ACIDITY OF 12-TUNGSTOPHOSPHORIC ACID AND ITS CESIUM DERIVATIVES

By

JOSÉ ALVES DIAS

A DISSERTATION PRESENTED TO THE GRADUATE SCHOOL
OF THE UNIVERSITY OF FLORIDA IN PARTIAL FULFILLMENT
OF THE REQUIREMENTS FOR THE DEGREE OF
DOCTOR OF PHILOSOPHY

UNIVERSITY OF FLORIDA

1997

This work is dedicated to my wife, whose love and faith in me were stronger than my own. This work would never have been achieved without her help, commitment and belief in a better future. I also dedicate this dissertation to my family for their constant support along all these years.

ACKNOWLEDGMENTS

I would like to thank the many people who have helped me throughout my career here at the University of Florida. First of all, I want to express my gratitude to my research advisor, Dr. Russell S. Drago, for helping me to come to the Department of Chemistry at the University of Florida. He is certainly one of the brightest minds that I have ever met. He taught me much of the chemistry that is beyond the textbooks. His perspective of analysis is unique and his capacity to solve problems seems unlimited. I will remember many of the discussions and ideas he always had to solve the difficulties. I would equally like to thank Ruth Drago whose kindness and hospitality helped a lot during these years. Maribel Lisk also deserves special thanks. Her friendship and assistance have been most appreciated.

On a personal note there are a few people I would like to mention. I would like to acknowledge one person specifically who has had the greatest impact on my life. This recognition goes to my wife, Sílvia C. L. Dias. It has been through her constant support, love and by her own example that I have been successful in what I have undertaken. Most importantly, I would like to thank my family. My father and mother, Sebastião and Luzia Dias, for their weekly supporting phone calls from Brazil. They did everything so that I could have and attain the best. They taught me by example that I could do anything

with hard work and determination. I would also like to thank my brothers, sister-in law and parents-in-law for constant prayers and support. To my family and friends for their prayers and calls, my deepest thanks and eternal gratitude.

There are people who should be noted for their important contributions: Dr. Thomas O. Maier for making the program used to analyze calorimetric data in homogeneous system (Chapter 2); Mr. John Osegovic for carrying out the ^{31}P MAS NMR analysis; Mr. Scott Baker for carrying out the ICP-MS measurements; and Mr. Jie Wu for carrying out the XRD experiments. I also want to thank the Drago group for all suggestions and discussions during this time.

I would also like to thank the Conselho Nacional de Desenvolvimento Científico e Tecnológico (CNPq) for the grant (proc. 200868/93-4) of a scholarship for pursuing Ph.D. at the University of Florida and the Universidade de Brasília (Brazil) for the leave of absence during this period.

TABLE OF CONTENTS

ACKNOWLEDGMENTS....iii

TABLE OF CONTENTS....v

LIST OF TABLES....vii

LIST OF FIGURES....ix

ABSTRACT....xii

CHAPTER 1: HETEROPOLY COMPOUNDS: CLASSES, STRUCTURES, AND RELEVANCE....1

Definition and Historical Aspects....1
Main Structures of Heteropolyanions....3
Structural Principles for Formation of Polyanions....7
Synthesis of Heteropoly Acids....11
Applications....13

CHAPTER 2: ACIDITY OF $H_3PW_{12}O_{40}$ IN HOMOGENEOUS SYSTEM....19

Introduction....19
Experimental....28
Results and Discussion....35
Conclusion....64

CHAPTER 3: ACIDITY $H_3PW_{12}O_{40}$ AND $Cs_xH_{3-x}PW_{12}O_{40}$ IN HETEROGENEOUS SYSTEM....66

Introduction....66
Experimental....69
Results and Discussion....74
Conclusion....109

CHAPTER 4: ACIDITY OF $H_3PW_{12}O_{40}$ SUPPORTED ON SILICA, ALUMINA, AND CARBON.....112

Introduction.....112
Experimental.....115
Results and Discussion.....116
Conclusion.....126

APPENDIX.....128

LIST OF REFERENCES.....154

BIOGRAPHICAL SKETCH.....161

LIST OF TABLES

Table page

1-1. Main Classes of Heteropolyanions......3

1-2. Effective Ionic Radii (Å) for Oxides (O^{-2} = 1.40 Å)......9

1-3. Organic Reactions Catalyzed by Heteropoly Acids......15

2-1. Fingerprint Bands of the Keggin Anion for $H_3PW_{12}O_{40}$......25

2-2. Results of Calorimetric Titrations (25 ±1 °C) with Pyridine for Different H_3PW Samples in CH_3CN Solvent......36

2-3. Heat Evolved (h'_{exp}) upon Addition of Pyridine to H_3PW in CH_3CN Solvent and Calculated (h'_{cal}) from Equilibrium Analysis $[H_3PW]_T = 1.39 \times 10^{-3}$ M......46

2-4. Thermodynamic Parameters for H_3PW-Base (25 ±1 °C) in CH_3CN Solvent......48

2-5. Results of ECW Fits for Reactions of H_3PW-Bases in CH_3CN Solvent......56

2-6. Enthalpies (kcal mol^{-1}) and Equilibrium Constants (25 ±1 °C) for the Reaction of Pyridine with Various Acids in CH_3CN Solvent $[Acid]_T = 1.39 \times 10^{-3}$ M......60

3-1. Chemical Analysis and Surface Area of $Cs_xH_{3-x}PW$ Compounds......70

3-2. Experimental Heat Evolved (h'_{exp}) in Cyclohexane upon Addition of Pyridine to H_3PW and Cs_2HPW for Different Thermally Treated Solids......76

3-3. Cal-ad Results for Three Types of Fit for H_3PW Reacting with Pyridine in Cyclohexane......78

3-4. XRD Patterns of H_3PW and Products of Reaction with Pyridine......89

3-5. Cal-ad Results for Reactions of $Cs_xH_{3-x}PW$ Compounds with Pyridine in Cyclohexane......93

3-6. Comparative Infrared Bands of the Keggin Anion for H_3PW and Cs_2HPW.............99

3-7. XRD Patterns of CsH_2PW, Cs_2HPW, $Cs_{2.5}H_{0.5}PW$, and Cs_3PW.............................104

4-1. Results of Calorimetric Titrations (25 ±1 °C) of SiO_2-H_3PW supported with Pyridine in Cyclohexane...117

4-2. Cal-ad Results for SiO_2^a-H_3PW supported (24.5 wt.%), $Al_2O_3^b$-H_3PW supported (19.4 wt.%), and Carbon^c-H_3PW supported (20.1 wt.%) with Pyridine in Cyclohexane..120

LIST OF FIGURES

Figure page

1-1. The Keggin Structure (α-$XM_{12}O_{40}$) Based on Tetrahedral Heteroatoms Represented
By (a) Bond, Polyhedral, and Space -filling Drawings; (b) One M_3O_{13} Group is
Removed to Show More Clearly the Iner Cavity that Accommodates the
Heteroatom.
The Black Dots Show the Oxygen Atoms Bonded to the Heteroatom........................4

1-2. The Silverton Structure of $CeMo_{12}O_{42}^{8-}$ Which is Based on 12-coordinated
Heteroatoms..6

1-3. The Dawson Structure of α-$P_2W_{18}O62^{6-}$...6

1-4. Comparative Structures of $M_7O_{24}^{n-}$ Anions in: **a** Anderson (D_{3d}), and **b** $Mo_7O_{24}^{6-}$
(C_{2v}) Symmetries..8

1-5. The Waugh Structure of $MnMo_9O_{32}^{6-}$...8

1-6. The Two Path Mechanism for Hydration of Isobutene Catalyzed by $H_4SiW_{12}O_{40}$....16

2-1. Structure of $H_3PW_{12}O_{40}$: (a) Primary, Shows the Four Types of Oxygen Atoms
in the Polyanion: (A) P-O; (B) W=O_t; (C) W-O-W_{edge}; (D) W-O-W_{corner};
(b) Secondary, Displays $H(H_2O)_2^+$ Bridging Four Polyanions for the Trihydrated
Acid...21

2-2. Thermal Analysis of $H_3PW_{12}O_{40}$ by: (a) DSC in air/He at 10 °C min^{-1};
(b) TGA in air at 10 °C min^{-1}..39

2-3. Isothermal TGA (300 °C min^{-1}) of $H_3PW_{12}O_{40}$ in Air at 10 °C min^{-1}........................40

2-4. FTIR of H_3PW in Mineral Oil. (—) H_3PW Treated at 162 °C for 4 hs under
Vacuum. (---) H_3PW Taken from the Bottle ($16H_2O$). Absorption Bands of
Mineral Oil (Aldrich, Dried on 3A Molecular Sieves) are on the Typical Range
of 2800-3000 cm^{-1} and 1400-1600 cm^{-1}. The Preparation of the Mull was made
in a Dry Box Filled with Nitrogen...41

2-5. Spectra of Absorption H_3PW with N-methylimidazole in CH_3CN (b = 0.1 cm).

The Concentration of H_3PW is 1.05 x10^{-4} mol L^{-1} (the Same for All Solutions). From Bottom to Top (λ = 230 nm), Concentration of N-methylimidazole in the Solutions are: 0; 2.17, 4.34, 6.51, and 8.68 x10^{-4} mol L^{-1} Respectively....................44

2-6. Figure 2-6. Spectra of Absorption H_3PW with Quinuclidine in CH_3CN (b = 0.1 cm). The Concentration of H_3PW is 1.57 x10^{-4} mol L^{-1} (for All Solutions). From Top to Bottom (λ = 230 nm), Concentration of Quinuclidine in the Solutions are Respectively: 1.67; 3.37, 5.05, 6.75, 8.37, 10.12, and 11.82 x10^{-4} mol L^{-1}................45

2-7 Isotherms of the Calorimetric Titrations of $H_3PW_{12}O_{40}$ with Bases. The Bases are: Quinoline (Qi), Pyridine (Py), Tetrahydrofuran (THF), N-methylimidazole (M-Im), Triethylphosphine (Tep), Quinuclidine (Qu), Dimethyl sulfoxide (DMSO), and N,N-dimethylacetamide (DMA)..53

2-8. Log K_1 versus $-\Delta H_1$ (kcal mol^{-1}) for the Reaction of H_3PW with Various Bases in CH_3CN Solvent. Bases are: Quinuclidine (Qu), Triethylphosphine (Tep), N-methylimidazole (M-im), Pyridine (Py), Quinoline (Qi), and Tetrahydrofuran (THF) respectively..55

2-9. Log K_1 versus ΔH_1 (kcal mol^{-1}) for the Reaction of Pyridine with Various Acids in CH_3CN Solvent. Acids are: 12-tungstophosphoric (H_3PW), triflic (TRIF), p-toluenesulfonic (PTS), sulfuric (H_2SO_4), trifluoroacetic (TFA), and m-chlorobenzoic (CB) respectively..61

3-1. Isotherms of Calorimetry and Adsorption for Reaction of H_3PW with Pyridine in Cyclohexane..77

3-2. Structure of $H_3PW_{12}O_{40}$: (a) Simple Unit Cell; (b) Extended Structure....................81

3-3. FTIR Spectra H_3PW (a) and Cs_3PW (b) after Reaction with Pyridine in Cclohexane..83

3-4. ^{31}P MAS NMR Spectra of: (a) H_3PW (δ = -12.05 ppm); (b) 1.04 mmol H_3PW-0.24 mmol Pyridine (δ = -16.53 ppm)....................................84

3-5. ^{31}P MAS NMR Spectra of: (a) 1.04 mmol H_3PW-0.08 mmol Pyridine (δ = -17.49 ppm); (b) 1.04 mmol H_3PW-0.12 mmol Pyridine (δ = -17.49 ppm)........86

3-6. XRD Pattern of H_3PW (dried at 162 °C/ 4 hs/ vacuum)..87

3-7. XRD Pattern of 1.04 mmol H_3PW-0.24 mmol Pyridine...88

3-8. XRD Pattern of 1.04 mmol H_3PW-0.08 mmol Pyridine...88

3-9. Calorimetric Isotherms of $Cs_xH_{3-x}PW$ Salts Reacted with Pyridine in Cyclohexane.91

3-10. Adsorption Isotherms of $Cs_xH_{3-x}PW$ Salts Reacted with Pyridine in Cyclohexane.92

3-11. FTIR Spectra CsH_2PW (a), Cs_2HPW (b) and $Cs_{2.5}H_{0.5}PW$ (c) after Reaction with Pyridine in Cclohexane..100

3-12. XRD Pattern of (a) CsH_2PW; (b) Cs_2HPW; (c) $Cs_{2.5}H_{0.5}PW$; and (d) Cs_3PW......102

3-13. ^{31}P MAS NMR Spectra of: (a) CsH_2PW(δ = -12.53 ppm); (b) Cs_2HPW (δ = -14.95 ppm); (c) $Cs_{2.5}H_{0.5}PW$ (δ = -15.51 ppm); (d) Cs_3PW (δ = -17.01 ppm)..106

4-1. Isotherms of Calorimetry and Adsorption for Reaction of SiO_2-H_3PW supported (24.5 wt.%) with Pyridine in Cyclohexane..118

4-2. FTIR Spectrum of SiO_2-H_3PW supported (24.5 wt.%)..121

4-3. Isotherms of Calorimetry and Adsorption for Reaction of Al_2O_3-H_3PW supported (19.4 wt.%) Reacted with Pyridine in Cyclohexane..123

4-4. FTIR Spectrum of Al_2O_3-H_3PW supported (19.4 wt.%)..124

4-5. Isotherms of Calorimetry and Adsorption for Reaction of carbon-H_3PW supported (20.1 wt.%) Reacted with Pyridine in Cyclohexane..125

Abstract of Dissertation Presented to the Graduate School
of the University of Florida in Partial Fulfillment of the
Requirements for the Degree of Doctor of Philosophy

ACIDITY OF 12-TUNGSTOPHOSPHORIC ACID AND ITS CESIUM DERIVATIVES

By

José Alves Dias

December 1997

Chairman: Dr. Russell S. Drago
Major Department: Chemistry

The objective of this work is to characterize the acidity $H_3PW_{12}O_{40}$ in different systems. This acid can catalyze reactions in homogeneous and heterogeneous systems. Acidity and solubility can be controlled by substituting the proton for different cations.

The calorimetric titration of $H_3PW_{12}O_{40}$ (H_3PW) with a series of bases in CH_3CN gives equilibrium constants and enthalpies for the three deprotonation steps. These results show that solutions of H_3PW in any solvent whose basicity is equal to or weaker than CH_3CN will furnish only one strong proton per molecule of acid for catalytic reactions. The best procedure to prepare the anhydrous H_3PW is established.

The ECW model gives a C_A^*/E_A^* ratio of 2.88, which indicates significant covalency in the interactions of this acceptor. The enthalpies of reactions of pyridine with a series of Brönsted acids in acetonitrile solvent leads to the acidity order: $H_3PW_{12}O_{40} > CF_3SO_3H > p\text{-}CH_3C_6H_4SO_3H \cong H_2SO_4 > CF_3COOH > m\text{-}ClC_6H_4COOH$.

Thermodynamic constants for H_3PW and $Cs_xH_{3-x}PW$ derivatives reacting with pyridine in cyclohexane solution are provided. The Cal-ad results indicate that the protons of H_3PW in the solid behave like those in solution, with all having different strengths. The enthalpy for reaction of the most acidic proton of H_3PW with pyridine is equivalent for the solid and in solution of acetonitrile.

Incomplete neutralization of the total available protons of H_3PW, CsH_2PW, and Cs_2HPW with pyridine in the calorimetric titrations and spectroscopic methods suggests formation of layered products. These methods also support that the distribution of the protons on the cesium salts is random and homogeneous in the solids.

Measurements of enthalpy of neutralization for the strongest protons in each compound lead to the following order of acidity: $H_3PW > Cs_2HPW \cong Cs_{2.5}H_{0.5}PW > CsH_2PW > Cs_3PW$.

Thermodynamic constants for H_3PW supported on silica, alumina, and carbon reacting with pyridine in cyclohexane solution are reported. Loading H_3PW up to 25 wt.% on these carriers does not increase the acidity of the free acid. However, Cal-ad results show that H_3PW is well dispersed on these supports.

The acidity order obtained is: H_3PW > SiO_2-H_3PW supported > Al_2O_3-H_3PW supported > Carbon-H_3PW supported.

CHAPTER 1
HETEROPOLY COMPOUNDS: CLASSES, STRUCTURES, AND RELEVANCE

Definition and Historical Aspects

Heteropolyanions are polymeric oxoanions represented by the general formula $[X_xM_mO_y]^{q-}$ ($x \leq m$) formed by the condensation of more than two different oxoanions [1]. Free acid or acid forms of these species are called heteropoly acids. For instance, reaction of tungstate with phosphate salts in acidic medium produce the heteropoly acid $H_3PW_{12}O_{40}$:

$$12WO_4^{2-} + HPO_4^{2-} + 26H^+ \rightarrow H_3PW_{12}O_{40} + 12H_2O$$

Of the elements comprising the structure, M is usually molybdenum, tungsten, vanadium, niobium, tantalum, or mixtures of these elements in their highest oxidation states (d^0, d^1), while X may comprise a wide variety of group I to VII elements (usually P, Si, As, Sb, etc.) [2].

The first heteropoly compound, now known as ammonium 12-molybdophosphate, was described by Berzelius in 1826 as the yellow precipitate that is produced when ammonium molybdate is added to phosphoric acid. This compound was introduced into analytical chemistry by Svanberg and Struve in 1848. The $PMo_{12}O_{40}^{3-}$ ion was used in quantitative determination of phosphate. When the tungstosilicic acid and its salts were discovered by Marignac in 1862, the analytical compositions of such heteropoly acids were precisely determined. By 1910, about sixty heteropoly compounds had been described [2].

The initial attempts to understand the composition of heteropolyanions were based on Werner's coordination theory. An advance occurred with the Miolati-Rosenheim theory, according to which, heteropolyanions are based on six-coordinate heteroatoms with MO_4^{2-} or $M_2O_7^{2-}$ anions as ligands or bridging groups. In 1929, Pauling [3] proposed that complexes with 12:1 ratio (M to X) had an arrangement of twelve MO_6 octahedra, each one sharing three corners with an adjoining octahedron, surrounding a central XO_4 tetrahedron. Although the detailed structure was not completely correct, the resulting formulas predicted the correct basicity and brought attention to the close relation of structural principles between heteropolyanions and infinite lattices. In 1933 Keggin [4a, 4b] determined the structure of $H_3PW_{12}O_{40}\cdot 5H_2O$ by X-ray diffraction showing that the anion was indeed based on WO_6 octahedral units linked by shared edges and as well as corners. Other isomorphous complexes were reported, but the next polyanion structure appeared in 1948 when Evans [5] described the structure of $TeMo_6O_{24}^{6-}$. A different structure for the ion ($H_6P_2Mo_{18}O_{62}$) was reported by Lindqvist [6a] in 1950, and later by Evans [6b]. Many other heteropoly compounds were isolated and their structures were determined. Taking into account those species with different m/x ratios, with more than one type of heteroatom, and with mixtures of polyatoms, the resulting field of heteropolyanions is vast, and several hundreds of complexes are known [2].

Main Structures of Heteropolyanions

A variety of polyanion structures exist with different formulas. A few examples include Keggin (α, β, γ, and ε-types; $XM_{12}O_{40}$), Silverton ($XM_{12}O_{42}$), Dawson ($X_2M_{18}O_{62}$), Anderson (XM_6O_{24}), and Waugh (XM_9O_{32}). The X element represents the central atom or heteroatom and M is called peripheral, poly or addenda atoms. Heteropoly compounds may be classified according to the ratio of the number of central atoms to the addenda atoms. Compounds with the same number of atoms in the anion usually are isomorphous and have similar chemical properties [7-10]. Typical heteropolyanions [11] are listed in Table 1-1.

Table 1-1. Main Classes of Heteropolyanions.

Ratio X:M	Structure	Polyatom (M)	Heteroatom (X)	Formula
1:12	Keggin	Mo, W	P(V), As(V), Si(IV), Ge(IV)	$[X^{n+}M_{12}O_{40}]^{(8-n)-}$
1:12	Silverton	Mo	Ce(IV), Th(IV)	$[X^{4+}M_{12}O_{42}]^{8-}$
2:18	Dawson	Mo, W	P(V), As(V),	$[X_2^{5+}M_{18}O_{62}]^{6-}$
1:9	Waugh	Mo	Mn(IV), Ni(V)	$[X^{4+}M_9O_{32}]^{6-}$
1:6	Anderson	Mo, W	Te(VI), I(VII)	$[X^{n+}M_6O_{24}]^{(12-n)-}$

The Keggin structure ($XM_{12}O_{40}$), illustrated in Figure 1-1, is based on tetrahedral heteroatoms [2-4]. The structure has an overall T_d symmetry and is formed by a central XO_4 tetrahedron surround by twelve MO_6 octahedra arranged in four groups of three edge-shared octahedra, M_3O_{13}. These groups (called M_3 triplets) are linked by shared corners to each other and have a common oxygen vertex to the central heteroatom. The

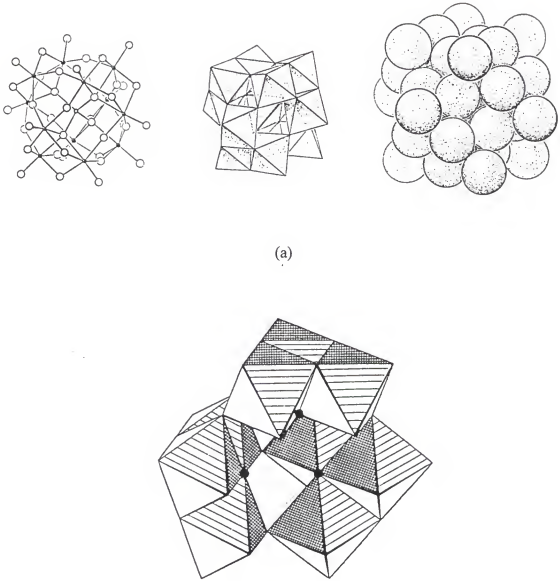

(a)

(b)

Figure 1-1. The Keggin Structure (α-$XM_{12}O_{40}$) Based on Tetrahedral Heteroatoms Represented by (a) Bond, Polyhedral, and Space-filling Drawings; (b) One M_3O_{13} Group is Removed to Show More Clearly the Inner Cavity that Accommodates the Heteroatom. The Black Dots Show the Oxygen Atoms bonded to the Heteroatom [1, 2].

existence of isomers for the Keggin anion has been established [12]. In the β-type, one of the three edge shared W_3O_{13} triplets of the α structure is rotated by 60^0 reducing the symmetry of the anion from T_d to C_{3v}. The other isomers involving the 60^0 rotation of two, three, and all four W_3O_{13} are called the γ, δ, and ε-type, respectively. A much more complex analysis is predicted for mixed Keggin anions of formula $XM_xM'_{12-x}O_{40}^{n}$, which presents numerous possibilities of what is known as positional isomers [2].

The Silverton structure ($XM_{12}O_{42}$) is based on icosahedral coordinated heteroatoms and faced-shared pairs of MO_6. This structure is observed for molybdenum complexes, but no analogous tungstates have been reported. The structure [2] is illustrated in Figure 1-2. The first anion described by the Silverton structure was $CeMo_{12}O_{42}^{8-}$. The icosahedron of CeO_{12} is surround by six face-shared Mo_2O_9 units, linked together by corner-sharing. The structure is known for molybdates with Ce(III and VI), Th(IV), U(IV and V), and Np(V) heteroatoms.

The Dawson structure ($X_2M_{18}O_{62}$) can be understood in terms of an intermediate lacunary Keggin anion. The stability of Keggin heteropolyanions of W and Mo in solution is dependent on the pH. As the pH increases, $X^{n+}M_{12}O_{40}^{(8-n)-}$ undergoes hydrolysis forming the lacunary $X^{n+}M_{11}O_{39}^{(12-n)-}$ (pH = 2) which degrades to give $X^{n+}M_9O_{31}^{(8-n)-}$ (pH = 8). Two units of that lacunary anion fuse to form the Dawson structure (Figure 1-3). There are three isomers, depending on the number of rotated M_3O_{13} groups [2].

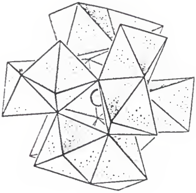

Figure 1-2. The Silverton Structure of $CeMo_{12}O_{42}^{8-}$, Which is Based on 12-coordinated Heteroatoms [2].

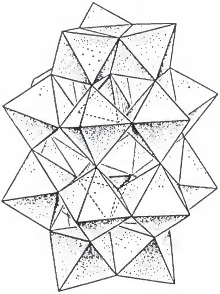

Figure 1-3. The Dawson Structure of α-$P_2W_{18}O_{62}^{6-}$ [2].

The Anderson structure (XM_6O_{24}) is based upon octahedral heteroatoms. The polyanion arrangement is made up of seven edge-shared octahedra with a planar structure averaging D_{3d} symmetry. Although this structure was originally proposed for the heptamolybdate anion ($Mo_7O_{24}^{6-}$), Lindqvist later demonstrated that the heptamolybdate had a bent structure with an averaged C_{2v} symmetry [2]. The first authentic Anderson structure [13] was observed for $TeMo_6O_{24}^{6-}$ (Figure 1-4). Heteroatoms in oxidation states +2, +3, +4, +6, and +7 have been observed in this heteropolyanion. With the lower oxidation states (+2, +3) the anion carries six non-acidic protons which are attached to the oxygens of the central XO_6 octahedron.

The Waugh structure (XM_9O_{32}) may be constructed from hypothetical XM_6 Anderson species. For instance [14], $Mn^{IV}Mo_9O_{32}^{6-}$ is composed by removing three alternate MoO_6 octahedra and placing three MoO_6 octahedra above and below the $MnMo_3$ unit (Figure 1-5). The final structure has a D_3 symmetry.

Structural Principles for Formation of Polyanions

The cluster structures discussed before belong to a more general class of compounds called metal-oxygen anions, which consist of so-called heteropoly and isopolyanions (polyanions formed by condensation of only one kind of oxoanion). These clusters contain highly symmetrical core assemblies of MO_x units (M = V, Mo, W) and frequently adopt quasi-spherical structures based upon Platonic solids of topological interest [15]. The structures of heteropoly and isopolyanions appear to be governed by the electrostatic and radius-ratio principles observed for extended ionic lattices.

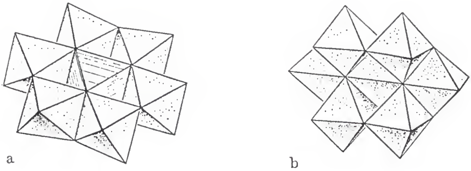

Figure 1-4. Comparative Structures of $M_7O_{24}^{n-}$ anions in: **a** Anderson (D_{3d}), and **b** $Mo_7O_{24}^{6-}$ (C_{2v}) Symmetries [2].

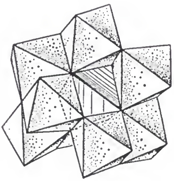

Figure 1-5. The Waugh Structure of $MnMo_9O_{32}^{6-}$ [2].

Thus, it is easier to describe these structures in terms of assemblages of metal-centered MO_x polyhedra that are linked by shared corners and edges, and occasionally, faces. The ionic radii for polyanion addenda atoms [16] are given in Table 1-2. In all cases, the metal ion is displaced from the center towards a vertex or edge of its own polyhedron.

Table 1-2. Effective Ionic Radii (Å) for oxides (O^{-2} = 1.40 Å).

Ion	T_d radius	O_h radius	Observed coordination number in polyanions
V^{+5}	0.49	0.68	4, 5, 6, 7
Nb^{+5}	0.62	0.78	6
Ta^{+5}	0.62	0.78	6
Mo^{+6}	0.55	0.73	4, 6, 7
W^{+6}	0.56	0.74	6

Polyoxometalates structures are governed by two general principles. First, each metal atom occupies an MO_x coordination polyhedron. The most common is an octahedron or square pyramid on which the metal atoms are displaced towards those polyhedral vertices that form the surface of the structure. This is a result of M-O π bonding. The second principle, the Lipscomb principle, establishes that structures with MO_6 octahedra do not contain more than two unshared oxygen atoms. This has been rationalized in terms of the strong trans influence of the terminal M-O bonds, which facilitates dissociation of neutral MO_3 from the cluster. However, a few examples of complexes have been characterized with anti-Lipscomb structures [17, 18] suggesting this rule is not absolute.

The existence of heteropoly and isopoly compounds is considered as a special class of compounds of d^0 metals of groups V and VI [19]. The two decisive factors are: (1) cis arrangement of the multiple-bonded ligands in octahedral complexes of d^0 metals in contrast to their trans arrangement in complexes of the d^2 metals; (2) the pronounced trans influence of the metal-ligand multiple bond, leading to considerable weakening and lengthening of the bond with its trans partner. When applied to oligomeric or polymeric oxygen compounds, the first factor results in localization of the π interaction in -M-O-M-O- chains of d^0 metals in M-O bonds through one, which leads to a cis arrangement of the M-O multiple bonds in each of the MO_6 octahedra. In none of the linked MO_6 octahedra of the anion can terminal oxygen atoms be found in a trans position to one another. Only linkage of octahedra along common edges is considered, since bonding by a common face results in metal atoms being too close to one another, and connection through a common vertex either keeps the trans arrangement of the terminal oxygen atom or leads to constructions with too low coordination numbers for the internal oxygen atoms. Therefore, the anion that satisfies this main requirement and has the least number of metal atoms is the trimer M_3O_{13}. Because the mean charge per oxygen atom for this species is too high (~0.6 e), this unit is metastable, and must form larger clusters promptly. The second and third factors are applicable to the distribution in the trans positions relative to M-O multiple bonds (in particular, the trans position relative to a terminal oxygen) of the oxygen atoms having the highest coordination number in relation to the metal. Taken together, all this leads to the appearance of oligomeric species constructed out of octahedra linked by common edges in such a way that multiple bonded oxygen atoms are peripheral and in the trans positions to them with the internal oxygen atoms having high coordination numbers.

Structures of the iso and heteropolyanion type disappear [19] on going to the metals of Groups VII and VIII, mainly because the d^1 and d^2 states, characteristic of these metals, take the place of d^0 state for Groups V and VI. In addition, the tendency towards localization of the π interaction is reversed, being delocalized for Groups VII and VIII. Those structures are also not encountered for the metals situated to the left of Groups V and VI because the trans influence disappears. With the increasing polarity of M-O bonds on moving across the Periodic Table, the π interaction is generally significant. There is also an increase in the tendency for coordination numbers higher than 6. An extra principle must be considered for understanding the appearance of iso and heteropolyanions. It relates solely to the ability of metal of Group V and VI to change their coordination number from 4 to 7 in relation to oxygen. Whatever the specific mechanism of polymerization of these polyanions in solution, they can proceed only with a change in the coordination number of the metal in the copolymerizing species and with the participation of protons forming hydroxyl and or water molecules.

Synthesis of Heteropoly Acids

Heteropolyanions are most commonly prepared by acidification of aqueous solutions of simple oxoanions and the necessary heteroatoms. When the central atom is not a transition element, a soluble molybdate or tungstate may be dissolved with a soluble salt containing the heteroatom in the appropriate oxidation state. Then, the mixture is acidified to an adequate pH range. When the central atom is a transition metal, a simple salt of that element is mixed hot with a soluble molybdate or tungstate in the proper pH range. If the central atom must be raised to an unusual oxidation state, peroxide, persulfate or bromine water are frequently employed or electrolytic oxidation may also be used [9]. Detailed syntheses of heteropoly acids are described in the literature [2, 9].

Isolation of the heteropoly acid, after acidification of an aqueous solution of the salt of the hetero element and the alkali metal molybdate or tungstate, is obtained through extraction with ether or ion exchange [2]. The solution of heteropolyanion is shaken with excess diethyl ether and three phases are formed, consisting of an ether layer, an aqueous layer, and a heavy oily etherate. The lowest layer is drawn off, shaken with excess ether to remove entrained aqueous solution, and separated again. The etherate is decomposed by the addition of water, the ether is removed, and the aqueous solution of the heteropoly acid is allowed to evaporate until crystallization occurs. The exact nature of the etherates [2] is not clear at present, although Et_2OH^+ has been detected by IR spectroscopy. Acids such as 12-tungstophosphoric, 12-tungstosilicic, and 12-molybdophosphoric are commercially available as crystalline hydrates

A new method using electrodialysis has been reported for preparation of $H_3PW_{12}O_{40}$ with much better yields and low by-product formation [20a, 20b]. The heteropoly acid is formed in the anode compartment of a dialyzer from Na_2WO_4 and H_3PO_4 in an aqueous solution. Acidification is provided by electrolysis of water. Na^+

ions are transferred by the electric potential from the anode to cathode through a cation-exchange membrane. As a result, pure $H_3PW_{12}O_{40}$ at the anode and NaOH at the cathode are formed. The heteropoly acid is isolated by crystallization in almost 100% yield.

Applications

Applications of polyoxometalates are mainly based on their unique properties, such as size, mass, electron-proton transfer, thermal stability, lability of lattice oxygen, and high Brönsted acidities. They have uses in many fields including analytical chemistry, biochemistry, solid state physics, and catalysis.

Analysis of P, As, Si, and Ge has been made by formation of $XMo_{12}O_{40}^{n-}$ anions, which can be either precipitated (gravimetry) or reduced (colorimetry) [21]. Variations contain the use of molybdate-vanadate or tungstate-vanadate mixtures [22]. A recent study uses differential-pulse anodic voltametry [23] to determine simultaneously P, Si, Ge, and As.

Salts of heteropolyanions have been shown to be biologically active. Such activity includes selective inhibition of enzyme functions, in vitro and in vivo antitumoral activity, antiviral activity (e.g., against rabies), and antiretroviral activity (e.g., against HIV infections connected with AIDS). The heteropolytungstate $NaSb_3O_7(SbW_7O_{24})^{18-}$ (called HPA-23) has been used [15] for treatment of AIDS patients in France. A few reasons can be pointed out [24] for biological activity of heteropoly acids, such as ionic size and shape, electron transfer and reservoir properties, stability or non-lability at micromolar concentrations and physiological pH.

Many properties of heteropoly compounds in solution are also observed in the crystalline salts and free acids, since the large anions tend to have very weak attractions to countercations and solvate molecules. Particularly, the electron- and proton-transfer characteristics are often conserved in the solid state. Crystalline acids such as $H_3PW_{12}O_{40} \cdot 21H_2O$ are protonic conductors and proton-conducting films [25a-c] have been described. Electrochromic and ion-selective electrodes have also been reported [26a, 26b].

The widest use of heteropolyanions lies in oxidation and acid catalysis. They are also excellent model systems [27] for investigating fundamental problems of catalysis. Recent reviews of catalytic chemical applications of heteropoly compounds in solution and solid state have been published, emphasizing homogeneous oxidations [28], synthesis of fine chemicals [29a, 29b], and acid catalysis [30, 31]. Table 1-3 summarizes some reactions [31] catalyzed by heteropoly compounds in homogeneous and heterogeneous solution.

Solubility of heteropolyanions in water and many polar organic solvents, and their insolubility in non-polar solvents makes these compounds useful for: liquid-phase homogeneous reactions (aqueous and organic media); liquid-phase heterogeneous reactions (non-polar solvents, e.g., hydrocarbons); vapor-phase heterogeneous reactions.

The mechanism of homogeneous acid catalysis [29a, 29b] by heteropoly acids involves their functioning as proton donors. In the simplest case, this catalysis can be represented by:

$$S + HA \rightleftharpoons SH^+ + A^- \quad (I); \qquad SH^+ \xrightarrow{(A^-)} P + HA \quad (II),$$

where S is the substrate, HA the acid catalyst, and P the product. As stronger acids, heteropoly acids are able to activate the substrate more effectively than the usual inorganic acids. However, heteropoly acids play other important roles in promoting reactions. They can stabilize organic intermediates or cause a strong salt effect on the reaction rate.

Table 1-3. Organic Reactions Catalyzed by Heteropoly Acids.

Reaction	**Substrate**
Isomerization	1-butene, m-xylene, p-xylene
Hydration	propene, isobutene, cyclohexene
Dehydration	2-propanol, cyclohexanol
Ether formation	methanol + isobutene (t-BuOH)
Esterification	carboxylic acid + alcohol (alkene)
Rearrangement	cumene hydroperoxide
Friedel-Crafts	alkylation, acylation
Prins reaction	styrene + formaldehyde
Polymerization	tetrahydrofuran
Methanol to gasoline conversion (MTG)	methanol

The hydration of isobutene is a known example [29a] to illustrate those features. A two path mechanism (Figure 1-6) is accepted for this reaction with formation of the intermediate carbenium ion, which operates with mineral acids (path I). Formation of a complex between the heteropoly acid and the olefin (path II) is responsible for promoting the reaction and increasing the order with respect to the heteropoly acid. The salt effect, established empirically, determines the formal order of isobutene hydration reaction with respect to heteropoly acids. In diluted solutions (0.02-0.1 M) the order is 1.2-1.5, while in concentrated solutions (up to 0.5 M) is 2.0-2.2.

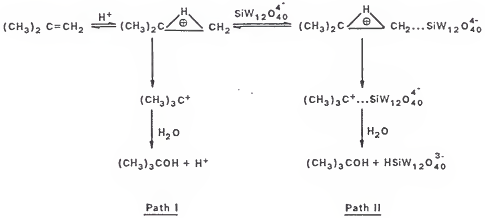

Figure 1-6. The Two Path Mechanism for Hydration of Isobutene catalyzed by $H_4SiW_{12}O_{40}$ [29a].

Most research in homogeneous catalysis by heteropoly compounds involves oxidation reactions [28]. The heteropolyanions comprise polyanions where the addenda atoms are substituted by d-electron transition metals. A number of reactions have been studied, mainly using monosubstituted heteropolyanions in different solvents. There are a variety of mechanisms, depending on the reaction. A recent review [28] describes many of the established mechanisms, which have been elucidated.

Three classes of catalysis have been identified [27] for heterogeneous systems (i.e., gas-solid and liquid-solid). For the first type, surface catalysis, reactions take place on the two-dimensional surface (outer surface or pore walls) of solid. The reaction rate is proportional to the catalyst surface. The second class, bulk type I catalysis, the reactants are absorbed into the solid, between the polyanions but not in the anion. Usually, these molecules substitute waters of crystallization or expand the lattice where reactions take place. The structure of the polyanion is intact. The reaction rate is proportional to the volume of the catalyst in the ideal case. The rate of an acid catalyzed reaction, for instance, is proportional to the total number of acidic groups in the solid bulk. The third class, bulk type II, occurs for some oxidation reactions at high temperatures. The principal reaction probably proceeds on the surface, the whole solid bulk takes part in redox catalysis owing to the rapid migration of proton and electron-redox reactants into the bulk. The rate is proportional to the volume of catalyst in the ideal case. Although the three classes are distinctly different from each other in the ideal case, the extent of contribution of the inner bulk of the solid to the catalysis depends on the rate of the catalytic reaction relative to the diffusion of the reactant and product molecules in the bulk type I catalysis and on the rate of diffusion of redox carriers for the bulk type II catalysis.

Heteropoly acids have been proven to be of value in fundamental studies and practical applications. The utility of these compounds is a consequence of the potential for design at the atomic and molecular level. Control of acidic and redox properties, multifunctionality, bulk-type and pseudoliquid behavior, and the unique basicity of the polyanion, makes these compounds very attractive to study.

The work presented in this dissertation is concerned with acidity characterization of 12-tungstophosphoric acid and its cesium derivatives. The heteropoly acid $H_3PW_{12}O_{40}$ offers a unique opportunity to be studied in homogeneous and heterogeneous system due to a variety of media in which this acid shows solubilities. Progressive substitution of the protons of $H_3PW_{12}O_{40}$ by cesium, forms compounds of the type $Cs_xH_{3-x}PW_{12}O_{40}$ which have very limited solubility. The acidities of the cesium compounds are compared to the parent acid in heterogeneous reaction because of their increasing importance in catalytic reactions. Moreover, characterization of $H_3PW_{12}O_{40}$ supported on solids such as silica, carbon, and alumina were carried out. Comparison with the unsupported acid allows for an investigation of the effects of surface area on the acidity of the solid. Mathematical models are used to interpret acidity of the acids in homogeneous and heterogeneous systems in attempt to obtain quantitative understanding. Thermodynamic data for these compounds may be used for comparing catalytic activity and acidity for different acid catalyzed reactions with the heteropoly acids studied.

CHAPTER 2
ACIDITY OF $H_3PW_{12}O_{40}$ IN HOMOGENEOUS SYSTEM

Introduction

The utility of heteropoly acids (HPAs) as catalysts for redox and acid catalyzed reactions has stimulated considerable interest in these compounds. Our interest in acid catalysis led us to investigate the acidity of these materials. The acid $H_3PW_{12}O_{40}$ (abbreviated as H_3PW) was selected for study because it is reported to be among the strongest acids in the series, it is commercially available as a crystalline hydrate and it has been thoroughly characterized [32a-c].

The 12-tungstophosphoric acid belongs to the Keggin class of heteropoly compounds. The complete structure of $H_3PW_{12}O_{40}{\cdot}nH_2O$ can be depicted by a primary and a secondary structure. The primary structure (Keggin polyanion) has twelve WO_6 octahedra surrounding a central PO_4 tetrahedron. The twelve WO_6 octahedra are better described as four groups of three edge-shared units of W_3O_{13} which are corner-shared to each other. These triplet groups actually do not exist independently, but they are the smallest block needed to build the entire Keggin anion. There are four kinds of oxygen atoms in this polyanion: 4 O_i (internal oxygen, connecting P and W), 12 O_e (edge-sharing oxygen, connecting W atoms), 12 O_c (corner-sharing oxygen, connecting W_3O_{13} units), and 12 O_t (terminal oxygen, bonded to one W atom). The W atoms are displaced outward

(0.3-0.4 Å) from the center of the WO_6 octahedron, giving the W-O_t bond some double bond character. The O_i is located inside the anion and the W-O_i-P bond is long and weak. The whole Keggin anion has a tetrahedral symmetry, and considering the anion as a sphere, it has a diameter of approximately 10 Å.

The secondary structure is dependent on the hydration degree, for example in the ($H_3PW_{12}O_{40}\cdot 6H_2O$) the polyanions constitute two sets of three-dimensional networks in which polyanions are connected by $H(H_2O)_2^+$ bridges. The two sets of networks penetrate each other, so that the arrangement of polyanions becomes the bcc type. This is the most dense secondary structure and is called type A. Types B, C, and D, which contain a greater number of water molecules, are also known. In the dehydrated compound, a proton located in the same position as $H^+(H_2O)_2$ interacts with the four O_t atoms. Since all terminal oxygens are equivalent, according to the magic angle ^{17}O NMR spectrum, the proton is proposed to exchange rapidly between the four O_t atoms [29a]. The primary and secondary structure of H_3PW is illustrated in Figure 2-1.

In solution, the structure of H_3PW depends upon its concentration and the solvent in which it is dissolved. Large angle X-ray scattering (LAXS) analysis of concentrated H_3PW solutions (> 10^{-2} mol L^{-1}) yields radial distribution curves which can be compared with those calculated from the known crystallographic dimensions of the presumed solute species. This method has shown [33a-d] that the structure of polyoxometalates are maintained when dissolved in water. Other evidence comes from similar UV spectra of solutions of isostructural compounds (e.g., $H_3PW_{12}O_{40}$, $H_4SiW_{12}O_{40}$, and $H_6[H_2W_{12}O_{40}]$), from IR, Raman, and ^{17}O NMR results of aqueous and non-aqueous solutions [32b].

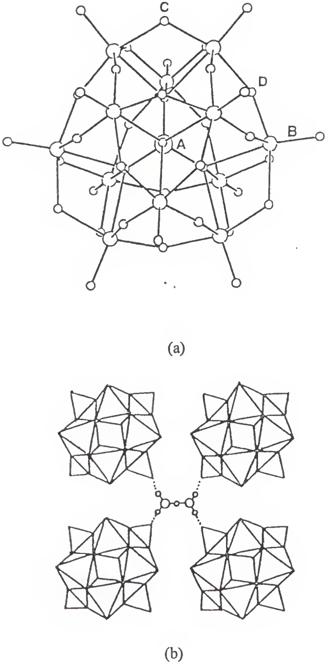

Figure 2-1. Structure of $H_3PW_{12}O_{40}$: (a) Primary, Shows the Four Types of Oxygen Atoms in the Polyanion: (A) P-O; (B) $W=O_t$; (C) $W\text{-}O\text{-}W_{edge}$; (D) $W\text{-}O\text{-}W_{corner}$. [51]
(b) Secondary, Displays $H(H_2O)_2^+$ Bridging Four Polyanions for the Trihydrated Acid [11].

H_3PW and many of its salts are fully dissociated in aqueous solution as a result of the large anion size, combined with a low surface density of the negative charge. The heteropolyanions are weakly solvated and behave as weak ligands [34]. H_3PW is a strong Brönsted acid. In solution at pH higher than 1.5, the following equilibrium reactions occur:

$$PW_{12}O_{40}^{3-} + 3H_2O \rightleftharpoons PW_{11}O_{39}^{7-} + WO_4^{2-} + 6H^+ \rightleftharpoons 12WO_4^{2-} + HPO_4^{2-} + 23H^+$$

Although the Keggin structure is preserved in concentrated aqueous solutions, degradative dissociation occurs in diluted solution [32b].

Acidities of heteropoly acids in solution have been studied by conductivity [35-36], Hammett acidity constants [37], and the ^{13}C shift of mesityl oxide [38]. Based on conductivity, it is claimed that in solvents of moderate polarity like ethanol, the first and second proton of H_3PW are completely dissociated while in acetic acid, H_3PW behaves as a monoprotic acid [32b, 38]. The pK_a for the dissociation of the protons in acetone are 1.6, 3.0, and 4.0. The pK_a values in ethanol are very similar to those in acetone. In water, the stepwise three step dissociation of H_3PW is not detected because of the leveling influence of the solvent. However, in acetic acid, pK_{a1} is equal to 4.77 [32b].

The most commonly reported criterion of acid strength for H_3PW has been Hammett acidity functions (H_0). H_3PW is pretreated under different thermal conditions, transferred to a solution of dry benzene, where small amounts of n-butylamine is added. Then, the solution is tested with a few drops of 0.1% solution of an appropriate indicator after equilibration. Each indicator has a strength, according to its dissociation constant in benzene. Then, the acidity is determined from the number of millimoles of n-butylamine which had to be added before the appropriated color change occurred. In this fashion, it has been determined [37] 0.90 mmol g^{-1} at H_0 -5.8 (strongest sites), and 3.09 mmol g^{-1} at H_0 6.8 (weakest sites) for H_3PW pretreated at 320 ^{0}C (best condition). It has also been reported [29a, 29b] the measurement of Hammet acidity in H_2O, H_2O-AcOH, H_2O-dioxane, H_2O-EtOH, and H_2O-Me_2CO mixtures. Other studies [39a-c] suggested that H_3PW is a superacid, based on the definition that a superacid is an acid with strength greater than that of 100% H_2SO_4, i.e., a value of $H_0 < -12$.

The ^{13}C shift of mesityl oxide upon reaction with H_3PW in acetic acid is interpreted to indicate that the three protons dissociate simultaneously and not consecutively [38]. Because of the size of the molecule, the negative charge of the conjugate base is claimed to be delocalized over the large Keggin structure, and there is no charge destabilization for the second and third ionizations. In all instances, the reported studies suggest that the acidity of H_3PW is greater than $HClO_4$ and H_2SO_4 [29a, 29b, 38].

In the solid state, H_3PW possess Brönsted acidity, which is claimed to be stronger than such conventional solid acids as SiO_2-Al_2O_3, H_3PO_4/SiO_2, and HX and HY zeolites [29a]. A microcalorimetric study [40] of the reaction of gaseous ammonia with solid H_3PW was carried out at 50 °C. The sample activated at 150 °C shows different behavior from one activated at 250 °C, which differs [41] from a sample activated at 300 °C and titrated at 150 °C. Another microcalorimetric study [42] at 150 °C claims that H_3PW, treated at 150 °C or 250 °C under vacuum, produces the anhydrous acid, whose acidity is greater than that of the anhydride prepared by vacuum drying at 400 °C. The anhydride is metastable decomposing into constituent oxides [42].

$H_3PW_{12}O_{40}{\cdot}nH_2O \rightarrow H_3PW_{12}O_{40} + nH_2O$ (Anhydrous acid)

$nH_3PW_{12}O_{40} \rightarrow [PW_{12}O_{38.5}]_n + 1.5nH_2O$ (Anhydride phase)

$[PW_{12}O_{38.5}]_n \rightarrow 0.5nP_2O_5 + 12nWO_3$ (Oxides)

The exotherms from the gas-solid calorimetric titration of studies of H_3PW with ammonia are complex. Initially enthalpies of 47.8 kcal mol^{-1} are reported dropping to 45 kcal mol^{-1} before 0.5 equivalents of ammonia are added. This is followed by a gradual drop to 39 kcal mol^{-1} up to 2.9 equivalents and a sharp drop thereafter. The three protons are reported to have comparable acidity. In the Cal-ad study [43] of HZSM-5, gas-solid calorimetry at elevated temperature was shown to contain both dispersion and acid-base components and to average into a single step different protons whose acidities differ by 30 kcal mol^{-1}.

Thermal methods such as TGA, DTA, TPR, and TPD have been used to characterize the stability and nature of the sites of H_3PW [32c, 44-47]. These data suggest that the Keggin structure is stable up to 450-500 ^{0}C. Water from the structure is considered zeolitic in nature, since its release does not affect the crystal lattice. In addition, desorption of pyridine has shown that the maximum uptake of pyridine is about three per Keggin anion, and occurs when the H_3PW is treated at 190-320 ^{0}C.

IR spectroscopy was also utilized to characterize the Keggin structure and to monitor reactions of basic probes with H_3PW [48-51]. Table 2-1 shows the vibrational bands assigned to the primary structure $PW_{12}O_{40}^{3-}$. Variable amounts of water do not cause shifts in these peaks. A peak about 1715 cm^{-1} indicates the presence of hydronion ($H(H_2O)_n^+$), which reacts with probes such as NH_3 or Pyridine.

Table 2-1. Fingerprint Bands of the Keggin Anion for $H_3PW_{12}O_{40}$.

Bond	Frequency (cm^{-1})
(P—O)	1081
(W — O_t)	984
(W — O_c — W)	892
(W —O_e — W)	794
(O —P— O)	595

The states of the protons and phosphate group in the solid H_3PW have been studied by solid state NMR spectroscopy of ^{31}P and ^1H [52-53]. Decreasing the amount of water in the structure reduces proton mobility, and leads to stronger bonding to the polyanion. This is indicated by broadening and weakening of a sharp proton resonance of $H_3PW \cdot 17H_2O$ ($\delta = 7.5$ ppm) to H_3PW dehydrated ($\delta = 9.2$ ppm). The ^{31}P NMR chemical shift is very dependent on the number of water molecules on $H_3PW \cdot nH_2O$, the values being for n=6 ($\delta = -15.1$ to -15.6 ppm), and n=0 ($\delta = -11.1$ to -10.5 ppm). It is suggested [29a] that the protons can move among four equivalent positions, $W{=}O{-}{-}H^+{-}{-}O{=}W$, attached directly to oxygen atoms of the Keggin units, while $H(H_2O)_2^+$ is connected to the heteropolyanion by hydrogen bonding at terminal oxygens.

The conflicting reports of the acidities of H_3PW have prompted further study. With a three step equilibrium possible, solution measurements are more easily interpreted than calorimetric studies of the solid. Enthalpies are measured as the criterion of acid strength, and they are expected to provide a temperature independent relative acidity scale for the temperature ranges used in acid catalysis. Work from this laboratory has emphasized [54-56] using the enthalpy of adduct formation in poorly solvating solvents as the criterion for measuring donor-acceptor strength. Most of the acceptors studied to date are neutral molecules that form neutral 1:1 adducts. The strong acid H_3PW, on reaction with moderately strong bases, forms ionic products, and the acid is insoluble in poorly solvating solvents. These properties afford an opportunity to extend the enthalpy criterion of acid strength to new acid-base reactions but require a reevaluation of the experimental conditions that will provide the most meaningful results.

Reaction of one molecule of base with a monoprotic acid, HX, is described by the following equilibria [57]:

$$\underset{}{B_{sol}} + \text{H-}X_{sol} \rightleftharpoons \underset{\text{(I)}}{\text{B--H-}X_{sol}} \rightleftharpoons \underset{\text{(II)}}{\text{B-H}^{+}\text{--}X^{-}_{sol}} \rightleftharpoons \underset{\text{(III)}}{BH^{+}_{sol} + X^{-}_{sol}} \qquad (2.1)$$

where (I) is the hydrogen bond adduct, (II) is an intimate ion pair with HX behaving as a Brönsted acid and (III) is the dissociated or solvent separated ion pair of the Brönsted acid, HX. In the solvent separated ion pair, the base and at least one solvent molecule is coordinated to the proton. Research leading to the Coordination Model [58] for non-aqueous solvents has shown that the position of the equilibrium between species (I), (II) and (III), in different pure bases as solvent, depends on the basicity and polarity of the solvent as well as the basicity of the conjugate base X^-. Both strong basicity and large polarity are needed to displace the anion from the acid by a neutral base.

To establish an acidity scale, the solvent should be held constant to minimize differences from non-specific solvation contributions to the measured enthalpy. The best solvents for studying Brönsted acids are non-protonic and weakly basic because of the leveling effect. Basic solvents drive the equilibrium in Equation (2.1) toward species (III) even when HX is a weak acid, i.e., those with strong conjugate bases. As a result, the enthalpy of reaction of a base with both weak and strong acids in basic solvents will be similar and will correspond to the enthalpy of the reaction (where S is a solvent molecule):

$$S_2H^+_{sol} + X^-_{sol} + B_{sol} \rightarrow BHS^+_{sol} + X^-_{sol} + S \qquad (2.2)$$

Slight differences in -ΔH may arise if the equilibrium between intimate and separated ion pairs (species II and III of Equation 2.1) differ. Thus, weakly basic solvents must be used to discriminate the relative acidity of strong acids.

The best solvents to study acidity should also be either non polar or only slightly polar, so the product of the reaction is species (II), or very polar, so the only product is species (III). In the studies reported here acetonitrile is selected as the weakly basic, polar solvent because solubility limitations of H_3PW require use of a polar solvent. When a strong, weakly polar base such as pyridine is added to H_3PW in a weakly basic polar solvent, solvent polarity will allow pyridine basicity to drive the reaction towards species (III) displacing X^- from the proton. The enthalpy measured will be the net of displacing X^- from the H^+ by pyridine plus the net non-specific solvation of the ionic products and reactants. The non-specific solvation is expected to be the smaller of the two contributions and relatively constant as the base is varied. Thus, in weakly basic polar solvents, relative basicities can be obtained from the enthalpies without varying contributions from the extent of ionizations of (II) to (III). When di- and tri-protic acids are studied, the above discussion for HX pertains to each step of the reaction.

With H_3PW, a series of reactions with different bases have been investigated to determine the influence of the base on the three steps of the H_3PW equilibria. The enthalpies for step 1 are correlated to the ECW model [56] to demonstrate that the basicity trends in acetonitrile toward Brönsted acids parallel those toward neutral acids in weakly solvating solvents. In order to compare the relative acid strength of H_3PW to other acids using this new scale, enthalpies for the reaction of pyridine with a variety of acids are also reported in CH_3CN solvent.

Experimental

Materials

Elemental and TG analysis of the H_3PW (obtained from Aldrich) revealed 16 moles of water per mole of H_3PW. Acetonitrile obtained from Fisher was purified by drying over 4A molecular sieves for 24 hours, and then distilled over P_2O_5. Pyridine obtained from Fisher was distilled over CaH_2. Quinuclidine, N-methylimidazole, N,N-dimethylacetamide and triethylphosphine (Aldrich), quinoline and dimethylsulfoxide (Fisher) were used as supplied. Sulfuric acid (97% as calculated by standardization), p-toluenesulfonic acid, and benzoic acid were obtained from Fisher. Triflic acid was obtained from Aldrich. Trifluoroacetic acid and m-chlorobenzoic acid were obtained from Kodak. Drying and standardization procedures for the acids followed literature guidelines. Dried samples were stored in a container with 4A molecular sieves.

Thermal Treatment and Calorimetric Titration of H_3PW

H_3PW was subjected to different thermal treatments. It was heated at 128 °C and 162 °C in a vacuum oven. In other treatments, it was heated at 200 °C, 300 °C, and 400 °C under dry air flow in a tube furnace. After each treatment, the H_3PW is transported immediately to a dry box and stored under nitrogen.

Samples of H_3PW were weighed and transferred to a vacuum insulated calorimetric cell, containing a stir bar. Since H_3PW is very hygroscopic, these weightings and transfers were done in a dry box. For each titration, 100 ml of acetonitrile is added to the cell. A calibrated syringe, filled with a solution of known concentration of base (e.g., 0.2 M), is inserted into the cell along with a thermistor and a heater coil. These operations were carried out in an inert atmosphere glove bag. The thermistor and heater coil were connected to an electronic circuit bridge, and a computer [59]. The thermistor was calibrated with the heater coil prior or immediately after each titration. A set of 12 calibrated brass stops were used for the syringe injections. After each injection the heat evolved from reaction of the base and H_3PW is measured. The heat from adding the base solution to the solvent is negligible. Each titration was repeated three times for each base studied. Titrations of acids other than H_3PW with pyridine were performed twice.

Spectral Analysis

A Perkin-Elmer Lambda 6 UV-vis spectrophotometer and suprasil quartz cells of 0.1 cm pathlength were employed. A Nicolet Model 5PC FTIR spectrophotometer and a NaCl cell of 0.1 mm pathlength or mull in a NaCl cell were employed.

Thermal Analysis

The DSC and TG analyses were carried out in a TA DuPont 2000 instrument (module 2910 DSC and module 2950 TGA) at rate of 10 $^{\circ}$C min^{-1}. Isothermal TGA's were run for 2 hours. The samples of H_3PW were taken directly from the bottle.

Calculations

The heat liberated in the reaction of strong bases with H_3PW in acetonitrile can be calculated according to the following set of equilibria, giving the respective thermodynamic parameters:

$$H_3PW + B \rightleftharpoons H_2PW^- + BH^+; \qquad K_1, \quad \Delta H_1 \tag{2.3}$$

$$H_2PW^- + B \rightleftharpoons HPW^{2-} + BH^+; \qquad K_2, \quad \Delta H_2 \tag{2.4}$$

$$HPW^{2-} + B \rightleftharpoons PW^{3-} + BH^+; \qquad K_3, \quad \Delta H_3 \tag{2.5}$$

For ease of representation, the acetonitriles attached to the protons of the H_3PW species are not shown. The equilibrium constants are represented by the expressions:

$$K_1 = \frac{[H_2PW^-][BH^+]}{[H_3PW][B]} \ (2.6) \qquad K_2 = \frac{[HPW^{2-}][BH^+]}{[H_2PW^-][B]} \ (2.7) \qquad K_3 = \frac{[PW^{3-}][BH^+]}{[HPW^{2-}][B]} \ (2.8)$$

where the brackets indicate concentration of the species (mol L^{-1}). The ionic strength for all solutions in this work was constant ($1.39x10^{-3}$ mol L^{-1}). Therefore, the activity coefficients are kept approximately constants and the concentration equilibrium constants calculated here are close to the true thermodynamic equilibrium constants. Transforming stepwise equilibrium constant expressions (Equations 2.6 to 2.8) to global formation constants, the following equations are obtained:

$$\beta_1 = K_1 = \frac{[H_2PW^-][BH^+]}{[H_3PW][B]} \tag{2.9}$$

$$\beta_2 = K_1K_2 = \frac{[HPW^{2-}][BH^+]^2}{[H_3PW][B]^2} \tag{2.10}$$

$$\beta_3 = K_1K_2K_3 = \frac{[PW^{3-}][BH^+]^3}{[H_3PW][B]^3} \tag{2.11}$$

The mass balance for this system is described by the total concentration (mol L^{-1}) of acid ($[H_3PW]_T$) and base ($[B]_T$):

$$[H_3PW]_T = [H_3PW] + [H_2PW^-] + [HPW^{2-}] + [PW^{3-}] \tag{2.12}$$

$$[B]_T = [B] + [BH^+] \tag{2.13}$$

Substituting the expressions for concentrations of H_2PW^-, HPW^{2-}, and PW^{3-} (based on Equations 2.9 - 2.11) in Equation (2.12), yields:

$$[H_3PW]_T = [H_3PW] + \beta_2[H_3PW]\frac{[B]^2}{[BH^+]^2} + \beta_1[H_3PW]\frac{[B]}{[BH^+]} + \beta_3[H_3PW]\frac{[B]^3}{[BH^+]^3} \tag{2.14}$$

$$[H_3PW]_T = [H_3PW](1 + \beta_1\frac{[B]}{[BH^+]} + \beta_2\frac{[B]^2}{[BH^+]^2} + \beta_3\frac{[B]^3}{[BH^+]^3}) \tag{2.15}$$

$$[H_3PW] = [H_3PW]_T / (1 + \beta_1 \frac{[B]}{[BH^+]} + \beta_2 \frac{[B]^2}{[BH^+]^2} + \beta_3 \frac{[B]^3}{[BH^+]^3}) \qquad (2.16)$$

The total calculated heat evolved (h'_{cal}) from that system, when acid reacts with base, is given by:

$$h'_{cal} = V([H_2PW^-]\Delta H_1^T + [HPW^{2-}]\Delta H_2^T + [PW^{3-}]\Delta H_3^T) \qquad (2.17)$$

where, V is the volume of the titration solution (L), and ΔH_i^T is the global enthalpy of deprotonation of H_3PW i.e., $\Delta H_1^T = \Delta H_1$, $\Delta H_2^T = \Delta H_1 + \Delta H_2$, and $\Delta H_3^T = \Delta H_1 + \Delta H_2 + \Delta H_3$, with ΔH_i being the stepwise formation enthalpy. Substituting the expressions for concentrations of H_2PW^-, HPW^{2-}, and PW^{3-} (based on Equations 2.9 - 2.11) in Equation (2.17), the following equations are obtained:

$$h'_{cal} = V[H_3PW](\beta_1 \frac{[B]}{[BH^+]} \Delta H_1^T + \beta_2 \frac{[B]^2}{[BH^+]^2} \Delta H_2^T + \beta_3 \frac{[B]^3}{[BH^+]^3} \Delta H_3^T) \qquad (2.18)$$

$$[H_3PW] = h'_{cal} / V(\beta_1 \frac{[B]}{[BH^+]} \Delta H_1^T + \beta_2 \frac{[B]^2}{[BH^+]^2} \Delta H_2^T + \beta_3 \frac{[B]^3}{[BH^+]^3} \Delta H_3^T) \qquad (2.19)$$

Equations (2.16) and (2.19) show the relation of free concentration of acid with the equilibrium constants and enthalpies of deprotonation. Setting Equations (2.16) to (2.19) equal to each other, and rearranging them, Equation (2.20) is obtained:

$$h'_{cal} = \frac{[H_3PW]_T V(\beta_1 \frac{[B]}{[BH^+]} \Delta H_1^T + \beta_2 \frac{[B]^2}{[BH^+]^2} \Delta H_2^T + \beta_3 \frac{[B]^3}{[BH^+]^3} \Delta H_3^T)}{(1 + \beta_1 \frac{[B]}{[BH^+]} + \beta_2 \frac{[B]^2}{[BH^+]^2} + \beta_3 \frac{[B]^3}{[BH^+]^3})} \qquad (2.20)$$

Considering $R = [B]/[BH^+]$ as the ratio of free base and protonated base concentrations (mol L^{-1}), the simplified expression of the calculated heat is given by Equation (2.21):

$$h'_{cal} = [H_3PW]_T V \frac{(\beta_1 R \Delta H_1{}^T + \beta_2 R^2 \Delta H_2{}^T + \beta_3 R^3 \Delta H_3{}^T)}{(1 + \beta_1 R + \beta_2 R^2 + \beta_3 R^3)} \quad (2.21)$$

A computer program was written to solve these equilibria in non aqueous solution (Appendix). K_1, K_2, K_3, the total concentration of H_3PW, and the total base concentration determine the concentration of all the species in solution using Equations (2.6 - 2.8). The ratio between free base and protonated base is obtained assuming an initial value, which allows the calculation of concentrations for all species. The routine adjusts the concentrations through a mass balance of the protons i.e., the protons on BH^+ must correspond to the ones lost from the initial acid. The calculation is repeated until the values are consistent. Knowing ΔH_1, ΔH_2, and ΔH_3 as well, Equation (2.21) can be solved for h'_{cal}. Actually, the values of the K's and ΔH's are unknown. Using initial estimates of these parameters, an iterative program is used to calculate the final values which give the minimum of the non-weighted sum of squares of the residuals (U) of Equation (2.22) by a non-linear routine.

$$U(\beta_i, \Delta H_i{}^T) = \Sigma (h'_{exp} - h'_{cal})^2 \quad (2.22)$$

The method of steepest descent is employed to find the best values of β_i and ΔH_i. The first derivatives, $\delta U/\delta\beta_i$ and $\delta U/\delta H_i$ are approximated as $\Delta U/\Delta\beta_i$ and $\Delta U/\Delta H_i$ which are easily calculated to give h'_{cal} (calculated heat). Using h'_{cal} and h'_{exp} (experimental heat), the minimum of the function (Equation 2.22) is obtained (e.g., a sample data fit is shown in Table 2-3).

In order to evaluate the adequacy of the proposed model, the experimental data were repeated. The residuals (h'_{exp} - h'_{cal}) were randomly distributed about the regression.

A comparison between the dispersion (variance) from the regression and one obtained by replication is made. To measure the dispersion of the experimental points (the external variance, σ^2_{ext}), the sum of squares of the residuals is obtained and divided by the degrees of freedom (number of measured points minus the number of fit parameters). An internal variance (σ^2_{int}) is calculated in a similar manner, but the sum of squares is based on the average of the replicates and the summation is done point to point without adding the heats. Since the heats are added up for analysis purposes, an error associated with each measurement is automatically inserted in each point. The system H_3PW-Pyridine, for instance, shows σ^2_{ext}=1.4903x10^{-4} and σ^2_{int}=1.1405x10^{-4}. Assuming that σ^2_{int} is constant for these calorimetric measurements, and the errors are normally distributed, both variances can be compared by means of an F test. The ratio $\sigma^2_{ext}/\sigma^2_{int}$ gives 1.30. At 10% probability for the F distribution (F= 3.05, $\phi_2 = \phi_1 = 6$) both measures of dispersion are equivalent. This test of the goodness of fit [60], although not completely rigorous in nonlinear modeling, has at least semiquantitative value, and can tell if the model provides a good to fit the data. Applying the F test to all systems gave similar results to the example shown.

Another method to evaluate the standard deviations for the K's and ΔH's uses a variance-covariance matrix of parameters [60], which gives errors as standard deviations. This analysis provides standard deviations that match those obtained by replicated data within ±5% of the reported value.

For all the data in Tables 2-2, 2-4 and 2-5, the values of the parameters are based on averaged data sets of duplicate or triplicate experiments and the errors are based on the standard deviations of the variance-covariance matrix. Since precision exceeds accuracy, interpretations of differences less than ±0.5 kcal mol^{-1} will not be made for $-\Delta H_1$ and less than 1-2 kcal mol^{-1} for ΔH_2 and ΔH_3.

Results and Discussion

Preparing Anhydrous H_3PW

As with any polyprotic oxyacid, drying is complicated by the conversion of dihydroxy functionality that gives rise to the Brönsted acidity to an anhydride with μ-oxo functionality. For heteropoly acids, the anhydride has been shown by gas-solid calorimetry to be a much weaker acid toward ammonia than the anhydrous acid. The hydrated acid is expected to be a weaker acid than the anhydrous acid because of the endothermic displacement of coordinated water. Thus it is critical for acidity and catalytic studies to use the anhydrous acid. In view of the conflicting reports in the literature [61-63] on the influence of pretreatment on acidity and reactivity, we decided to determine the optimal drying procedure to produce the strongest acid. The total heat released, equilibrium constants and enthalpies from calorimetric titrations with pyridine are given in Table 2-2 for samples prepared by different thermal treatments.

The samples in Table 2-2 were analyzed by UV-vis, FTIR, XRD, DSC and TGA. No differences in the UV-vis [64] or FTIR [48-51] spectra of acetonitrile solutions were observed confirming that the Keggin structure is intact in all samples. Powder XRD results are identical except for the sample calcined at 400 °C where a slight broadening of

Table 2-2. Results of Calorimetric Titrations (25±1°C) with Pyridine for Different H_3PW Samples in CH_3CN Solvent.

Sample[a] (°C/hs)	Total Heat Evolved (cal)	$-\Delta H_i$ [b] (i=1, 2, 3) (kcal mol^{-1})	K_i [b] (i=1, 2, 3)
128 / 4	6.187	19.8	$1.6x10^3$
		15.3	$1.1x10^2$
		13.9	$2.4x10^1$
128 / 8	6.365	20.5	$3.6x10^2$
		9.4	$6.5x10^1$
		20.0	$5.2x10^1$
162 / 1	5.548	18.5	$4.6x10^2$
		9.2	$1.2x10^2$
		15.3	$4.2x10^1$
162 / 2	5.768	19.9	$2.2x10^3$
		9.3	$1.2x10^3$
		16.7	$2.9x10^1$
162 / 4	6.647	21.0	$2.2x10^3$
		11.8	$2.4x10^2$
		18.6	$4.2x10^1$
200 / 2	5.511	18.6	$2.2x10^3$
		10.1	$5.8x10^2$
		17.5	9.2
300 / 2	4.338	17.7	$4.5x10^4$
		11.1	$3.2x10^3$
		3.0	$1.5x10^2$
300 / 16	3.827	11.4	$4.8x10^3$
		7.7	$8.5x10^2$
		9.0	$5.5x10^1$
400 / 2	1.307	8.2	$1.5x10^3$
		0.3	$6.4x10^2$
		3.3	$3.2x10^{-1}$

Table 2-2. continued

a. Samples of H_3PW treated at different Temperature (°C) / Time (hs). Samples at 128 and 162°C were evacuated and those at 200, 300, and 400°C were calcined under air flow. Two samples of $H_3PW \cdot 16H_2O$ (as purchased) were titrated with pyridine solution providing -12.9 and -5.4 kcal mol^{-1} for ΔH_1 and ΔH_2 with errors of 3% and 6% respectively, and 6.8x10^3 and 1.6x10^3 for K_1 and K_2 with errors of 10% and 27% respectively.

b. Based on variance-covariance matrix analysis, standard deviation are 1%, 2% and 5% of ΔH_1, ΔH_2, and ΔH_3, and 5%, 20%, and 25% of K_1, K_2 and K_3 respectively. Conclusions are based on a error estimate of ±0.5 kcal mol^{-1} for ΔH_1 and ±1-2 kcal mol^{-1} for ΔH_2, and ΔH_3.

the lines and loss of intensity occurs. Similar XRD results [46] are reported for a sample of H_3PW calcined at 400°C.

DSC and TG analyses give two endothermic peaks, corresponding to loss of water at 92 and 215 °C, and a third peak at about 550 °C (Figure 2-2). After the initial weight loss, isothermal TGA's at 150, 200, 300, and 400 °C for 2 to 4 hours do not show any further change (Figure 2-3). A DTA study [44] of H_3PW reports decomposition at about 590 °C forming WO_3. TGA [46] and TPD [45] studies claim that decomposition of H_3PW results from mass loss of phosphorous, as P_2O_5, occurring at 500 °C depending on the duration of heating. Traces of green and yellow powder are seen on the surface of H_3PW for 300/2, 300/16, and 400/2, (°C/hr), samples. The color changes suggests formation of anhydrous WO_3 (yellow) and reduced W_nO_{3n-1} (blue) which accounts for the green color. When WO_3 is heated in vacuum, reduction occurs forming a variety of tungsten blue materials [1].

The results of Table 2-2 clearly show that the sample treated at 162°C for 4 hours (162/4) under vacuum is the strongest acid, which should be the anhydrous acid. Reported gas phase calorimetry and TGA results also indicate that this treatment will produce the anhydrous acid [42]. The FTIR of this 162/4 sample compared to the purchased sample of $H_3PW \cdot 16H_2O$, Figure 2-4, shows the absence of the characteristic broad absorption band for water around 3500 cm^{-1}.

In order to substantiate that 162/4 produces the anhydrous acid with the data in Table 2-2, a calorimetric titration of 162/4 with water as base in CH_3CN was carried out giving a $-\Delta H_1$ of 4.2 kcal mol^{-1} and $K_1 = 1.0 \times 10^3$. The large K indicates that any excess

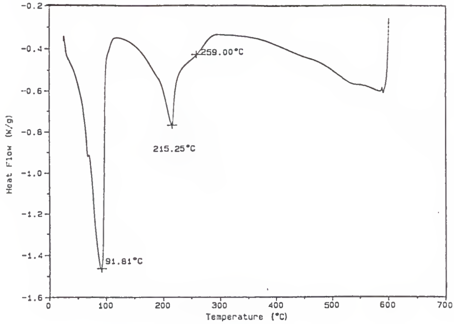

(a)

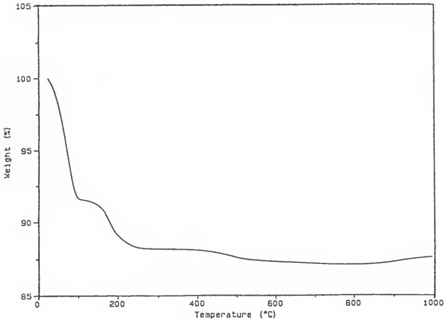

(b)

Figure 2-2. Thermal Analysis of $H_3PW_{12}O_{40}$ by: (a) DSC in air/He at 10 °C min^{-1}; (b) TGA in air at 10 °C min^{-1}.

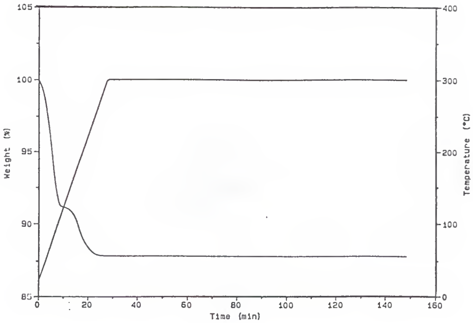

Figure 2-3. Isothermal TGA (300 °C) of $H_3PW_{12}O_{40}$ in air at 10 °C min^{-1}.

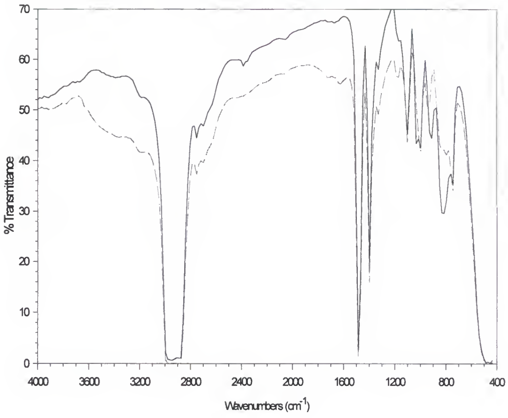

Figure 2-4. FTIR of H_3PW in Mineral Oil. (—) H_3PW Treated at 162 °C for 4 hs under Vacuum. (---) H_3PW Taken from the Bottle ($16H_2O$). Absorption Bands of Mineral Oil (Aldrich, dried on 3A Molecular Sieves) are on the Typical Range of 2800-3000 cm^{-1} and 1400-1600 cm^{-1}. The Preparation of the Mull was Made in a Dry Box Filled with Nitrogen.

water in the samples of Table 2-2 would be coordinated to H_3PW. Since the $-\Delta H_1$ values for the vacuum dried samples, 128/4, 162/1 and 162/2 (°C/hr) are smaller than 162/4 by an amount less than the 4 kcal mol^{-1} found for the monohydrate, we can conclude that 128/4, 162/1, and 162/2 are partially wet. The sample 128/8 is almost as dry as 162/4 but the total heat evolved indicates a very small amount of water remains. Flowing air is not as efficient as vacuum for drying as shown by the 200/2 versus the 162/2 (°C/hr) result. Since the flowing air samples 300/2, 300/16 and 400/2 (°C/hr) are expected to have less water than 200/2, the lower enthalpies suggest some degree of reduction and anhydride formation consistent with the observed color changes on the surface of the solid. A large decrease in the total heat evolved for titration of sample 400/2 is consistent with the decreased acidity reported in the gas-solid calorimetric results [42] and illustrates the insensitivity of the XRD pattern to the changes occurring on drying. The calorimetric results in Table 2-2 would mitigate against use of H_3PW as an acid catalyst at or above 300°C.

The hydrated $H_3PW\cdot16H_2O$ was also titrated with pyridine giving a $-\Delta H_1$ of 12.9 kcal mol^{-1}. Subtracting $-\Delta H_1$ for the reaction of H_3PW with water (4.2 kcal mol^{-1}) from 21.0 kcal mol^{-1} for the pyridine reaction with anhydrous H_3PW produces $-\Delta H_1 = 16.8$ for the reaction of the monohydrate with pyridine. Solution species of higher water molecularity in $H_3PW\cdot16H_2O$ than in the monohydrate lead to a more endothermic water displacement. Other complications from the presence of water are evident. With all bases used in this study, properly dried H_3PW leads to the enthalpy order of $-\Delta H_1 > -\Delta H_2 < -\Delta H_3$ (vide Table 2-4). In some instances, this is not observed in Table 2-2. Since the reactions involved in steps 2 and 3 for wet samples are not known, the possible incorrect formulation of the equilibria precludes a more detailed analysis of the results in Table 2-2. These experiments accomplish their main objective by showing that the treatment 162/4 produces a sample that evolves the largest total heat, gives the highest $-\Delta H_1$ comparable to that of CF_3SO_3H (vide infra), is driest and most likely is the anhydrous acid. Unless noted otherwise, all of the results reported in the next sections of this study were obtained on H_3PW samples dried under vacuum at 162 °C for 4 hours.

Solution Species

The reaction of H_3PW in CH_3CN with various bases was monitored by UV-vis spectra. The absorption maximum for H_3PW in CH_3CN occurs at $\lambda = 266$ nm. The spectra are essentially unchanged when excess of most of the bases over that required for neutralization of the three protons is added to H_3PW in acetonitrile (e.g., Figure 2-5). Quinuclidine is an exception to this behavior. With this base, the spectra are essentially unchanged up to a 1:1 ratio of base to H_3PW. A slight decrease in absorbance but no band shift is observed up to a 2:1 ratio. At the ratios of quinuclidine to H_3PW greater than 2:1, a band shift from 266 nm to 251 nm is observed leading to an isosbestic point at 255 nm (Figure 2-6). Different spectral behavior of H_3PW in different organic solvents has been noted [65-68]. ^{1}H, ^{17}O, ^{31}P, and ^{183}W NMR and electronic absorption spectroscopy [67], of complexes of $[DP_2H^+]_3[PW^{3-}]$ (where DP = N-methylpyrrolidinone (NMP), 1,1,3,3,-tetramethylurea (TMU), and 1,3-dimethyl-2-imidazolidinone (DMEU)) attribute the changes to reversible intermolecular electron donor-acceptor complexes in

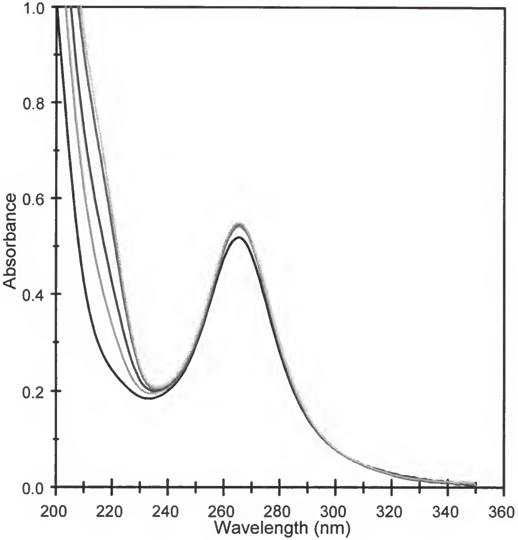

Figure 2-5. Spectra of Absorption H_3PW with N-methylimidazole in CH_3CN (b = 0.1 cm). The Concentration of H_3PW is 1.05 $\times 10^{-4}$ mol L^{-1} (the Same for All Solutions). From Bottom to Top (λ = 230 nm), Concentration of N-methylimidazole in the Solutions are: 0; 2.17, 4.34, 6.51, and 8.68 $\times 10^{-4}$ mol L^{-1} Respectively.

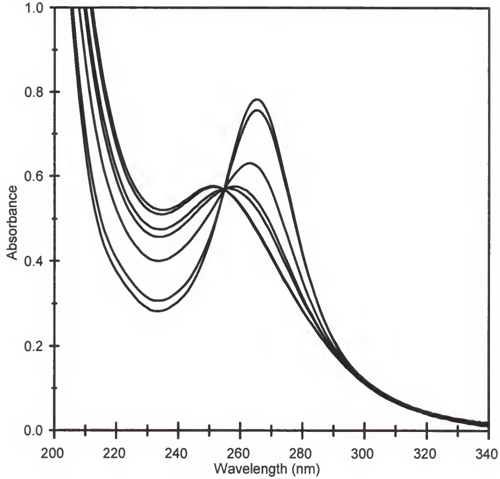

Figure 2-6. Spectra of Absorption H_3PW with Quinuclidine in CH_3CN (b = 0.1 cm). The Concentration of H_3PW is 1.57 $x10^{-4}$ mol L^{-1} (for All Solutions). From Top to Bottom (λ = 230 nm), Concentration of Quinuclidine in the Solutions are Respectively: 1.67; 3.37, 5.05, 6.75, 8.37, 10.12, and 11.82 $x10^{-4}$ mol L^{-1}.

solution. The cause of the change with quinuclidine was not pursued in view of predominant interest in the 1:1 species in this work, vide infra.

Calorimetry

The measured amounts of heat (h'_{exp}) evolved from the calorimetric titration of H_3PW with pyridine in acetonitrile are shown in Table 2-3 along with the calculated values, h'_{cal}, from the data fit to a three step equilibrium. Attempts to fit the data to a one step equilibrium (three protons reacting with the same strength) or to a two step equilibrium (one different and two equivalent) lead to larger sums of the squares of the deviations and meaningless parameters.

The values of K_1, K_2 and K_3 for the pyridine reaction are 2100, 240, and 41 respectively. The corresponding enthalpies,$-\Delta H_1$,$-\Delta H_2$, and$-\Delta H_3$, are 21.0, 11.8 and 18.6 kcal mol^{-1}. The thermodynamic data in Table 2-4 reveal a very interesting pattern and each step will be interpreted separately.

The first step of the equilibria existing in solutions of H_3PW in CH_3CN is given by Equation (2.23):

$$CH_3CN + (CH_3CN)_3H_3PW \rightleftharpoons (CH_3CN)_2H^+ + (CH_3CN)_2H_2PW^- \qquad (2.23)$$

To simplify the discussion, coordination number two is assumed for the proton, anionic H_2PW^- species will be assumed to have two acetonitriles coordinated, and no attempt will be made to distinguish intimate ion-pairing from hydrogen bonding, i.e., species I and II of Equation (2.1). The position of the equilibrium in Equation (2.23) is unknown but the pK_a of perchloric acid in acetonitrile [69] is 2 and the pK_{a1} for H_3PW in acetone is 1.6.

Table 2-3. Heat Evolved (h'_{exp})^{a} upon Addition of Pyridine to H_3PW in CH_3CN Solvent and Calculated (h'_{cal}) from Equilibrium Analysis. $[H_3PW]_T = 1.39 \times 10^{-3}$M.

Base Added x 10^4 (M)	h'_{exp} (cal)	h'_{cal} (cal)
2.43	0.499	0.504
4.54	0.932	0.936
6.74	1.377	1.372
9.05	1.827	1.813
13.6	2.624	2.621
18.1	3.325	3.341
23.5	4.146	4.147
27.1	4.690	4.683
31.7	5.374	5.372
36.1	6.011	6.012
40.6	6.458	6.459
45.2	6.647	6.648

a. The base added and h'_{exp} values are summed giving the total base and the total heat after each addition i.e., 4.54×10^{-4} M and 0.932 calories are the sums for the first two additions.

Table 2-4. Thermodynamic Parameters[a] for H_3PW-Base[b] (25±1°C) in CH_3CN Solvent.

	Qi	Py	M-Im	Tep	Qu[c]	H_2O	DMA	THF
K_1	$4.8x10^2$ (±9.5)	$2.1x10^3$ (±4.0)	$1.5x10^4$ ($\pm1.8x10^2$)	$3.5x10^4$ ($\pm7.4x10^2$)	$1.1x10^6$ ($\pm1.4x10^3$)	$1.0x10^3$ (±0.5)	$6.1x10^6$ ($\pm5.5x10^5$)	$9.2x10^1$ (±1.2)
K_2	$2.6x10^2$ ($\pm3.9x10^1$)	$2.4x10^2$ (±3.4)	$1.1x10^4$ ($\pm4.8x10^3$)	$4.5x10^3$ ($\pm1.7x10^3$)	$9.2x10^5$ ($\pm5.2x10^5$)	$3.8x10^2$ ($\pm6.8x10^1$)	$2.4x10^6$ ($\pm3.1x10^5$)	$5.6x10^1$ ($\pm1.7x10^1$)
K_3	$5.2x10^1$ ($\pm1.3x10^1$)	$4.1x10^1$ (±5.8)	$6.5x10^1$ (±7.1)	$7.5x10^2$ ($\pm9.9x10^1$)	$1.3x10^2$ ($\pm4.6x10^1$)	7.1 (±0.7)	4.7 (±2.6)	
$-\Delta H_1$	18.1 (±0.4)	21.0 (±0.2)	29.5 (±0.4)	32.2 (±0.7)	42.6 (±2.1)	4.2 (±1.0)	13.2 (±2.0)	11.4 (±0.5)
$-\Delta H_2$	7.1 (±0.2)	11.8 (±0.3)	16.3 (±0.5)	15.3 (±0.3)	18.6 (±0.4)	0.9 (±0.5)	3.4 (±0.5)	0.3 (±0.1)
$-\Delta H_3$	15.9 (±0.7)	18.6 (±0.5)	23.4 (±0.8)	18.0 (±0.8)	26.0 (±1.1)	2.1 (±2.6)	12.0 (±1.9)	
$-\Delta G_1$	3.7	4.5	5.7	6.2	8.3	4.1	9.3	2.7
$-\Delta G_2$	3.3	3.2	5.6	5.0	8.1	3.5	8.7	2.4
$-\Delta G_3$	2.3	2.2	2.5	3.9	2.9	1.2	0.9	
$-\Delta S_1$	48.3	55.1	79.8	87.1	115.0	0.3	13.3	29.2
$-\Delta S_2$	12.9	28.8	36.0	34.7	35.1	-8.8	-18.0	-7.0
$-\Delta S_3$	45.4	55.1	70.0	47.3	77.4	3.0	37.2	

Table 2-4. continued

a.The units for ΔH_i and ΔG_i, and are kcal mol^{-1}. The unit of ΔS_i is cal Kelvin^{-1} mole^{-1}.
b. Bases are listed as Quinoline (Qi), Pyridine (Py), N-methylimidazole (M-im), Triethylphosphine (Tep), Quinuclidine (Qu), N,N-Dimethylacetamide (DMA), and Tetrahydrofuran (THF). The errors are standard deviations calculated by variance-covariance matrix analysis. Deviations for ΔH_2 and ΔH_3 reflect cumulative errors on the measured heat values (h'_{exp}). Since the equilibrium constants are calculated from h'_{exp} values, small errors on these measurements cause large errors on equilibrium constants. Our main criterion for acidity is the enthalpy and these are very well determined.

c. UV-vis spectral changes indicate this data may reflect a more complex reaction.

Slight ionization, Equation (2.23), is expected in acetonitrile from these comparisons and $-\Delta H_1$ for the reaction with pyridine corresponds predominantly to displacement of $(CH_3CN)_2H_2PW^-$ to form $C_5H_5NHCH_3CN^+$ (Equation 2.24, more accurate representation of Equation 2.3). Both basicity and solvent polarity are needed to dissociate the anion or form a solvent separated ion-pair [58].

$$(CH_3CN)_3H_3PW + B \rightleftharpoons BHCH_3CN^+ + (CH_3CN)_2H_2PW^- \quad (2.24)$$

It must be take into account that Equation (2.23) as well as the second and the third proton dissociation steps of H_3PW should be combined with the expression for the protonation of the base ($B + (CH_3CN)_2H^+ \rightleftharpoons BHCH_3CN^+ + CH_3CN$) in order to deduce the expressions for the equilibrium constant defined in Equations (2.3) to (2.5).

The second and third ionization steps for H_3PW in acetonitrile proceed to a very small extent and are given in Equations (2.25) and (2.26).

$$CH_3CN + (CH_3CN)_2H_2PW^- \rightleftharpoons (CH_3CN)_2H^+ + (CH_3CN)HPW^{2-} \quad (2.25)$$

$$CH_3CN + (CH_3CN)HPW^{2-} \rightleftharpoons (CH_3CN)_2H^+ + PW^{3-} \quad (2.26)$$

Reaction of the second proton of H_3PW with pyridine involves reaction of the species in Equation (2.25). The lower $-\Delta H_2$ than $-\Delta H_1$ for all bases studied (e.g., 11.8 vs. 21.0 kcal mol^{-1} for pyridine) clearly shows that step 2 involves a weaker acid than step 1. Had the reactions in Equations (2.23) and (2.25) gone to completion when H_3PW is added to CH_3CN, $-\Delta H_2$ would equal $-\Delta H_1$ because the titration reaction would involve displacement of CH_3CN from $(CH_3CN)_2H^+$ (Equation 2.2) in both instances. This resolves the literature differences by showing that the first two protons removed from H_3PW are not comparable in acidity. Step 2 predominantly involves titration of

$(CH_3CN)_2H_2PW^-$, shown in Equation (2.25), giving a smaller $-\Delta H_2$ than $-\Delta H_1$ for all bases studied. The question then arises, why is a large K_2 and a small $-\Delta H_2$ observed for all bases studied, (Table 2-4)? When base reacts with $(CH_3CN)_2H_2PW^-$, the endothermic loss of CH_3CN molecules could occur to form HPW^{2-} as shown in Equation (2.27).

$$(CH_3CN)_2H_2PW^- + B \rightleftharpoons BHCH_3CN^+ + HPW^{2-} + CH_3CN \qquad (2.27)$$

With acetonitrile being bound less completely or not at all to the weaker acid HPW^{2-}, ΔS_2 increases and $-\Delta H_2$ decreases for the second step, Equation (2.27).

Equation (2.27), a more accurate representation of Equation (2.4), also accounts for the smaller K and larger $-\Delta H$ observed for step 3. Since endothermic CH_3CN displacement is not involved in step 3, a larger $-\Delta H$ and $-\Delta S$ results than for step 2. Equation (2.28) best represents the equilibrium given in Equation (2.5) for the third step.

$$CH_3CN + B + HPW^{2-} \rightleftharpoons BHCH_3CN^+ + PW^{3-} \qquad (2.28)$$

Note that in contrast to step 1 where one pyridine coordinates, there is an enthalpy contribution from one molecule of pyridine and one of acetonitrile coordinating to the displaced proton in step 3. With weaker donors, step 3 could involve formation of a hydrogen bonded adduct instead of PW^{3-} and the equilibria would be incorrectly formulated in Equation (2.5) of our analysis. Both steps 2 and 3 may be more complicated than shown above because of reaction of $BHCH_3CN^+$ with added base to form B_2H^+ instead of or in addition to the reactions in Equations (2.27) and (2.28). Complexes of heteropoly acids with organic molecules with formula $[(B_2H^+)_3][PX^{3-}]$ (X = Mo, W) have been prepared [65-68]. X-ray studies of these complexes show that the B_2H^+ units do not interact with the polyoxoanions. Spectral studies [65-68] also suggest that the structure of these complexes in solution are similar to those in the solid state. Because of the complications from competing reactions and extents of CH_3CN displacement, our focus will be on step 1 for acidity comparisons and no further interpretation of steps 2 and 3 will be offered. Clearly, our analysis has accomplished the primary objective by demonstrating that the three protons of H_3PW have very different strengths.

Reactions of H_3PW with Other Bases

Calorimetric titrations were carried out using the bases quinoline (Qi); N-methylimidazole (M-Im); quinuclidine (Qu); triethylphosphine (Tep); tetrahydrofuran (THF); water; N,N-dimethylacetamide (DMA); and dimethylsulfoxide (DMSO). Figure 2-7 shows the calorimetric isotherms for all bases titrated. The reactions described above for pyridine explain the consistent pattern of $K_1 > K_2 > K_3$ and $-\Delta H_1 > -\Delta H_3 > -\Delta H_2$ for all bases. For THF, the total heat evolved is 1.610 calories, and the exotherm virtually stops when base is added above a 2:1 mol ratio of THF to H_3PW. Therefore, K_3 and ΔH_3 can not be determined in CH_3CN with these experimental conditions, and the data are analyzed with a two step equilibrium. When the experimental heats (h'_{exp}) from the titration curves of DMSO are analyzed with a three step equilibrium, meaningless equilibrium constants and enthalpies result. A reasonable fit is obtained with a 2:1 model when base additions up to a 2:1 mole ratio of DMSO to H_3PW are used. This limited data is fit to a two step equilibrium giving values of $K_1 = 1.6$ (±0.6), $K_2 = 6.6\text{x}10^{-2}$ (±$4.2\text{x}10^{-2}$), $-\Delta H_1 = 22.5$ (±0.3), and $-\Delta H_2 = 9.2$ (±4.8) kcal mol^{-1} respectively.

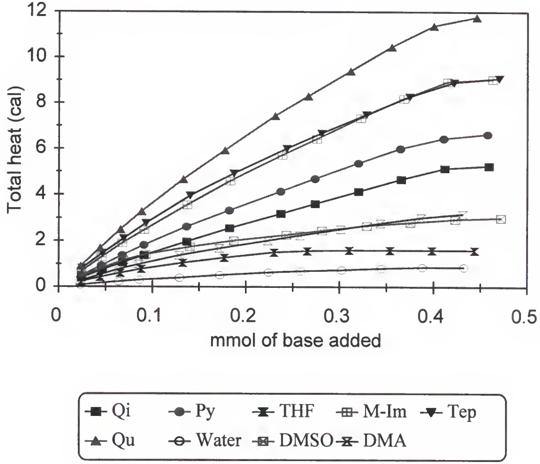

Figure 2-7. Isotherms of the Calorimetric Titrations of $H_3PW_{12}O_{40}$ with Bases. The Bases are: Quinoline (Qi), Pyridine (Py), Tetrahydrofuran (THF), N-methylimidazole (M-Im), Triethylphosphine (Tep), Quinuclidine (Qu), Dimethyl sulfoxide (DMSO), and N,N-dimethylacetamide (DMA).

Figure 2-8 shows an excellent linear relation of log K_1 to $-\Delta H_1$ for all bases except DMA, water and DMSO. DMA and water lie above the line while DMSO falls below. DMSO and DMA also show a poor correlation of $-\Delta H_1$ to the ECW model. Discussion of the complications encountered with these donors and limitations on the interpretation of these enthalpies will be treated in the section on the ECW analysis. The large experimental errors for K_2 and the small range of K_3 values preclude meaningful log K vs. $-\Delta H$ plots for steps two and three.

Enthalpy Analysis with the ECW Model

The ECW approach has been successfully employed [54-56] to correlate many neutral base neutral acceptor adduct formation enthalpies to the equation:

$$-\Delta H = E_AE_B + C_AC_B + W \tag{2.29}$$

E_AE_B and C_AC_B describe electrostatic and covalent contributions for the donor (B)-acceptor (A) reaction. The W term is zero for simple donor-acceptor adduct reactions in poorly solvating media, but for a more complex reaction, it incorporates any constant contributions of a particular acid that is independent of the base it reacts with. Equation (2.29) has, for the most part, been applied to 1:1 adduct formation enthalpies. Recently, a successful correlation of the enthalpies of reaction of CF_3SO_3H with various bases [70] to form an ion-pair in dicloroethane has been reported [71]. This encouraged us to attempt a correlation of the $-\Delta H_1$ values for the ionic products of the reaction of a Brönsted acid with the bases in Table 2-4. The result is an excellent data fit to Equation (2.29) shown in Table 2-5 for most of the bases studied giving $E_A^* = 2.56 \pm 0.23$, $C_A^* = 7.38 \pm 0.07$, and

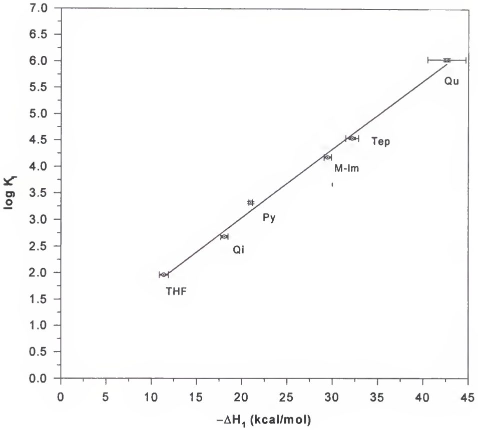

Figure 2-8. Log K_1 versus $-\Delta H_1$ (kcal mol^{-1}) for the Reaction of H_3PW with Various Bases in CH_3CN Solvent. Bases are: Quinuclidine (Qu), Triethylphosphine (Tep), N-methylimidazole (M-im), Pyridine (Py), Quinoline (Qi), and Tetrahydrofuran (THF) respectively.

Table 2-5. Results of ECW Fits for Reactions of H_3PW - Bases in CH_3CN Solvent.[a]

Base	C_B/E_B	$-\Delta H_{exp}$	$-\Delta H_{ECW}$[b]
Pyridine	1.99	21.0	21.3
Quinoline	1.27	18.1	17.8
N-methylimidazole	4.24	29.5	29.9
THF	1.33	11.4	10.9
Quinuclidine	8.40	42.6	42.2
Triethylphosphine	19.75	32.2	32.1
Acetonitrile	0.43	0.0	0.07

a. Unit for ΔH is kcal mol^{-1}.

b. Calculated with 2.56 (±0.22) E_B + 7.38 (±0.07) C_B - 9.36 (±0.0). Values of E_B and C_B for the bases listed above can be obtained in reference [56]. Parameters for triethylphosphine are $E_B = 0.28$, $C_B = 5.53$.

W = -9.36. The E_A^* and C_A^* parameters characterize the acceptor properties of CH_3CNH^+ in acetonitrile. The W value incorporates constant net solvation energies of products and reactants and the endothermic enthalpy of dissociation of the anion from $(CH_3CN)_3H_3PW$.

The E_A^* and C_A^* values of 2.56 and 7.38 for CH_3CNH^+ compared to the reported value of E_A^* and C_A^* of 4.51 and 5.70 for CF_3SO_3H in dichloroethane suggest that the former is more covalent and much less electrostatic than CF_3SO_3H. With different C_A^*/E_A^* ratios for the different acids involved, the enthalpies of reaction for a series of different bases reacting with H_3PW in CH_3CN and CF_3SO_3H in 1,2-dichloroethane are not expected to plot up linearly.

The fit of the H_3PW enthalpies to ECW is an important result for it indicates that the same base properties that correlate neutral donor-acceptor reactions in poorly solvating solvents also determine the basicity order when ionic products are formed from Brönsted acids in acetonitrile. The acid concentration should be held constant to establish basicity orders because variation in the extent of ion-pairing with acid concentration will influence the enthalpy measured. The ECW fit shows that enthalpy contribution from the basicity and polarity of acetonitrile solvent in facilitating ionization of HX is either a constant factor or is linear with basicity. As a result, with the acid concentration constant, $-\Delta H$ for reaction of a base in this solvent provides a measure of the donor strength and substantiates earlier discussion on the selection of acetonitrile as a solvent for studying Brönsted acidity.

The enthalpy data for DMSO, H_2O and DMA do not obey the ECW correlation and reveal some interesting conclusions regarding reactivity. The DMSO reaction could involve bonding to sulfur which is expected for acceptors with a large C_A^*/E_A^*. With the E_B and C_B values reported [56] for DMSO referring to oxygen coordination, even an equilibrium mixture of S and O coordination would give an average $-\Delta H$ larger than that predicted by ECW. Unfortunately overlap of the S=O stretching frequency with H_3PW and CH_3CN bands precludes testing this explanation. Water was not included in the ECW analysis because E_B and C_B parameters are only available for the gas phase monomer and these cannot be used for water aggregates in solution. Solutions of heteropoly acids in DMA are reported to be photochemically redox active [65-68]. The solution resulting from our titration of H_3PW with DMA has a bluish tint and we attribute the discrepancy with ECW to enthalpy contributions from redox reactions.

The ECW analysis is not only a correlation and predictive tool but can provide thermodynamic data for reactivity that cannot be measured directly. Using E_A^* and C_A^* with E_B and C_B for CH_3CN, the enthalpy of coordinating CH_3CN to $(CH_3CN)H^+$ in acetonitrile is calculated to be 9.4 kcal mol^{-1}. Comparing this quantity to the W value of 9.4 indicates that $(CH_3CN)H^+$ coordinates acetonitrile and $(CH_3CN)_2H_2PW^-$ with equal strength, so displacement of the anion by acetonitrile would have a zero enthalpy contribution. Adding W of 9.4 kcal mol^{-1} to $-\Delta H_1$ measured in acetonitrile, gives $-\Delta H$ for reactions of bases with CH_3CNH^+ as an acid in acetonitrile.

An Acidity Scale in CH_3CN toward Pyridine

In order to provide a comparison of relative acidity, the enthalpies of reactions of a series of other acids with pyridine were measured in CH_3CN. Results of the calculated K's and ΔH's are presented in Table 2-6. Since the position of the ionic equilibria in Equation (2.1) will be concentration dependent, an acid concentration of 1.39×10^{-3} M is used in all experiments and is a defined quantity for our acetonitrile acidity scale. Because of variation in ion-pairing, differences less than ±0.5 kcal mol^{-1} are not considered significant. The $-\Delta H_1$ values furnish an acidity order :

$H_3PW > CF_3SO_3H > p\text{-}CH_3C_6H_4SO_3H \sim H_2SO_4$ (97%) $>> CF_3COOH >> ClC_6H_4COOH$.

A plot of log K_1 vs. $-\Delta H_1$ for the acids studied in Table 2-6 is shown in Figure 2-9. The linear free energy-enthalpy relation supports a similar reaction type for all acids. H_3PW is the strongest acid that can be measured with this scale because an acid that is completely ionized in acetonitrile will exist as $(CH_3CN)_2H^+$ and it was shown earlier that acetonitrile and $(CH_3CN)_2H_2PW^-$ have similar enthalpies of displacement from $(CH_3CN)H^+$.

An enthalpy for the reaction of pyridine with $p\text{-}CH_3C_6H_4SO_3H$ in acetonitrile is reported [72]. At low base concentration, a -ΔH of 18.3 kcal mol^{-1} results from a limiting reagent estimate in good agreement with our value of 18.7. When the limiting reagent approach is used with a ten fold excess of acid an enthalpy of 18.6 kcal mol^{-1} is reported [72]. The -ΔH is reported to decreases with base concentration and this is attributed to a base dependent heat of reaction. Our magnitude for K shows this behavior is expected from incomplete protonation of all the base added as a 1:1 ratio is approached and the true enthalpy of product formation is base concentration independent.

Table 2-6. Enthalpies (kcal mol^{-1}) and Equilibrium Constants (25±1°C) for the Reaction of Pyridine with Various Acids[a] in CH_3CN Solvent. $[Acid]_T = 1.39 \times 10^{-3}$ M.

Acid	K_1	K_2	K_3	$-\Delta H_1$	$-\Delta H_2$	$-\Delta H_3$
H_3PW	2.1×10^3 $(\pm 4.0 \times 10^1)$	2.4×10^2 $(\pm 3.4 \times 10^1)$	4.1×10^1 (±5.8)	21.0 (±0.2)	11.8 (±0.3)	18.6 (±0.5)
H_2SO_4[b]	1.5×10^2 $(\pm 2.0 \times 10^1)$	7.9 (±5.8)		18.4 (±0.2)	0.2 (±0.5)	
CF_3SO_3H	6.1×10^2 $(\pm 5.0 \times 10^1)$			19.9 (±0.2)		
$CH_3C_6H_4SO_3H$	2.1×10^2 $(\pm 5.5 \times 10^1)$			18.7 (±0.2)		
CF_3COOH	2.8×10^1 $(\pm 1.2 \times 10^1)$			14.2 (±1.0)		
ClC_6H_4COOH	2.1×10^{-1} $(\pm 1.0 \times 10^{-1})$			6.5 (±1.9)		

a. Standard deviations are based on variance-covariance matrix analysis.

b. Concentrated sulfuric acid used for preparation of standard solution of H_2SO_4 in acetonitrile was 97% w/w, calculated by standardization.

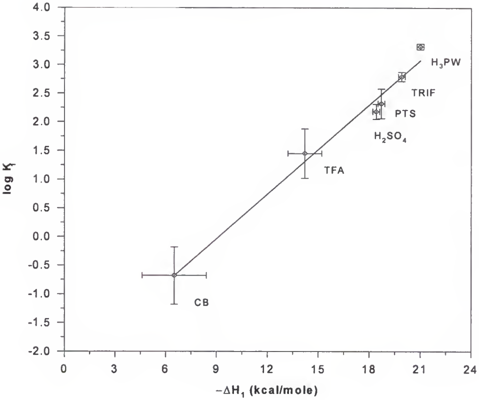

Figure 2-9. Log K_l versus ΔH_l (kcal mol^{-1}) for the Reaction of Pyridine with Various Acids in CH_3CN Solvent. Acids are: 12-tungstophosphoric (H_3PW), triflic (TRIF), p-toluenesulfonic (PTS), sulfuric (H_2SO_4), trifluoroacetic (TFA), and m-chlorobenzoic (CB) respectively.

The reaction of pyridine with triflic acid in CH_3CN gives an enthalpy of 19.9 kcal mol^{-1}. In acetonitrile the enthalpy of reaction of $(CH_3CN)H^+$ with pyridine is calculated as -30.4 kcal mol^{-1}. The difference in the measured enthalpy and this quantity gives 10.5 kcal mol^{-1} as the enthalpy of dissociating the $CF_3SO_3^-$ from CH_3CNH^+ in acetonitrile compared to the W value of 9.4 for dissociating $(CH_3CN)_2H_2PW^-$. Assuming that all acids in the above series form $(CH_3CN)H(C_5H_5N)^+$, similar calculations for the other acids provide an enthalpy scale of conjugate base strengths toward this acid.

An extensive compilation of the dissociation constants (pK_a) in acetonitrile is available [69]. For the acids employed in this work, pK_a of 7.8, 8.7, and 12.6 are given for sulfuric, p-toluenesulfonic, and trifluoroacetic, respectively. The pK_a trend is in good agreement with our enthalpy trend which provides a direct measure of bond strength.

Comparison of Solution and Solid Calorimetric Data

Comparison of the solution enthalpies with those from gas-solid calorimetry is informative. As reported [43], the gas-solid data contains a dispersion component not present in solution leading to larger measured -ΔH values than those corresponding to the donor-acceptor component. Furthermore, the differential heat of gaseous ammonia adsorption at 50 °C for the solid sample treated[17] at 250 °C is claimed to show that all three protons of the solid are titrated producing the same -ΔH of ≅ 35 kcal mol^{-1}. There is no solvent leveling or displacement in the gaseous ammonia reaction but this can not account for three protons of equivalent acidity. Unfortunately equilibrium constants are not measured in reported gas-solid calorimetric studies [43]. If K_1, K_2, and K_3 decrease slightly for the gas phase reaction, simultaneous reaction of all three protons would occur leading to averaged heat evolution and an average -ΔH of 35 kcal mol^{-1}. The -ΔH could in reality correspond to the average of large, medium and small enthalpies with similar K's. Slightly decreasing equilibrium constants would account for a -ΔH slightly higher than 35 with 0.1 moles of NH_3 to 1 mole of H_3PW added and the small -ΔH of ≈ 20 kcal mol^{-1} based on a limiting reagent assumption for the remaining weakest site up to a 3:1 NH_3 to H_3PW mole ratio. Titration of samples with varying water content are reported[17] [40] but as described above (Table 2-2) interpretation of these measurements is difficult. Calorimetric titration with ammonia [42] at 150 °C on samples activated at 150 and 200 °C are also reported. Reaction is practically complete for 2.89 moles of added base with the differential heat decreasing from 48 to 36 kcal mol^{-1} during the titration. At this higher temperature the step equilibrium constants, for steps with decreasing enthalpies, will be closer in magnitude than at lower temperatures. Without a knowledge of the three step equilibrium constants, the interpretation of the results from a gas-solid enthalpy titration is ambiguous because the measured heat evolved cannot be resolved into contributions from the different steps [43].

Solution calorimetry unequivocally shows the three protons are not strong acids of equal strength and the discussion offered in this work is relevant to measuring acidity in homogeneous systems. Solid acids have the conjugate base anion as part of the crystal lattice and proton transfer from a Brönsted site produces an intimate ion-pair. The lattice energy of the ion-pair compared to that of the solid acid contributes to -ΔH. Thus, any direct comparison of enthalpies for homogeneous and heterogeneous systems should take into account the differences in the reactions involved.

Conclusions

This study provides thermodynamic parameters for the three step equilibria of H_3PW reacting with a series of bases in acetonitrile solution. The results indicate that the three protons are not of equal strength as proposed from gas-solid calorimetry measurements. Only one strong proton per molecule of acid is furnished for stoichiometric or catalytic reactions in any solvent of basicity equal to or less than CH_3CN. Consistent with literature claims of superacidity, the enthalpies in acetonitrile show that, as a monoprotic acid toward pyridine, H_3PW is comparable to triflic acid and is stronger than sulfuric acid, and p-toluenesulfonic acid.

The enthalpies of reactions for the first protonation process were successfully correlated to the ECW model, leading to substantial covalent character ($C_A^* / E_A^* = 2.88$) in the donor-acceptor reactions of the species $(CH_3CN)H^+$. With a database of more than one hundred bases in the ECW correlation, enthalpies of reaction of all these bases with H_3PW can be predicted. Of even more significance is the ability of the solvation minimized ECW parameters for neutral donor acceptor interactions to predict enthalpies for the reaction of Brönsted acids in acetonitrile solvent. This justifies arguments presented for using enthalpies in acetonitrile as a Brönsted acidity scale.

The dehydration of H_3PW is complicated by decomposition, and it must be dried carefully in order to obtain the anhydrous acid. A procedure for accomplishing this is reported. The demonstrated instability of H_3PW at 300 °C precludes its use as an acid catalyst at this or higher temperatures.

In any acid catalyzed reaction occurring in the condensed phase, the reactivity will depend upon the number of protons provided as well as the strength of interaction of the acid with the substrate. Hammett indicators, which provide a measure of the number of acid species supplied, do not measure the strength of the acid-substrate bond. Calorimetry at low base concentration, assuming complete complexation, can provide a measure of the strength of the interaction for monoprotic acids or when $K_1>K_2$ for diprotic acids. The determination of both K and $-\Delta H$ furnishes a complete characterization of the strength and amount of acid species. With a linear log K vs. $-\Delta H$ plot (Figure 2-9), the trend in amount and strength are the same for H_3PW in acetonitrile. Thus, the calorimetric measurement of $-\Delta H$ for different acids in acetonitrile solvent provides a temperature independent Brönsted acidity scale of relevance to homogeneous catalytic reactions in which unusual entropy effects are absent. We emphasize that this is a one parameter scale and should be applied in a manner consistent with the limitations [73] of such a scale.

CHAPTER 3
ACIDITY OF $H_3PW_{12}O_{40}$ AND $Cs_XH_{3-X}PW_{12}O_{40}$ IN HETEROGENEOUS SYSTEM

Introduction

Research in heteropoly acids has focused attention in their industrial use as homogeneous and heterogeneous catalysts for redox and acid catalyzed reactions [32a]. $H_3PW_{12}O_{40}$ (abbreviated as H_3PW) is the strongest heteropoly acid, and it has been characterized recently as a monoprotic, superacid in solution by calorimetry [74] resolving conflicting reports from NMR [52], IR [48-51], UV-vis [64], thermal methods (TG, DSC, TPR, TPD) [44-45, 47], microcalorimetry with ammonia absorption [40-42], Hammett acidity constants [37], conductivity [36], and the ^{13}C shift of mesityl oxide [38].

The crystal structure of $H_3PW_{12}O_{40}$ [4a, 4b] is demonstrated with X-ray and neutron diffraction [75] to be a hexahydrate. The structure can be divided into primary (anion) and secondary (protons and water) parts. The complete structure of the phosphotungstic acid has been described in more details in chapter 2.

Recently $Cs_xH_{3-x}PW_{12}O_{40}$ (abbreviated as $Cs_xH_{3-x}PW$) derivatives have gained attention because of their claimed superacidity and shape-selectivity in alkylations reactions [76-78]. Unlike H_3PW, the $Cs_xH_{3-x}PW$ salts have limited solubility in water or organic solvents and are used as heterogeneous catalysts. They show higher catalytic activity and higher thermal stability in some reactions than the parent acid [27]. In

Cs_3PW, the Cs^+ occupies the positions of $H_5O_2^+$ in the hydrate [27] having the same cubic structure of hexahydrated H_3PW, but with a smaller lattice constant. The structure of the other $Cs_xH_{3-x}PW$ are not completely established. The proposed structure of cesium complexes with $x< 3$ are reported to be mixtures of H_3PW and $Cs_xH_{3-x}PW$. A study of the precipitates [79] from the reaction of H_3PW with Cs_2CO_3 evaporated to dryness together with the solution concludes that in the range of $0 < x \leq 2$ are mainly Cs_2HPW. Compounds prepared in the range of $2 < x \leq 3$ are Cs_3PW, although $Cs_{2.5}H_{0.5}PW$ is considered a mixture of Cs_2HPW and Cs_3PW. Reported XRD spectra for $Cs_xH_{3-x}PW$ ($x = 0, 1, 2$, and 3) [80] claims that CsH_2PW is a mixture of H_3PW and Cs_2HPW which is transformed in a nearly homogeneous acidic salt after thermal treatment of the precipitate at 300 °C. The lattice constants values for those cesium salts indicate all of them belong to cubic system. The XRD pattern is very similar for Cs_2HPW and Cs_3PW, but distinct enough from H_3PW and CsH_2PW. The $Cs_xH_{3-x}PW$ ($x = 2, 2.5$, and 3) were studied by ^{31}P NMR [81]. The ^{31}P spectrum of Cs_2HPW has four peaks, which were interpreted as a mixture of four species ($x = 0, 1, 2$, and 3). The results for $Cs_{2.5}H_{0.5}PW$ claimed that this compound is a mixture of Cs_2HPW and Cs_3PW. Supported H_3PW on Cs_3PW presents the same ^{31}P spectrum as $Cs_{2.5}H_{0.5}PW$ [81], accounting to the exchange between H^+ and Cs^+ during the heating process. In all those studies [79-81] the cesium derivatives were prepared similarly [77], though the thermal treatment before analysis of the solids were not always the same.

The tertiary structures of these cesium salts are important. The tertiary structure is composed of the size of the primary and secondary particles, distribution of protons and cations, and pore structure [27]. Porosity is important in catalysis [80] and leads to shape-selectivity [82]. There is a remarkable change of surface area in going from H_3PW to Cs_3PW. H_3PW has a surface area of 5-6 $m^2 g^{-1}$, which decreases slightly as the cesium content is increased up to CsH_2PW (1 $m^2 g^{-1}$). Above two cesiums, the surface area increases rapidly, for instance, $Cs_{2.5}H_{0.5}PW$ is reported to have 135 $m^2 g^{-1}$ of area [77]. Micropores form in these solids [77, 82] when the proton is substituted by cesium. Adsorption studies with different probes (e.g., nitrogen, benzene, etc.) [77] give the pore sizes for $Cs_{2.2}H_{0.8}PW$ as 6.2-7.5 Å and those for $Cs_{2.5}H_{0.5}PW$ are larger than 8.5 Å. Microporosity studies of $Cs_xH_{3-x}PW$ carried out by ^{129}Xe NMR [82] indicate slightly smaller pores.

Studies of the microporosity of monovalent salts of the heteropoly compounds have been reported [83-86] using nitrogen adsorption-desorption and X-ray diffraction analysis. The solids are reported to contain interstitial voids set apart from each other by the terminal oxygen atoms of the polyanions. Widening of the interstices occurs as the size of the cation increases. These studies demonstrate that the pore sizes can be controlled in heteropoly acids substituting the proton with different cations.

In an earlier report [74], thermodynamic data describing the acidity of H_3PW was measured in acetonitrile solution by calorimetric titration. The Keggin structure of crystalline H_3PW is maintained in solution [2]. This chapter aims to characterize the acidity of solid H_3PW and the solid $Cs_xH_{3-x}PW$ salts in their reactions with pyridine in cyclohexane using combined measurements from a calorimetric titration and adsorption isotherm measurement, Cal-ad [87, 59, 43]. A multiple-site Langmuir equation is used to solve both measurements simultaneously and calculates the number of sites (n_i), equilibrium constants (K_i), and enthalpies (ΔH_i) for different acid sites on these solids. Thus, the Cal-ad analysis provides a total characterization of solid acid strength and furnishes enthalpies for different sites to provide a temperature independent acidity scale. Differences in the reactivity of solid H_3PW and acetonitrile solutions of this acid are discussed.

Experimental

Materials and Preparation of Cesium Derivatives

Elemental and TG analysis of the H_3PW (purchased from Aldrich) revealed 16 moles of water per mole of H_3PW. Cyclohexane obtained from Fisher was purified by drying over 4A molecular sieves for 24 hours, and then distilled over P_2O_5. Pyridine obtained from Fisher was distilled over CaH_2. Dried samples were stored in a container with 4A molecular sieves. $Cs_xH_{3-x}PW$ (x=1, 2, 2.5, and 3) was prepared by adding predetermined amounts of a 0.2 mol L^{-1} aqueous solution of Cs_2CO_3 to a 0.08 mol L^{-1} solution of H_3PW at a rate of 1 mL min^{-1} at room temperature. A white precipitate formed in the solutions. The solutions were left to stand overnight at room temperature. Then, according to the literature [77], the solutions were evaporated to dryness at 40 °C. It is interesting to note that as the cesium content increases in the compounds, the product appears whiter. The extent of proton exchange by cesium is in close agreement with the expected stoichiometric value, as determined by ICP-MS (Table 3-1).

Table 3-1. Chemical Analysis[a] and Surface Area[b] of $Cs_xH_{3-x}PW$ Compounds.

Sample	Cs per K.U. (x)	Surface Area ($m^2\ g^{-1}$)
CsH_2PW	0.9	1
Cs_2HPW	1.8	63
$Cs_{2.5}H_{0.5}PW$	2.3	119
Cs_3PW	2.7	92

a. Cesium contend was determined by ICP-MS after dissolving the compounds in 0.01 mol L^{-1} NaOH solutions.
b. Surface area values were obtained in reference 78.

Drying Procedures

H_3PW was dried at 162 °C for 4 hours under vacuum [74]. The $Cs_xH_{3-x}PW$ dried at 200 °C for 4 hours under vacuum gave higher heats of reaction with pyridine in cyclohexane than at 300 °C.

The apparatus for drying H_3PW and $Cs_xH_{3-x}PW$ consisted of a glass fixed bed reactor with two stopcocks at the ends to close the system. An external small opening under the reactor bed contains a wire thermocouple to control and measure the temperature of the reactor. The sample is weighed, placed into the reactor, and evacuated. The reactor is filled with argon and evacuated two to three times during the drying period to remove equilibrium water vapor from the reactor. After 4 hours, the sample is cooled to room temperature, the reactor is filled with argon and transported to a inert atmosphere box. The samples are stored in vials in a dry box until used. The same apparatus has been successfully used to dry zeolites in this laboratory [43].

Spectral Analysis

A Perkin-Elmer Lambda 6 UV-vis spectrophotometer and quartz cells of 1.0 cm pathlength were employed for the adsorption experiment. Infrared spectra were obtained with a Nicolet Model 5PC FTIR spectrophotometer in nujol (Aldrich) mulls on NaCl plates. Mulls of dried samples were prepared inside the inert atmosphere box. The determination of cesium was measured for ^{133}Cs by inductively coupled plasma mass spectrometry with a Finningan MAT SOLA ICP-MS. The powder X-ray diffraction data were obtained with a Siemens General area detector (XRDS) with x-ray tube power at 50 kV and 40 mA (adding time of 10000 seconds).

The ^{31}P NMR spectra of H_3PW, H_3PW-Py, and $Cs_xH_{3-x}PW$ compounds were taken on a Unity 500 NMR using a Varian MAS probe tuned to 202.640 MHz. Samples were loaded into silicon nitride rotors. Packing of the rotor with the solids was accomplished by filling the rotor 2/3 of the way full with the sample, and then packing the remainder with silica gel. This prevented the samples, specially $Cs_{2.5}H_{0.5}PW$, from sticking to the inside of the rotor, and allowed the rotor cap to be removed after acquisition. The magic angle was tuned using $K^{79}Br$. A recycle delay of 2 seconds was used. The acquisition time was set to 0.02 s, with the FID no longer showing the evolution of signal after 0.01 s. Signals were indirectly referenced to 85 wt.% phosphoric acid. One hundred plus transients were obtained.

Calorimetric Titrations and Adsorption Measurements

For solid acids, a pyridine solution is added to a slurry of the solid in cyclohexane, and the measurement of heat evolved and the equilibrium amount of base in solution is determined in two independent experiments. The calorimetric data generates an isotherm of total heat evolved versus the total moles of base added. Calorimetry does not account for the amount of base in solution, but the adsorption measurement provides this information producing an isotherm of moles of base adsorbed versus moles of base in solution. It is important that the concentrations of base added and the ratio (V/g) between the volume of solution (V) and the mass of solid used (g) be the same in both calorimetric and adsorption experiments to interchange the data. Samples of H_3PW or $Cs_xH_{3-x}PW$, are weighed and transferred to a vacuum insulated calorimetric cell containing a stir bar. For each titration, 100 mL of cyclohexane is added to the cell. A calibrated syringe, filled with a solution of known concentration of pyridine (e.g., 0.1 mol L^{-1}) is inserted into the cell along with a thermistor and a heater coil. All these operations are carried out in an inert atmosphere glove bag. The thermistor and heater coil are connected to an electronic bridge, and a computer [59]. The thermistor is calibrated with the heater coil prior to or immediately after each titration. A set of 12 calibrated brass stops are used for the syringe additions. After each addition the heat evolved from reaction of the base with the samples is measured. The heat from adding the base solution to the solvent is negligible. Each titration was repeated two times.

The adsorption experiments are carried out using 1 g of solid, weighed inside the dry box, and added to a sealed three neck round bottom flask with 100 mL of cyclohexane. The same syringe and calibrated brass stops used in the calorimetric experiment are used for addition of pyridine in this experiment. After each addition of base, at least 3 min is allowed for equilibrium to be reached. Then, a 1 mL sample of solution is removed from the flask and placed into a quartz cell of 1 cm pathlength and 1 mL volume. One milliliter of cyclohexane is added back into the flask in order to maintain a constant volume. The absorbance of pyridine is measured at 251 nm to determine its equilibrium concentration in solution. Since the amount of pyridine added is known, the amount of base adsorbed by the solid is calculated by difference. Each adsorption experiment was repeated two times.

Cal-ad Calculations

The Cal-ad analysis is based on simultaneously solving data from calorimetric and adsorption experiments [87, 59, 56, 43]. The model employs multiple-site equilibrium for the different acid sites present in a solid acid. A Langmuir-type equation is summed over all sites of the solid, according to Equation (3.1):

$$h/g = \sum (n_iK_i[B]/(1 + K_i[B]))\Delta H_i \tag{3.1}$$

where h is the sum of the heat evolved (cal) from the calorimetric titration; g is the mass of solid (g); [B] is the concentration of base in solution at equilibrium (mol L^{-1}); n_i is the number of each different site; K_i is the equilibrium constant for each site; and ΔH_i is the enthalpy of reaction for each site on the solid.

A Simplex routine is used to calculate the parameters. The data adjusted to the model consist of the mol adsorbed and equilibrium concentration in solution (adsorption), and the sum of the heat and equilibrium concentration in solution (calorimetry). As the calorimetric titration does not measure the equilibrium concentration in solution, this information is obtained through a polynomial series, according to this expression:

$$(V/g)[T] = x^n[B]^n + x^{n-1}[B]^{n-1} + x^{n-2}[B]^{n-2} + x^{n-3}[B]^{n-3} + \dots \qquad (3.2)$$

where (V/g) is the ratio of volume of solution (L)/mass of solid (g); [T] is the total concentration of base added for each addition in the calorimetric experiment (mol L^{-1}); [B] is the equilibrium concentration of base in solution (mol L^{-1}). The polynomial is one degree higher than the number of sites (e.g., for two sites a third degree polynomial is used as shown in Equation 3.2). The x^n terms have the following meaning for a two site adjustment: $x^3 = K_1K_2(V/g)$; $x^2 = n_1\ K_1K_2 + n_2\ K_1K_2 - (V/g)K_1K_2[T] + (V/g)K_1 + (V/g)K_2$; and $x = n_1K_1 + n_2K_2 - (V/g)K_1[T] - (V/g)K_2[T] + (V/g)$. Estimates of n's and K's are obtained from a Langmuir analysis of the adsorption data using Equation (3.3):

$$S_TB = \Sigma\ n_iK_i[B]/(1 + K_i[B]) \qquad (3.3)$$

where S_TB is the total number of moles of base adsorbed per gram of solid. Cal-ad has been successfully applied for calculation of K's , n's, and ΔH's for the solid acids silica gel [59], ZSM-5 [43], and sulfated zirconia [88].

Results and Discussion

Drying the Solids

As pointed out in a previous report [74] the dehydration of H_3PW to the anhydrous acid is complicated by decomposition into constituent oxides. We have shown

[74] that treatment of the H_3PW at 160-200 °C for 4 hours under vacuum results in the anhydrous acid.

The drying of the $Cs_xH_{3-x}PW$ compounds was investigated using the maximum total heat released in the titration with pyridine as a criterion of dryness [74]. Temperatures of 200 and 300 °C for 4 hours under vacuum were used and the former gave better results, Table 3-2. All cesium salts were dried at 200 °C for 4 hours under vacuum.

Cal-ad Analysis of Solid H_3PW

The results of the calorimetric titration and adsorption experiments for pyridine reacting with a slurry of H_3PW in cyclohexane are shown in Figure 3-1. Cyclohexane was chosen as the solvent because it is a non-specific interacting solvent in which H_3PW is insoluble. The heat evolved from the reaction indicates that not all of the 1.04 millimoles of protons in one gram of H_3PW are titrated. After 0.24 mmol of pyridine are added (about 24% of the moles of protons in a gram of solid), heat evolution practically stops and the adsorption of pyridine by the solid also reaches a plateau.

Three possible equilibria were evaluated and the results are presented in Table 3-3. The Cal-ad data were analyzed by assuming a one site fit, i.e., all of the protons titrated have the same strength and equilibrium constant. The results obtained are: $\Delta H = -25.6 \pm 1.1$ kcal mol^{-1}, $K = 3.5\times10^4 \pm 8.1\times10^3$ and $n = 0.185 \pm 0.005$ mmol g^{-1}. This fit shows a higher sum of squares and higher errors than a fit to two sets of non-equivalent protons. The two site fit produces: $\Delta H_1 = -32.7 \pm 0.3$ kcal mol^{-1}, $K_1 = 3.7\times10^5 \pm 2.0\times10^3$, $n_1 = 0.079 \pm 0.002$, $\Delta H_2 = -19.6 \pm 4.8$ kcal mol^{-1}, $K_2 = 2.9\times10^3 \pm 1.0\times10^3$, $n_2 = 0.159 \pm 0.056$ mmol g^{-1}. The deviations in the experimental and calculated heat evolved in the titration

Table 3-2. Experimental Heat Evolved (h'_{exp}) in Cyclohexane Upon Addition of Pyridine[a] to H_3PW and Cs_2HPW for Different Thermally Treated Solids[b].

	h'_{exp} (cal)			
mmol py added	H_3PW (162/4)	H_3PW (200/4)	Cs_2HPW (200/4)	Cs_2HPW (300/4)
0.0123	0.365	0.363	0.299	0.221
0.0230	0.693	0.688	0.540	0.391
0.0341	1.029	1.009	0.754	0.558
0.0458	1.381	1.338	0.862	0.674
0.0690	2.076	1.992	1.018	0.806
0.0920	2.704	2.628	1.152	0.928
0.1197	3.279	3.315	1.294	1.063
0.1382	3.613	3.684	1.390	1.141
0.1615	3.946	4.062	1.467	1.208
0.1842	4.198	4.376	1.538	1.270
0.2074	4.421	4.568	1.598	1.335
0.2311	4.618	4.651	1.658	1.397

a. The millimoles of pyridine added and the heat evolved values are summed along the titration.

b. Thermal treatments refer to temperature (°C) and time (hs) which the solid was heated under vacuum.

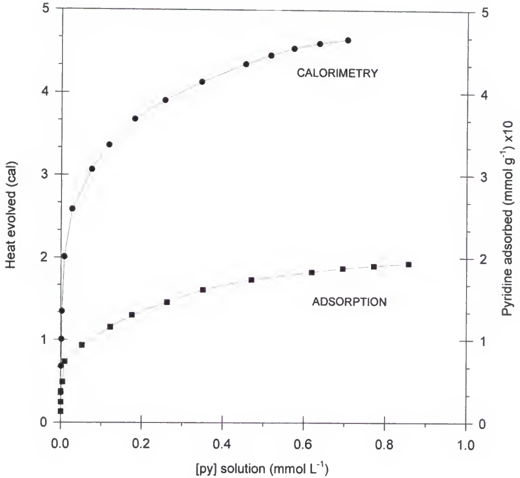

Figure 3-1. Isotherms of Calorimetry and Adsorption for Reaction of H_3PW with Pyridine in Cyclohexane.

Table 3-3. Cal-ad Results for Three Types of Fit for H_3PW Reacting with Pyridine in Cyclohexane.

	1 site fit	2 site fit	3 site fit
n_1 (mmol g^{-1})	0.186 ± 0.005	0.079 ± 0.002	0.081 ± 0.002
K_1 (M^{-1})	$3.5x10^4 \pm 8.1x10^3$	$3.7x10^5 \pm 2.0x10^3$	$3.6x10^5 \pm 2.3x10^3$
$-\Delta H_1$ (kcal mol^{-1})	25.6 ± 1.1	32.7 ± 0.3	32.1 ± 0.3
n_2 (mmol g^{-1})		0.16 ± 0.05	0.08 ± 0.05
K_2 (M^{-1})		$2.9x10^3 \pm 1.0x10^3$	$3.0x10^3 \pm 2.6x10^3$
$-\Delta H_2$ (kcal mol^{-1})		19.6 ± 4.8	25.0 ± 5.6
n_3 (mmol g^{-1})			0.09 ± 0.08
K_3 (M^{-1})			$2.5x10^3 \pm 1.9x10^3$
$-\Delta H_3$ (kcal mol^{-1})			15.1 ± 12.2
U[a]	$1.60x10^{-1}$	$6.59x10^{-3}$	$1.65x10^{-3}$

a. The quantity U is the sum of squares of residuals, calculated for calorimetry as: $\sum (h'_{exp}-h'_{calc})^2$.

are close to the sum of the squares of the experimental error (1.65×10^{-2}). The two site model also gives a value for the sum of the sites that is in good agreement with the estimate of the moles of pyridine reacted from the calorimetric exotherm. There is a four-fold improvement in the sum of squares for the three site fit compared to the two but the improvement in the deviations in the data fit are not significant compared to experimental error. Within experimental error a three site fit cannot be distinguished from the two site fit. This leads to a choice of the two site fit and the next concern is with the assignment of the sites.

The number of surface protons reported [89] for H_3PW, 0.008 mmol g^{-1}, agrees with our estimate from its surface area (5 m^2 g^{-1}) and the diameter of an assumed spherical Keggin anion (10 Å). This is an order of magnitude less than calculated site1. Thus, in addition to reacting with the protons on the surface, pyridine also penetrates into and partially reacts with those in the bulk solid. This result is consistent with reports [90] that the absorption of polar molecules by solid H_3PW lead to catalytic reactions in the bulk of the crystal as well as on the surface. The solid behaves like a concentrated solution and this behavior is described as a pseudoliquid phase [11]. Non-polar molecules are not absorbed.

In this titration, not all of the protons react. In order to determine if incomplete reaction is caused by forming a layer of product on the surface that could not be penetrated by pyridine, a sample of the same calcined solid was ground to finer particles inside the inert atmosphere box and titrated with pyridine. An identical isotherm resulted demonstrating that restricting diffusion from a surface constraining is not a problem.

Pyridine does not access certain protons in the structure. The reaction with pyridine may require a slight lattice expansion. In order to understand how an expansion in the structure produce a layered material, it is necessary keep a clear image of the complete structure of H_3PW. Figure 3-2(a) illustrates the unit cell of H_3PW. This unit cell consists of a total of two anions, 8 anions at the vertices of a cube shared by eight cubes and 1 unshared anion in the center. Six of the protons are positioned on the center of faces and shared by two units cells. Twelve of protons bridge Keggin ions and are located on 12 edges. The edge protons are shared by four unit cells giving the six protons needed to charge compensate the two Keggin anions to produce the molecular formula H_3PW. The quantity of protons titrated (24%), suggests that on average one layer is neutralized out of every four. In a given layer, four of the protons neutralized in the unit cell are shared with four unit cells and the face proton is shared by two. This gives rise to a 2:1 ratio of different type protons labeled edge and face in Figure 3-2(b). This ratio corresponds to the ratio of sites calculated from Cal-ad with enthalpies of -32.7 ±0.3 consisting of 0.08 mmol g^{-1} and those with enthalpies of -19.6 ±4.8 kcal mol^{-1} consisting of 0.16 mmol g^{-1}. Thus we assigned the strongest sites to the face protons. It is important to realize that all protons on the H_3PW structure are equivalent, as can be observed in the extended structure. The two sites arise when pyridine starts to react with the protons and therefore it creates a non symmetric environment of the remained protons.

The Cal-ad results with pyridine differ from microcalorimetry of gaseous ammonia adsorption [40-42]. With ammonia the three protons on H_3PW react and the enthalpy decreases from -48 to -39 kcal mol^{-1} over the titration. The ammonia enthalpies are larger for they contain both donor-acceptor and dispersion contributions. In contrast

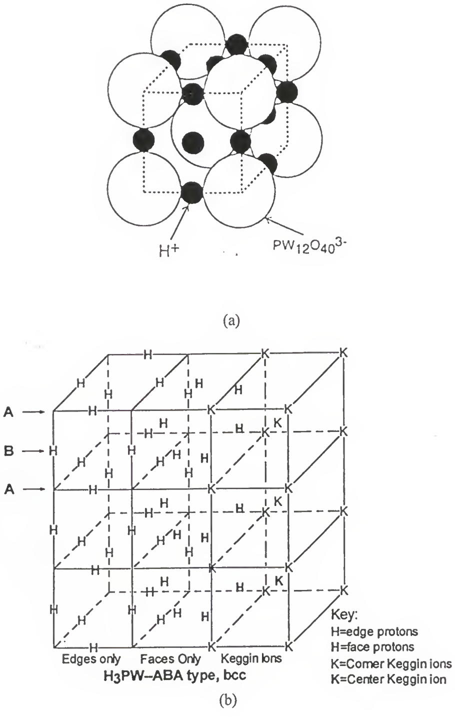

Figure 3-2. Structure of $H_3PW_{12}O_{40}$: (a) Simple Unit Cell; (b) Extended Structure.

to all protons reacting, Cal-ad reaction of H_3PW with pyridine indicate that only 24% of the available protons react with pyridine and these have different strengths (-32.7 and -19.6 kcal mol^{-1}). The differences in numbers of protons reacted is attributed to the small size of ammonia which enables it to occupy positions occupied by water in the hydrate without appreciable change in lattice dimensions.

Results of FTIR, ^{31}P MAS NMR and XRD for H_3PW

FTIR spectra of samples produced from the reaction of H_3PW with pyridine contain unchanged characteristic Keggin bands. The region between 1700-1450 cm^{-1} is informative for it contains bands at 1540 cm^{-1} and 1485 cm^{-1} which have been assigned to pyridinium ion [91]. Coordinated pyridine or hydrogen-bonded pyridine shows a band at 1612 cm^{-1} [91]. The pyridinium band is clearly observed (Figure 3-3) for H_3PW, but only a small band at 1612 cm^{-1} is shown. The relative ratio based upon the height of the bands at 1612 cm^{-1} to that at 1540 cm^{-1} is 0.2. This ratio is different that obtained by Cal-ad calculations from n_2 over n_1 (2.0). Thus, site 2 can not be considered as hydrogen-bonded pyridine to H_3PW, which is consistent with the high enthalpy for that site ($\Delta H_2 = -19.6$ kcal mol^{-1}). Both protons, assigned as site 1 and 2, in H_3PW are Brönsted type.

The ^{31}P MAS NMR spectrum of H_3PW contains a single sharp peak at -12.05 ppm relative to an external 85 wt.% H_3PO_4 reference (Figure 3-4a). This compares favorably with the literature reports of -10.9 ppm [81], -11.1 ppm [52] and -12.4 ppm [92]. The spectrum of the product of the pyridine titration gave a single resonance at -16.53 ppm (Figure 3-4b). This is a surprising result because only 24% of the protons in H_3PW have reacted but is not unexpected in view of the mobility of the protons. The

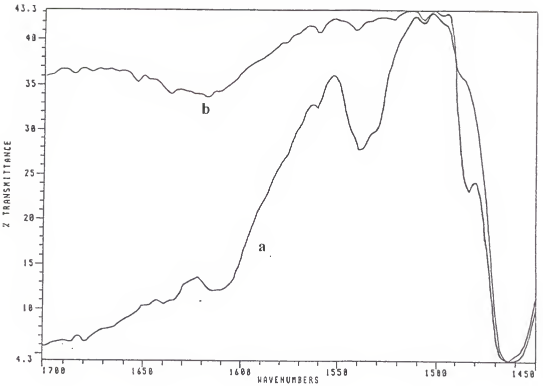

Figure 3-3. FTIR Spectra of H_3PW (a) and Cs_3PW (b) after Reaction with Pyridine in Cyclohexane.

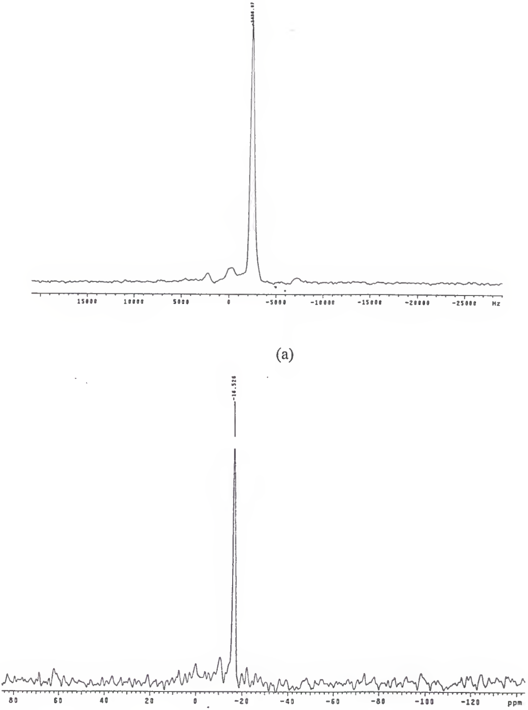

(a)

(b)

Figure 3-4. ^{31}P MAS NMR Spectra of: (a) H_3PW ($\delta = -12.05$ ppm); (b) 1.04 mmol H_3PW-0.24 mmol Pyridine ($\delta = -16.53$ ppm).

single peak suggests that the remaining protons not titrated are not symmetrically located between the unit cells of the average four layer units but are displaced in the bridges toward the anionic layer. In this way the negative charge formed by reaction of the protons with pyridine in a given layer is distributed over the structure making the electron density on all the anions similar. Spectra of ^{31}P NMR for 1.04 mmol of H_3PW reacting with 0.08 and 0.12 mmol of pyridine also show a single peak at -17.49 ppm suggesting the protons are mobile in the structure (Figure 3-5).

The XRD spectrum of H_3PW gives a pattern similar to the reported in the literature [78] (Figure 3-6). The main peaks, related to the strongest reflections, are present at $2\theta = 10.40$, 20.90, and 25.40. The broader peaks indicates loss of crystallinity, as reported for H_3PW dried at different conditions [45, 93]. The XRD pattern of the product of the reaction of 1.04 mmol (1 gram) of H_3PW with 0.24 mmol of pyridine shows various new reflections (Figure 3-7). The most intense peak now occurs at $2\theta = 25.57$. The peak at $2\theta = 10.40$ split up in two less intense shoulders at $2\theta = 10.30$ and 10.52. Two new reflections at $2\theta = 9.27$ and 9.98 are present in the powder pattern. These results confirms formation of a different compound. No extensive change was observed in the XRD pattern when 1.04 mmol of H_3PW was reacted with 0.08 mmol of pyridine (site 1 of Cal-ad), except that a more crystalline spectrum was obtained Figure 3-8). The main peaks with the intensities in the XRD spectra of those compounds are presented in Table 3-4.

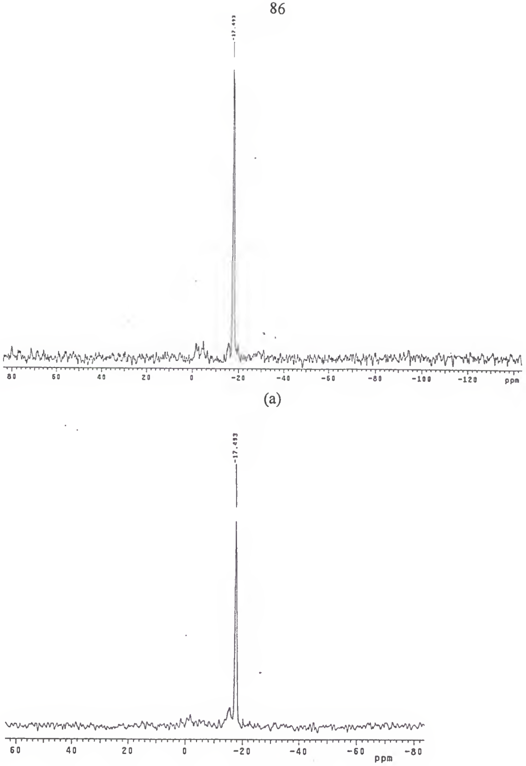

(a)

(b)

Figure 3-5. ^{31}P MAS NMR Spectra of: (a) 1.04 mmol H_3PW-0.08 mmol Pyridine (δ = -17.49 ppm); (b) 1.04 mmol H_3PW-0.12 mmol Pyridine (δ = -17.49 ppm).

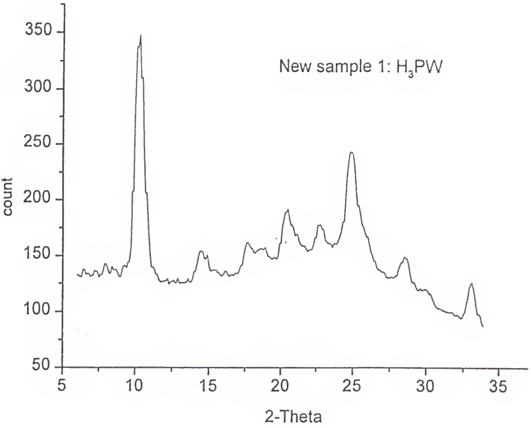

Figure 3-6. XRD Pattern of H_3PW (dried at 162 °C/ 4 hs/ vacuum).

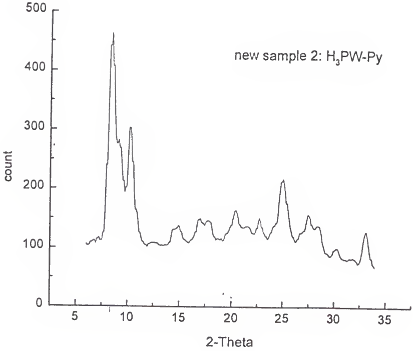

Figure 3-7. XRD Pattern of 1.04 mmol H_3PW-0.24 mmol Pyridine.

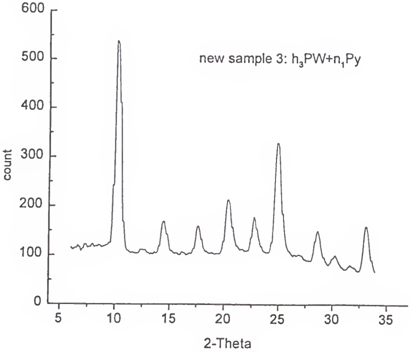

Figure 3-8. XRD Pattern of 1.04 mmol H_3PW-0.08 mmol Pyridine.

Table 3-4. XRD Patterns of H_3PW and Products of Reaction with Pyridine.

2θ Angle (degree)	d-spacing (Å)	Intensity (V)
H_3PW (162 °C/ 4 hs/ vacuum)		
10.40	8.51	61.5
14.90	5.95	6.3
18.10	4.90	7.0
20.90	4.25	10.3
23.20	3.83	7.6
25.40	3.51	32.7
29.00	3.08	7.5
33.50	2.68	7.6
1.04 mmol H_3PW-0.24 mmol Pyridine		
9.27	9.53	8.7
9.98	8.86	19.7
10.30	8.58	27.3
10.40	8.51	60.0
10.52	8.41	42.9
18.13	4.89	36.2
21.00	4.23	9.41
23.30	3.82	8.2
25.57	3.48	142.5
29.20	3.06	20.6
1.04 mmol H_3PW-0.08 mmol Pyridine		
10.40	8.51	47.8
18.10	4.90	19.1
20.90	4.25	7.4
23.30	3.82	10.4
25.60	3.48	84.9
29.20	3.06	20.77

Cal-ad Acidity of $Cs_xH_{3-x}PW$ Compounds

Calorimetric and adsorption isotherm curves for the reaction of $Cs_xH_{3-x}PW$ salts with pyridine in cyclohexane are shown in Figures 3-9 and 3-10 respectively. The results of the Cal-ad analysis are reported in Table 3-5. Fits of the combined calorimetric and adsorption data on all systems were attempted for both one and two processes. For all solids, the one site fit gave large errors in the resulting K, n, and ΔH values as well as the calculated heats and moles adsorbed. Meaningful parameters with improved errors and a decrease in the sum of the squares of the fit residuals result when two sites are employed. FTIR spectra of cesium salts, except Cs_3PW, after reaction with pyridine also supports this choice, since they indicate both Brönsted and hydrogen-bonded pyridine bands (vide infra). The second site present on the analysis of Cs_3PW is determined because formation of pores in this compound, which is responsible for pyridine physisorbed. It is important also to keep in mind the results of cesium analysis (Table 3-1) when interpreting the numbers of sites and moles of protons reacted obtained by Cal-ad.

The CsH_2PW titration with pyridine involves about 0.10 mmol g^{-1} of acid sites (16% of the total 0.66 mmol of protons present in one gram of solid). With Cs_2HPW, about 0.12 mmol g^{-1} react with pyridine (38% of the total 0.32 mmol of protons present in one gram of solid). There are 0.16 mmol of protons in one gram of $Cs_{2.5}H_{0.5}PW$, and they all react with pyridine. In Cs_3PW, there are 0.09 mmol g^{-1} of the residual protons in the solid. The higher number of second sites formed for Cs_3PW is attributed to physisorbed pyridine. Cs_3PW has the same structure of H_3PW [27], but with a higher surface area. The presence of micropores in Cs_3PW allows some pyridine to be adsorbed in the solid.

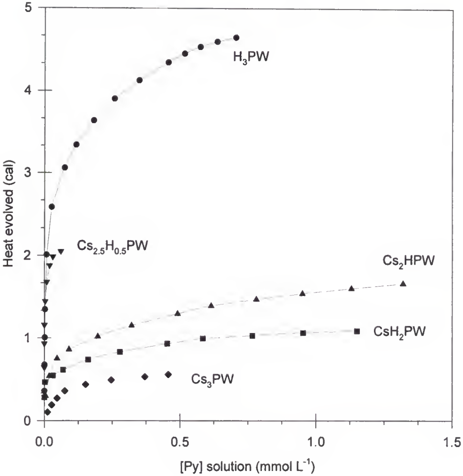

Figure 3-9. Calorimetric Isotherms of Cs$_x$H$_{3-x}$PW Salts Reacted with Pyridine in Cyclohexane.

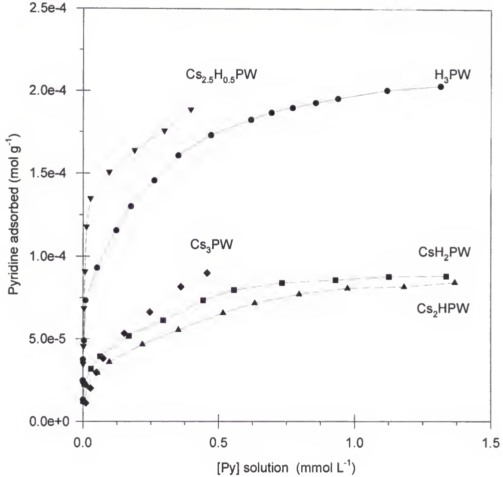

Figure 3-10. Adsorption Isotherms of $Cs_xH_{3-x}PW$ Salts Reacted with Pyridine in Cyclohexane.

Table 3-5. Cal-ad Results for Reactions of $Cs_xH_{3-x}PW$ Compounds with Pyridine in Cyclohexane.

	CsH_2PW	Cs_2HPW	$Cs_{2.5}H_{0.5}PW$	Cs_3PW
n_1 (mmol g^{-1})	0.022 ±0.001	0.027 ±0.001	0.053 ±0.005	0.043 ±0.003
K_1 (M^{-1})	$1.5x10^7$ ±$3.1x10^4$	$1.2x10^5$ ±$1.8x10^3$	$5.0x10^6$ ±$6.2x10^4$	$2.1x10^4$ ±$1.2x10^3$
$-\Delta H_1$(kcal mol^{-1})	20.8 ±0.3	28.3 ±0.6	27.4 ±0.5	12.7 ±0.5
n_2 (mmol g^{-1})	0.08 ±0.02	0.09 ±0.03	0.14 ±0.09	0.15 ±0.15
K_2 (M^{-1})	$3.6x10^3$ ±$9.9x10^2$	$1.5x10^3$ ±$5.7x10^2$	$4.6x10^4$ ±$3.1x10^4$	$1.1x10^3$ ±$9.9x10^2$
$-\Delta H_2$(kcal mol^{-1})	9.3 ±2.3	15.1 ±2.7	6.4 ±4.6	1.4 ±1.8
Total H^+ [a] (mmol g^{-1})	0.66	0.32	0.16	0.09
H^+ reacted [b] (mmol g^{-1})	0.10	0.12	0.19	0.19

a. This amount is based on the stoichiometric formula of each compound, except Cs_3PW where the actual formula was used.

b. This amount is based upon the number of sites ($n_1 + n_2$) obtained by Cal-ad.

The residual protons of Cs_3PW are mainly on the surface, which are homogeneously distributed after thermal treatment of the solid.

The enthalpies are informative when compared to the enthalpies of reaction of H_3PW with pyridine. For Cs_3PW, the magnitude of the ΔH_1 (-12.7 kcal mol^{-1}) is comparable to the hydrogen bond site for reaction of pyridine with silica gel [59] (ΔH_1 = -12.6 kcal mol^{-1}). The IR spectrum (Figure 3-3) does not contain the band assigned to pyridinium ion but only the hydrogen-bonded adduct band is observed at 1614 cm^{-1} [91], confirming the nature of this site for Cs_3PW.

For CsH_2PW, the ΔH_1 = -20.8 kcal mol^{-1} is close to the value of ΔH_2 obtained for H_3PW (-19.6 kcal mol^{-1}). The FTIR spectrum of this solid (vide infra) after reaction with pyridine shows a very small peak at 1540 cm^{-1} (pyridinium ion), which is assigned to the strongest site. A second band at 1614 cm^{-1} corresponds to hydrogen-bonded pyridine to the solid CsH_2PW. Compared to FTIR spectrum of H_3PW reacted with pyridine (Figure 3-3), CsH_2PW shows a larger band for hydrogen-bonded pyridine. As discussed before, this pyridinium band is consistent to be assigned to the strongest site. Having the same enthalpy of site 2 for H_3PW, this CsH_2PW compound has fewer strong sites responsible for the higher enthalpy obtained. This is compatible with the Cal-ad results, demonstrating site 1 for CsH_2PW has the same nature of second site for H_3PW.

The enthalpy result for site 1 on CsH_2PW indicates that the site 1 protons in H_3PW were completely neutralized by cesium and there is no accessible H_3PW in the solid. Only 16% of the available protons in the solid are titrated which is lower than the 24% titrated for H_3PW. Considering that 0.34 mmol g^{-1} of solid are cesium atoms and

0.10 mmol g^{-1} are the total protons reacted with pyridine, 0.44 mmol g^{-1} of the total 1.04 mmol g^{-1} reacted from the H_3PW. These 42% of the original 1.04 mmol of protons from H_3PW correspond to a ratio of 4:1 between the protons positioned at the edges and on the faces. That ratio is close to the one obtained by Cal-ad from site 2 to site 1 (3.6). This suggests that reaction with pyridine, on average, occurs in one out of every two layers in the solid. Coupled with the ^{31}P NMR results (vide infra) which shows no free H_3PW, we conclude that the reacted layer is mainly cesium atoms which combined with the low surface area prevents access to most of the protons in the solid. The lower enthalpy of reaction for site 2 (9.3 kcal mol^{-1}) is attributed to hydrogen-bonded pyridine, as confirmed by the presence of a large band at 1614 cm^{-1} in the FTIR spectrum.

The enthalpies of reaction of pyridine with Cs_2HPW together with the quantity of acidic protons (n_1 = 0.03 mmol g^{-1}) are significantly larger than CsH_2PW. The larger n_1 is attributed to the tertiary structure which leads to formation of pores and therefore higher surface area. The strongest acid site for Cs_2HPW (ΔH_1 = -28.3 kcal mol^{-1}) is a weaker acid than the first site of H_3PW. This can be qualitatively evidenced by a smaller band at 1540 cm^{-1} for Cs_2HPW than for H_3PW. However, this band is a little larger than the one obtained by CsH_2PW, which is concordant with the higher enthalpy of Cs_2HPW (vide infra).

The ^{31}P NMR (vide infra) shows only one peak (-14.95 ppm) for Cs_2HPW and no signal at -12.05 ppm (free H_3PW). A previous report [81] based on ^{31}P NMR results, pointed out that Cs_2HPW is a mixture of four different species of $Cs_xH_{3-x}PW$ (x= 0, 1, 2, and 3). According to our results, this compound is a homogeneous solid with the protons being homogeneously distributed in the structure. The preparation from aqueous solution might generate a series of equilibria in solution involving up to four species, but after thermal treatment ^{31}P NMR shows the cesium atoms are homogeneously distributed in the solid Cs_2HPW. Considering that thermal treatment for this solid was the same that one reported (200 °C under vacuum) [81], the differences demonstrates that structurally different solids were obtained. This fact is confirmed by the XRD spectrum (vide infra) which shows small differences from the one reported [80].

The magnitude of the enthalpy values of ΔH_1 (-28.3 kcal mol^{-1}) and ΔH_2 (-15.1 kcal mol^{-1}) for Cs_2HPW show this solid is a weaker acid than H_3PW and is not a simple mechanical mixture of the H_3PW and the other cesium salts. The IR spectrum (vide infra) also confirms the presence of a Brönsted site (1540 cm^{-1}) and a weaker hydrogen-bonded site (1612 cm^{-1}).

The distribution of the protons in the structure is considered from the 0.68 mmol of cesium per gram of Cs_2HPW and the total protons reacted (0.12 mmol g^{-1} of solid). Thus 0.80 mmol of protons per gram reacted from 1.04 mmol g^{-1} of H_3PW. The 77% of the original protons of H_3PW correspond to a ratio of 3:1 between protons positioned at the edges and on the faces. That ratio is close to that obtained by Cal-ad from site 2 to site 1 (3.3). This suggests that on average, reaction of Cs_2HPW with pyridine occurs in four out of every five layers in the solid.

It is observed that the strong acid site in all these solids is only a fraction of the protons available, but this fraction increases with the amount of cesium atoms. The strength decreases in the order $H_3PW > Cs_2HPW > CsH_2PW$. This order is not expected on the basis of charge on the conjugate base and suggests that the lattice energy changes that accompany reaction with pyridine make a significant contribution to the enthalpy measured.

Solid $Cs_{2.5}H_{0.5}PW$ is reported to be a mixture of Cs_2HPW and Cs_3PW [81]. Our results from ^{31}P NMR pointed out that only one type of compound is present (vide infra). The increased amount of acidic sites going from CsH_2PW to $Cs_{2.5}H_{0.5}PW$ indicates that exposure of protons are markedly dependent of the surface area for these cesium heteropoly compounds. The formation of pores are also well evidenced from the adsorption of pyridine on $Cs_{2.5}H_{0.5}PW$ (Figure 3-10). As the surface area increases, more protons can be accessed and titrated.

FTIR spectrum of $Cs_{2.5}H_{0.5}PW$ (vide infra) shows a larger band for the pyridinium ion (1540 cm^{-1}) compared to the Cs_2HPW and CsH_2PW, in this order respectively. This agrees to the Cal-ad results where the $Cs_{2.5}H_{0.5}PW$ is as strong as Cs_2HPW, and more protons are accessible. Our Cal-ad results suggests that every single layer of the $Cs_{2.5}H_{0.5}PW$ salt reacts with pyridine. This can be obtained considering that 0.87 mmol of cesium per gram of $Cs_{2.5}H_{0.5}PW$ plus the total protons reacted (about 0.17 mmol g^{-1} of solid) leads to 1.04 mmol of protons per gram reacted from 1.04 mmol g^{-1} of H_3PW. The 100% of the original 1.04 mmol of protons from H_3PW correspond to a ratio of 3:1 between protons positioned at the edges and on the faces. That ratio is close to that obtained by Cal-ad from site 2 to site 1 (2.6). Thus, all layers of $Cs_{2.5}H_{0.5}PW$ have been titrated with pyridine.

The magnitude of the ΔH_1 for $Cs_{2.5}H_{0.5}PW$ (-27.5 kcal mol^{-1}) as well as the higher number of acidic protons (n_1 = 0.05 mmol g^{-1}), compared to only 0.008 mmol g^{-1} for surface protons on H_3PW, show why this compound is more effective in some alkylation reactions than H_3PW. With presence of pores in its structure and higher surface area than H_3PW, $Cs_{2.5}H_{0.5}PW$ have more surface protons available to catalytic reactions.

Results of FTIR, XRD and ^{31}P MAS NMR of $Cs_xH_{3-x}PW$ Compounds

FTIR spectra of $Cs_xH_{3-x}PW$ salts were taken before and after reaction of the compounds with pyridine. A comparative analysis, presented in Table 3-6, concludes the Keggin anion is practically not altered by substitution of H^+ by Cs^+, as observed for K^+ and Al^{3+} salts [51]. Reaction with pyridine does not change the characteristic Keggin bands. However, the region between 1700-1450 cm^{-1} shows the pyridinium ion through the presence of the bands at 1540 cm^{-1} and 1485 cm^{-1} [91]. Coordinated or hydrogen-bonded pyridine shows a band at 1612 cm^{-1} [91]. Those bands were observed (Figure 3-11) for all cesium salts except Cs_3PW which presents only a wide band at 1612 cm^{-1}. The ratio, based on the relative height of the bands, between the hydrogen-bonded pyridine band (1612 cm^{-1}) to the pyridinium band (1540 cm^{-1}) are 3.9 for CsH_2PW, 3.1 for Cs_2HPW, and 2.4 for $Cs_{2.5}H_{0.5}PW$. Compared to Cal-ad analysis these ratio of the bands support the choice of two site fit for the cesium salts, since the ratio between n_2 to n_1 are 3.6 for CsH_2PW, 3.3 for Cs_2HPW, and 2.6 for $Cs_{2.5}H_{0.5}PW$. Based on these results the nature of second site for CsH_2PW, Cs_2HPW and $Cs_{2.5}H_{0.5}PW$ are assigned as hydrogen-bonded pyridine in the solid, while the strongest site 1 is a Brönsted type site.

Table 3-6. Comparative Infrared Bands (cm^{-1}) of the Keggin Anion for H_3PW and Cs_2HPW.

Group	H_3PW^a	H_3PW dry^b	$H_3PW16{\cdot}H_2O$	H_3PW-Py	Cs_2HPW^c	Cs_2HPW-Py
P-O	1081	1082	1076	1080	1078	1078
$W-O_t$	984	991	978	978	984	984
$W-O_c-W$	892	895	916	891	889	889
$W-O_e-W$	794	801	734	806	799	799

a. Values obtained for $H_3PW6{\cdot}H_2O$ from reference [51].
b. Values obtained for H_3PW dried at 162 °C/4 hs/vacuum from reference [74].
c. Cs_2HPW dried at 200 °C/4 hs/vacuum. The other cesium salts have the same bands.

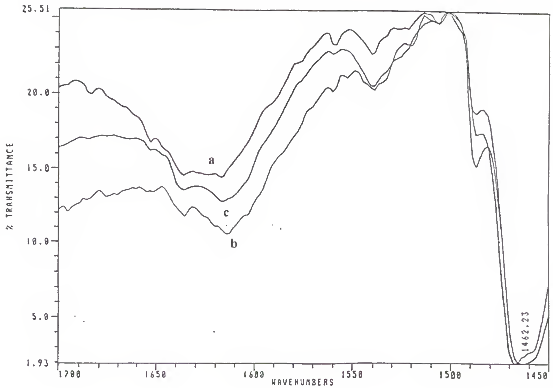

Figure 3-11. FTIR Spectra of CsH_2PW (**a**), Cs_2HPW (**b**) and $Cs_{2.5}H_{0.5}PW$ (**c**) after Reaction with Pyridine in Cyclohexane.

The XRD patterns for the cesium salts were recorded. The results are presented in Figure 3-12(a-d). It is observed that the main peaks present on the free H_3PW are shifted toward higher angles in CsH_2PW and Cs_2HPW. This result is consistent with the smaller cubic lattice parameters obtained for these compounds in the literature [80]. However, $Cs_{2.5}H_{0.5}PW$ and Cs_3PW shows shifts to lower angles, compared to H_3PW, which indicates these prepared compounds may be different from the ones reported in the literature [80]. In fact, no XRD pattern is reported for $Cs_{2.5}H_{0.5}PW$ in the literature. The spectra display only small differences going from CsH_2PW to Cs_3PW, but a carefully analysis of the reflections in Table 3-7 demonstrates they are distinct, although they probably have similar structures.

Spectra of ^{31}P MAS NMR were taken on all cesium derivatives. The results are presented in Figure 3-13. Contrary to the literature [81], the spectra show only a single peak for each cesium containing compound. There is an approximately linear shift to lower field in the ^{31}P NMR spectra going from H_3PW to Cs_3PW. Exchange of protons for cesium atoms causes increased electronic density at the phosphorous core because the protons are less mobile in these structures. The lower mobility of the protons in the cesium containing compounds causes the observed shielding shift. These single peaks suggest that the protons are located in random positions in the structure of each of the cesium derivatives. This result conflicts with another report [81] but is consistent with all other measurements performed in these solids. No evidence of mixtures of the cesium compounds with free H_3PW could be assigned in this report.

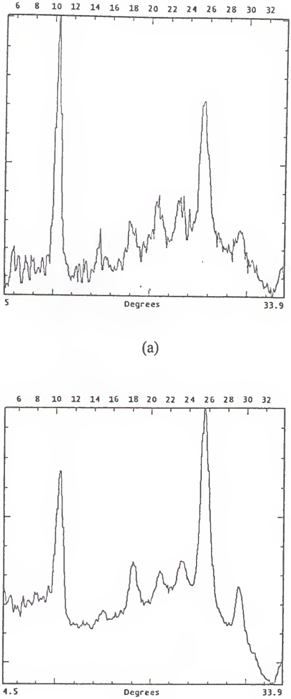

(a)

(b)

Figure 3-12. XRD Pattern of: (a) CsH_2PW; (b) Cs_2HPW.

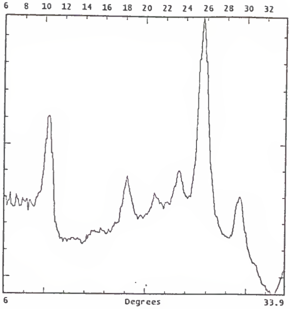

(c)

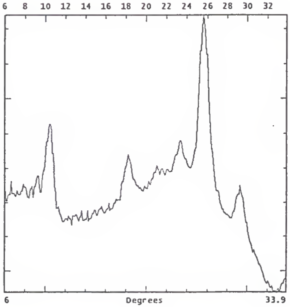

(d)

Figure 3-12. XRD Pattern of: (c) $Cs_{2.5}H_{0.5}PW$; (d) Cs_3PW.

Table 3-7. XRD Patterns of CsH_2PW, Cs_2HPW, $Cs_{2.5}H_{0.5}PW$, and Cs_3PW.

2θ Angle (degree)	d-spacing (Å)	Intensity (V)
CsH_2PW		
10.40	8.51	27.1
18.20	4.87	14.6
21.00	4.23	5.5
23.30	3.82	7.7
25.60	3.48	56.4
29.30	3.05	16.4
Cs_2HPW		
10.60	8.35	46.0
15.10	5.87	7.8
18.60	4.77	7.6
21.10	4.21	12.3
25.80	3.45	23.8
29.60	3.02	3.8

Table 3-7. continued

2θ Angle (degree)	d-spacing (Å)	Intensity (V)
$Cs_{2.5}H_{0.5}PW$		
8.30	10.65	173.0
9.00	9.83	61.4
10.20	8.67	40.3
14.80	5.99	15.0
16.90	5.25	18.0
17.80	4.98	14.4
20.30	4.37	22.9
22.60	3.93	6.8
25.00	3.56	60.6
27.50	3.24	27.6
28.40	3.14	19.1
33.00	2.71	32.5
Cs_3PW		
10.20	8.67	256.7
12.50	7.08	1.9
14.40	6.15	39.1
17.70	5.01	33.3
20.30	4.38	63.2
22.70	3.92	42.3
24.80	3.59	133.1
28.50	3.13	29.0
33.00	2.71	47.2

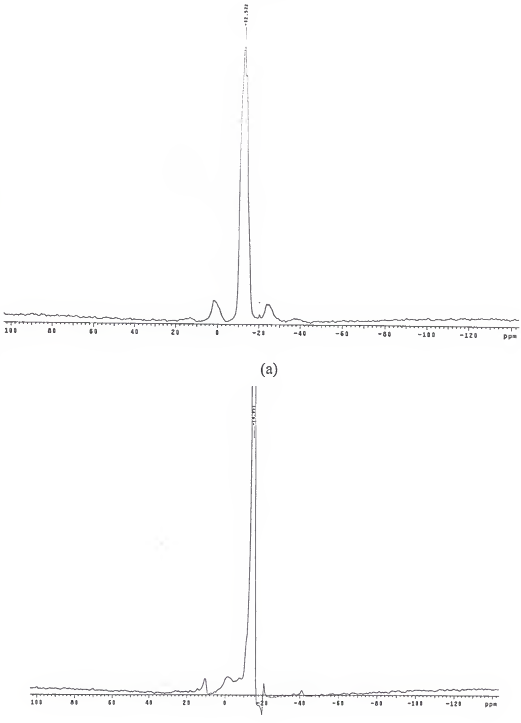

(a)

(b)

Figure 3-13. ^{31}P MAS NMR Spectra of: (a) CsH_2PW(δ = -12.53 ppm); (b) Cs_2HPW (δ = -14.95 ppm).

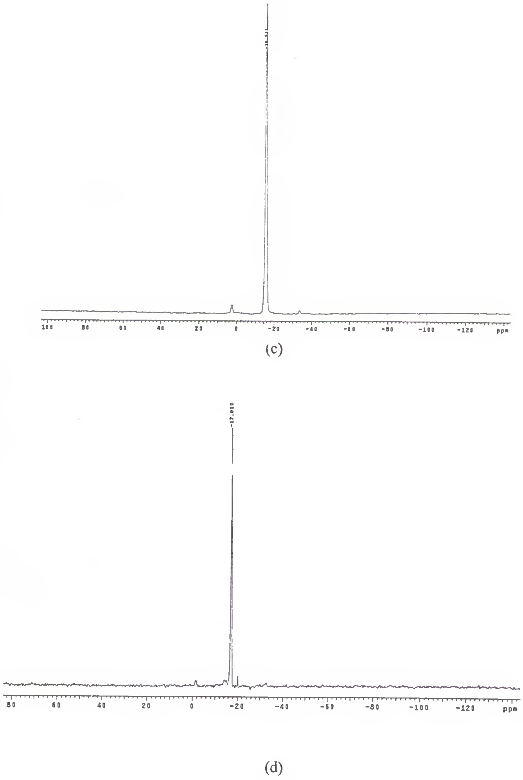

Figure 3-13. ^{31}P MAS NMR Spectra of: (c) $Cs_{2.5}H_{0.5}PW$ (δ = -15.51 ppm); (d) Cs_3PW (δ = -17.01 ppm).

Comparison of Acidity of H_3PW in Homogeneous and Heterogeneous System

Acidity of H_3PW was measured in solution of CH_3CN using calorimetry [74]. In homogeneous solution of a solvent of equal or lower basicity than acetonitrile, H_3PW behaves as a triprotic acid with the first proton stronger, but only partially dissociated. According to ECW analysis [74], the first proton has an enthalpy of -30.4 kcal mol^{-1} when it reacts with pyridine (corrected for the enthalpy of displacement of CH_3CN) . The value obtained in this work (-32.7 kcal mol^{-1}) is in good agreement with the former study. This demonstrate that the use of enthalpies to compare neutral donor-acceptor reactions and ionic products are possible in low polarity solvents, like acetonitrile, as well as non polar solvents, like cyclohexane. This is only possible if the contribution of solvation of the polar solvent can be factor out. Using the ECW model [74] an estimate of the net solvation energies of products and reactants together with the endothermic enthalpy of dissociation of the anion from $(CH_3CN)_3H_3PW$ was obtained.

As pointed out [74], in solution of acetonitrile an equilibrium mixture between the completely dissociated ion pair and hydrogen bonding species is possible for the H_3PW equilibria, especially for the second and third steps of its dissociation:

$$B_{sol} + H\text{-}X_{sol} \rightleftharpoons \underset{(a)}{B\text{--}H\text{-}X_{sol}} \rightleftharpoons \underset{(b)}{B\text{-}H^{+}\text{--}X^{-}_{sol}} \rightleftharpoons \underset{(c)}{BH^{+}_{sol} + X^{-}_{sol}} \qquad (3.4)$$

The solvent may influence the association, proton-transfer, and dissociation steps. The main factor which determines the position of a Brönsted acid-base equilibrium in Equation 3.4 is the differential solvation of the covalent and the ionic hydrogen-bonded complexes (a) and (b). For H_3PW in CH_3CN, second and third proton dissociations have shown possible mixtures between species (b) and (c) [74].

In cyclohexane much less complications are related to the solvent. H_3PW is not soluble in this solvent. Cyclohexane is a non specific interacting solvent. It has a low dielectric constant, and therefore is expected formation of only ion pairs in solution (products b and c from Equation 3.4). H_3PW is a strong Brönsted solid acid and formation of ion-pair product in cyclohexane is expected, where the proton is completely transferred to the base (product b in Equation 3.4).

Comparison of the second enthalpy in cyclohexane (ΔH_2 = -19.6 kcal mol^{-1}) with that obtained in CH_3CN (ΔH_2 = -21.2 kcal mol^{-1}), considering the displacement of the anion $(CH_3CN)_2HPW^{2-}$ to be equal to -9.4 kcal mol^{-1} (the same order of magnitude of the dissociation of $(CH_3CN)_2H_2PW^{-}$) shows a close agreement between enthalpy measurements in solution and in the solid. The enthalpy of the second site in solid H_3PW is considerably reduced over that of the first. This could result from an endothermic contribution from expanding the lattice of H_3PW^{-}. Titration of the protons on the edges of the cube expand the structure, while the strong acid site on the face of the unit cell is accessed in the solid structure. In solution, the lower enthalpy is attributed to the higher energy bonding of the proton to the polyanion resulting from the dissociation of the first proton.

Conclusions

This work provides thermodynamic constants for H_3PW and $Cs_xH_{3-x}PW$ (x = 1, 2, 2.5, and 3) reacting with pyridine in cyclohexane solution. The Cal-ad results indicate that the protons of H_3PW in the solid behaves like in solution, with all having different strengths. This achievement disagrees with previous claims by gas-solid calorimetry that all protons on solid H_3PW are equivalent. Similar to solutions of low basicity solvents such as CH_3CN, where H_3PW behaves as a strong monoprotic acid, in solid state it can donate protons with different levels of acidity. Restrictions of size and polarity of the donor molecule and polarity of medium can influence the effectiveness of the proton transfer. Two kinds of protons with different strengths are assigned for solid H_3PW, according to its cubic unit cell: face protons (site 1) and edge protons (site 2). The enthalpies for reaction of the most acidic proton (site 1) with pyridine (ΔH_1 = -32.7 kcal mol^{-1}) and site 2 (ΔH_2 = -19.6 kcal mol^{-1}) are in good agreement with the value obtained in solution of acetonitrile (ΔH_1 = -30.4 kcal mol^{-1} and estimated ΔH_2 = -21.2 kcal mol^{-1}) respectively.

The incomplete neutralization of the total available protons of H_3PW with pyridine in cyclohexane is explained by formation of a layered product. On average, one out of every four layers of H_3PW is neutralized out by pyridine. This result is confirmed by Cal-ad through the ratio of the number of sites for site 2 (assigned to protons on the edge) to site 1 (assigned to protons on the face).

Measurements of enthalpy for the strongest protons in each compound lead to the following order of acidity: $H_3PW > Cs_2HPW \cong Cs_{2.5}H_{0.5}PW > CsH_2PW > Cs_3PW$. The increased acidity with the surface area in the cesium series confirms $Cs_{2.5}H_{0.5}PW$ as a strong catalyst, having an acidity comparable to Cs_2HPW. Cs_3PW presents only residual protons and the concentration of protons becomes very low and so does the acidity as measured by Cal-ad. The CsH_2PW compound has a smaller surface area than H_3PW which explains its comparatively lower acidity.

The ^{31}P MAS NMR, XRD, FTIR and Cal-ad results confirm that $Cs_xH_{3-x}PW$ compounds are not simple mixtures of H_3PW with the exchanged cesium derivatives. The positions of proton and cesium atoms in the salt structures are random and homogeneously distributed. Based on the Cal-ad results for the relative amount of sites 1 and 2 in the cesium derivatives an attempt to distribute the proton and cesium atoms in the structure is proposed.

Reaction with pyridine of the cesium derivatives shows incomplete neutralization of the total available protons for each compound, except for $Cs_{2.5}H_{0.5}PW$ and Cs_3PW. For $Cs_{2.5}H_{0.5}PW$, all protons available react with pyridine, which concludes that every single layer in the solid is titrated. Cs_3PW has only residual protons and all react with pyridine. For CsH_2PW, one out of every two layers reacts with pyridine, while for Cs_2HPW four out of every five layers reacts with pyridine. This proposition is supported by the Cal-ad results as well as the other spectroscopic methods used.

CHAPTER 4

ACIDITY OF $H_3PW_{12}O_{40}$ SUPPORTED ON SILICA, ALUMINA, AND CARBON

Introduction

Keggin-type heteropoly acids (HPAs) have been extensively studied because they possess strong acidic and redox properties [32]. The different acidity and relatively high thermal stability of the heteropoly acids allows them to be used in several acid-catalyzed reactions in homogeneous solution, liquid-solid and gas-solid heterogeneous reactions. It has been demonstrated that HPAs are much more effective in acid catalysis than protonic mineral and organic acids such as sulfuric and p-toluenesulfonic acids [31].

HPAs have been supported on different solids to increase the surface to find a better catalyst for reactions of non polar molecules with heteropoly compounds. It is known that HPAs can absorb polar molecules into their bulk leading to a pseudoliquid-phase type of catalysis. Non-polar molecules react only on the surface or between surface layers of the crystals [11]. Because the surface area of HPAs are usually very low, increasing the surface area of supported HPAs could produce a catalyst with higher activity for reactions involving non polar substrates.

Silica gel is the most often used carrier for HPAs. SiO_2-H_3PW supported has been characterized by XRD and TPD of ammonia [94], microcalorimetry with ammonia adsorption [41, 95], and NMR [92, 96]. No distinct diffraction peaks appear on the XRD spectrum, but when loading is higher than 20 wt.% a broad peak occurs at $2\theta = 10^{\circ}$, characteristic of H_3PW. Mechanical mixtures of H_3PW and SiO_2 show this peak with amounts of heteropoly acid as low as 5 wt.% [94]. According to TPD of ammonia absorption [94], the strength of SiO_2-H_3PW supported is independent of amount of the heteropoly acid, but the total acidity increases with the H_3PW content. TPD [94] and microcalorimetry [41, 95] with NH_3 indicate that H_3PW supported on SiO_2 is weaker than the pure acid. The nature of interaction between H_3PW and SiO_2 has been elucidated by ^1H and ^{31}P MAS NMR. No difference in the ^1H NMR spectra of SiO_2 and SiO_2-H_3PW supported is observed up to 50 wt.% of H_3PW, except that the Si-OH line intensity drops as loading of H_3PW increases [92]. It is concluded that at concentrations below 50 wt.% of H_3PW over SiO_2 the proton structure is different from that crystalline H_3PW. This is also confirmed by the shift in the ^{31}P NMR spectra for 3-20 wt.% of H_3PW supported on SiO_2 [92, 96]. The interaction of SiO_2 with H_3PW is attributed to the formation of $(\equiv SiOH_2^+)(H_2PW_{12}O_{40}^-)$ species [96]. At concentrations up to 20 wt.% of H_3PW supported, the surface species are isolated, while at higher than 50 wt.% content crystals of free H_3PW are formed on the silica surface [92]. Various forms of the polyanions are observed on the silica surface using TEM (transmission electron spectroscopy). Isolated molecules and clusters of 50 to 500 Å in size are identified [97], depending on the HPA loading.

Alumina is usually considered as unsuitable as a support because it decomposes the Keggin structure of HPAs [27, 11]. This decomposition is controversial for $H_3PMo_{12}O_{40}$ [98, 99]. Studies by ^{31}P NMR indicate that the interaction between H_3PW

and γ-Al_2O_3 is not strong and the Keggin structure is maintained. If γ-Al_2O_3-H_3PW supported is heated above 200 °C, the ^{31}P signal broadness suggesting decomposition of the polyanion structure [98]. Comparison of the catalytic activity of H_3PW supported on γ-Al_2O_3 and SiO_2 for cumene cracking, toluene disproportionation and n-hexane isomerization indicate that centers of different acid strength are present on both catalysts with the same loading of heteropoly acid [100]. It is claimed [100] that the interaction of H_3PW with alumina forms aluminum salts, for contents up to 10 wt.% of the acid. The aluminum salts of H_3PW are reported [50] to contain both Lewis-acid centers (coordinatively unsaturated aluminum cations) and Brönsted-acid sites. The IR spectrum of alumina-H_3PW supported shows bands of very low intensity with no distinct peaks in the region of Keggin vibrations [100].

Activated carbon entraps HPAs in pores forming insoluble compounds that do not leach any acid from the catalyst support. The catalyst can be used for liquid-solid and gas-solid organic reactions in polar media. Leaching of HPAs has been tested by extraction of the polyacids with water and methanol [101]. The fraction of HPA dissolved out of the carbon support (Calgon F-300) depends upon the initial loading and the solvent employed, but a final concentration of 7-14 wt.% is left after about 20 hs of extraction. Characterization of carbon-H_3PW supported performed by microcalorimetry with NH_3 adsorption [102] shows that interaction of H_3PW with activated carbon is strong. H_3PW supported on carbon (Darco) is a weaker acid than the pure acid, and the heat is dependent upon the polyanion loading. It is claimed [103] that supporting H_3PW on various oxides (e.g., silica) does not cause such a drastic decrease in acidity. It is proposed [104] that proton transfer occurs from the heteropoly acid to the basic groups (e.g., alcohols, amines) on the carbon support. Nonetheless, results of microcalorimetry are interpreted assuming only coulombic interactions of H_3PW with the surface groups on carbon [103]. Potentiometric titrations and ^{31}P MAS NMR experiments [103] of H_3PW supported on carbon confirms no degradation of the Keggin structure when it is deposited on carbon black.

The objective of this research is to characterize the acidity of H_3PW supported on different carries, such as silica gel, alumina, and carbon by Cal-ad. Cal-ad determines the number of sites (n_i), equilibrium constants (K_i), and enthalpies (ΔH_i) for different acid sites on these solids. Comparison with the Cal-ad results of free H_3PW are discussed.

Experimental

Materials and Preparation of H_3PW Supported

Elemental and TG analysis of the H_3PW (purchased from Aldrich) revealed 16 moles of water per mole of H_3PW. Cyclohexane obtained from Fisher was purified by drying over 4A molecular sieves for 24 hours, and then distilled over P_2O_5. Pyridine obtained from Fisher was distilled over CaH_2. Dried samples were stored in a container with 4A molecular sieves. The support was Davisil® silica gel grade 62, obtained from Aldrich, with particles within 60-200 mesh and a surface area of 260 $m^2\ g^{-1}$. Brokman® activated acidic aluminum oxide obtained from Fisher, was used with particles within 80-200 mesh and a surface area of 155 $m^2\ g^{-1}$. The support supplied by Rohm and Haas was Ambersorb® 572 with 100-200 mesh particles and with a surface area of 1160 $m^2\ g^{-1}$.

The H_3PW supported catalysts were prepared by impregnation. Aqueous solutions of H_3PW in 0.1 mol L^{-1} of HCl were prepared using concentrations that depend upon the desired loading of the support (e.g., 20 wt.% H_3PW). The support was added to a volume of solution needed to form a suspension. The suspension was stirred with a magnetic bar/stir plate and evaporated in a oil bath at 80 °C to dryness. Then the solid was ground to fine particles and dried in a reactor under vacuum. No pretreatment of supports was carried out, except for Ambersorb® 572 which was washed with a solution of 0.1 mol L^{-1} of HCl for 6 hours and then dried at 100 °C overnight under vacuum, before impregnation with H_3PW. All H_3PW supported samples were dried under vacuum at 200 °C for 6 hours, except carbon-H_3PW supported which was dried at 100 °C for 12 hours.

FTIR, Calorimetric and Adsorption Measurements

Calorimetric, FTIR, and adsorption measurements were performed on the H_3PW supported samples according to the procedures described in Chapter 3. The analysis by the Cal-ad method was also explained in Chapter 3.

Results and Discussion

Cal-ad Analysis of Silica-H_3PW Supported

Calorimetric titrations with pyridine were performed on H_3PW supported on silica with different loadings of the polyacid. Loadings of H_3PW ranging from 8-24 wt.% were studied. The level of coverage to produced a monolayer in SiO_2 with a surface area of

300 m^2 g^{-1} is about 20 wt.% of H_3PW. The results of average enthalpy (calculated based on limiting reagent assumption) for reaction of these solids are presented in Table 4-1.

Table 4-1. Results of Calorimetric Titrations (25 ± 1 °C) of SiO_2-H_3PW supported with Pyridine.

wt.% H_3PW	mmol H_3PW/g of solid	mmol H^+/g of solid[a]	$-\Delta H_{AVG}$ (kcal mol^{-1})[b]
24.5	0.084	0.252	27
19.5	0.068	0.204	26
15.3	0.053	0.159	24
7.6	0.026	0.078	21

a. Value based on the amount of H_3PW.
b. The average enthalpy is based on the first two or three additions of pyridine in the calorimetric titration.

This semi-quantitative result shows that the interaction of H_3PW with SiO_2 is strong (ΔH_{AVG} = -26 kcal mol^{-1}) and almost independent of the heteropoly acid content in the range from 15-24 wt.% of H_3PW. Loading 8 wt.% of H_3PW gives lower enthalpy (ΔH_{AVG} = -21 kcal mol^{-1}). Based upon these observations, full Cal-ad analysis was made on the SiO_2-H_3PW supported 24.5 wt.% sample. The calorimetric and adsorption isotherms of its reaction with pyridine in cyclohexane are shown in Figure 4-1.

The Cal-ad data were analyzed assuming the presence of two sites and three sites. Three site fit gives a meaningless result for site 3 with high standard deviation errors for the parameters. The two site fit gives better standard deviations on the parameters and has the sum of squares of residuals of the same order of magnitude as the experimental

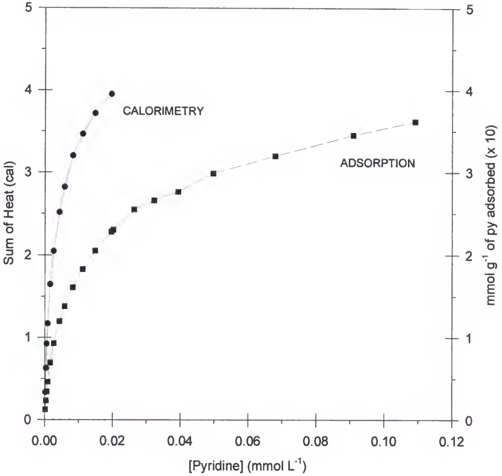

Figure 4-1. Isotherms of Calorimetry and Adsorption of SiO_2-H_3PW supported (24.5 wt.%) Reacted with Pyridine in Cyclohexane.

error. Table 4-2 reports the thermodynamic parameters for the interaction with pyridine of H_3PW supported on silica.

The enthalpy of interaction with pyridine for site 1 (ΔH_1 = -27.9 kcal mol^{-1}) is smaller than the enthalpy of pure H_3PW (ΔH_1 = -32.7 kcal mol^{-1}), but the number of sites are slightly higher (0.10 mmol g^{-1}) for H_3PW supported on silica than for the free acid (0.08 mmol g^{-1}). The second site enthalpy is 10.1 kcal mol^{-1} and a number of sites of 0.31 mmol g^{-1}, while free H_3PW shows ΔH_2 = -19.6 kcal mol^{-1} with n_2 = 0.16 mmol g^{-1}. These results suggest that H_3PW is well dispersed on silica gel. The total protons available from H_3PW (0.255 mmol g^{-1}) are titrated as shown by the sum of n_1 and n_2 (0.41 mmol g^{-1}). A strong interaction between H_3PW and silica is indicated by ^1H and ^{31}P NMR [92, 96]. At concentrations up to 20 wt.% the species on the surface are considered isolated [92]. Therefore it can be concluded that reaction occurs between H_3PW and SiO_2 forming a weaker acid than the free acid. The FTIR spectrum (Figure 4-2) shows that the Keggin structure is practically intact when H_3PW is supported on silica. After reaction with pyridine the formation of pyridinium ion is indicated by the band at 1540 cm^{-1} [91]. Hydrogen-bonded pyridine is also indicated by a band at 1620 cm^{-1}.

Cal-ad Analysis of Alumina-H_3PW Supported

Cal-ad results for alumina-H_3PW supported are shown in Table 4-2 while isotherms from calorimetry and adsorption experiments are given in Figure 4-3. The values obtained for site 1 (ΔH_1 = -22.6 kcal mol^{-1}, n_1 = 0.15 mmol g^{-1}) and site 2 (ΔH_2 = -12.0 kcal mol^{-1}, n_2 = 0.20 mmol g^{-1}) demonstrate this is a weaker solid acid than H_3PW. However, the quantity of sites are considerable higher than that of pure H_3PW. This

Table 4-2. Cal-ad Results for SiO_2^a-H_3PW supported (24.5 wt.%), $Al_2O_3^b$-H_3PW supported (19.4 wt.%), and Carbon[c]-H_3PW supported (20.1 wt.%) with Pyridine in Cyclohexane.

	H_3PW/SiO_2	H_3PW/Al_2O_3	H_3PW/Carbon
n_I (mmol g^{-1})	0.102 ± 0.005	0.152 ± 0.007	0.129 ± 0.002
K_I (M^{-1})	$6.7x10^5 \pm 1.3x10^4$	$1.2x10^5 \pm 2.3x10^3$	$1.2x10^7 \pm 3.2x10^4$
$-\Delta H_I$ (kcal mol^{-1})	27.9 ± 0.7	22.6 ± 0.2	22.4 ± 0.1
$-\Delta G_I$ (kcal mol^{-1})	7.9	6.9	9.7
ΔS_I (cal K^{-1} mol^{-1})	-66.7	-52.7	-42.8
n_2 (mmol g^{-1})	0.31 ± 0.06	0.20 ± 0.04	0.21 ± 0.11
K_2 (M^{-1})	$3.8x10^4 \pm 7.2x10^3$	$4.9x10^3 \pm 8.7x10^2$	$8.6x10^4 \pm 4.8x10^4$
$-\Delta H_2$ (kcal mol^{-1})	10.1 ± 2.9	12.0 ± 1.1	6.0 ± 4.9
$-\Delta G_2$ (kcal mol^{-1})	6.2	5.0	6.7
ΔS_2 (cal K^{-1} mol^{-1})	-12.8	-23.4	2.4
Total H^+ (mmol g^{-1})[d]	0.255	0.202	0.209

a. Davisil® silica gel grade 62 with surface area of 260 m^2 g^{-1}.
b. Brokman® activated acidic aluminum oxide with surface area of 155 m^2 g^{-1}.
c. Ambersorb® 572 carbonaceous adsorbent with surface area of 1160 m^2 g^{-1}.
d. Total millimoles of H^+ is based on the H_3PW content.

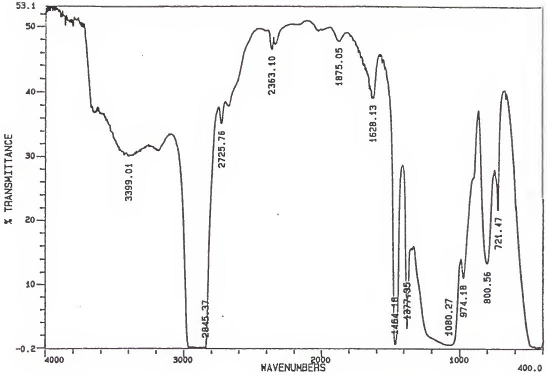

Figure 4-2. FTIR Spectrum of SiO_2-H_3PW supported (24.5 wt.%).

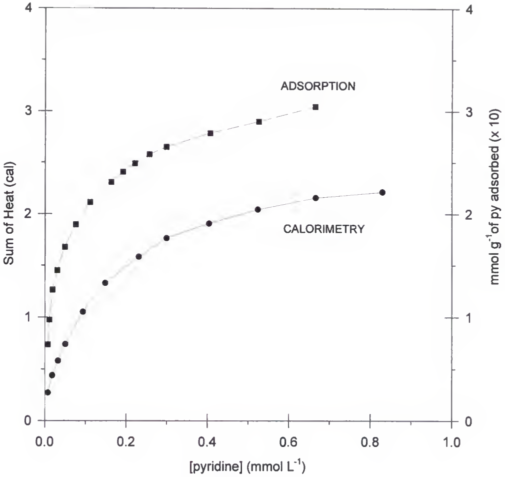

Figure 4-3. Isotherms of Calorimetry and Adsorption of Al_2O_3-H_3PW supported (19.4 wt.%) Reacted with Pyridine in Cyclohexane.

suggests that H_3PW is better dispersed on alumina than silica, even though the later carrier has a higher surface area. Other evidence of good dispersion comes from the total acidic protons presents from the H_3PW loading. About 75% of the total 0.202 mmol of protons per gram of solid are titrated as site 1. The nature of this site is quite different from pure H_3PW or alumina. The strength and quantity of sites for γ-Al_2O_3 [105] are $\Delta H_1 = -15.2$ kcal mol^{-1}, $n_1 = 0.16$ mmol g^{-1} and $\Delta H_2 = -6.7$ kcal mol^{-1}, $n_2 = 0.25$ mmol g^{-1} for site 1 and 2 respectively. These results imply that reaction of H_3PW with alumina produces new sites stronger than pure alumina but weaker than the heteropoly acid non-supported. The FTIR spectrum (Figure 4-4) of H_3PW supported on alumina shows that the Keggin bands are not well defined and shifts of the bands from the parent acid suggests some degree of decomposition of the heteropoly acid on the surface of alumina. After reaction of H_3PW supported on alumina with pyridine, FTIR spectrum shows two bands, one corresponding to pyridinium ion at 1540 cm^{-1} and one assigned to weakly coordinated pyridine at 1630 cm^{-1}.

Cal-ad Analysis of Carbon-H_3PW Supported

Ambersorb® 572 (A-572) load with 20.1 wt.% of H_3PW reacts with pyridine to give the calorimetric and adsorption isotherms shown in Figure 4-5. The results of Cal-ad (Table 4-2) shows 0.13 mmol per gram of solid and an enthalpy of -22.4 kcal mol^{-1} for site 1. The acid H_3PW on A-572 is much weaker than H_3PW ($\Delta H_1 = -32.7$ kcal mol^{-1} and $n_1 = 0.08$ mmol g^{-1}). The amount of strongest sites shows that H_3PW is well dispersed on the surface of the carbon. Although the supported acid is weaker than the pure H_3PW,

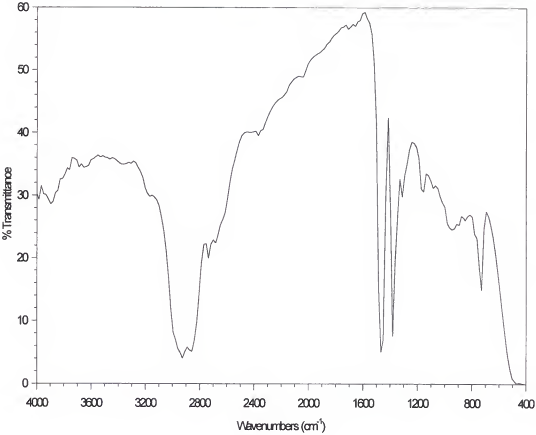

Figure 4-4. FTIR Spectrum of Al_2O_3-H_3PW supported (19.4 wt.%)

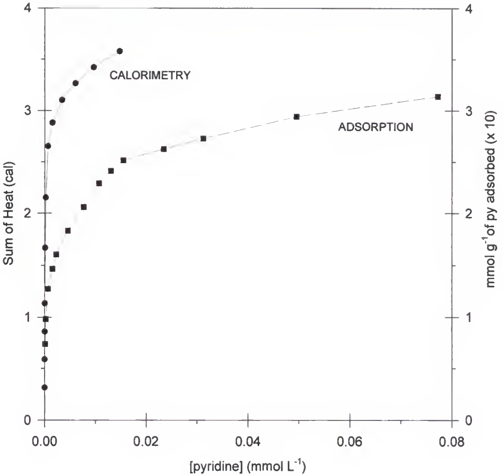

Figure 4-5. Isotherms of Calorimetry and Adsorption of Carbon-H_3PW supported (20.1 wt.%) Reacted with Pyridine in Cyclohexane.

77% of the 0.202 mmol of protons per gram of solid are titrated as site 1. This shows an increase in relation to pure H_3PW where only 8% of 1.04 mmol of protons per gram are titrated with pyridine as site 1. For reactions demanding solid acids with enthalpies about 25 kcal mol^{-1} H_3PW supported on carbon is a viable choice. The Cal-ad results help to explain why some reactions show better activity for carbon-H_3PW supported than the unsupported acid. The higher surface area leads to a higher number of relatively strong sites. The carbonaceous adsorbent used (A-572) has been characterized using gas-solid adsorption with nonpolar gases [106]. This material, a macroreticular sulfonated polystyrene resin which is pyrolyzed, does not show any measurable acidity. Titration of the carbon with pyridine yield no detectable heat. Therefore, all acidic properties of the H_3PW supported on Ambersorb® 572 carbon is provided by the H_3PW. The thermodynamic parameters for the second site of carbon-H_3PW supported ($\Delta H_2 = -6.0$ kcal mol^{-1} and $n_2 = 0.21$ mmol g^{-1}) correspond to weak hydrogen-bonding site. Physisorption of pyridine by H_3PW supported on A-572 can be seen in the adsorption curve (Figure 4-5). This contributes to the low enthalpy of site 2.

Conclusions

This work reports thermodynamic constants for H_3PW supported on silica, alumina, and carbon reacting with pyridine in cyclohexane solution. Loadings of H_3PW up to 25 wt.% on these carriers decrease the acidity of the free acid. However, the Cal-ad results show that H_3PW is well dispersed on these supports. The number of the strongest sites increases compared to the free H_3PW. This trend does not follow parallel the surface area of the different supports, as expected. The amount of the strongest sites increases in the order: H_3PW/alumina > H_3PW/carbon > H_3PW/silica, while the surface area is carbon >>silica > alumina.

The acidity order is consistent with the literature results where H_3PW > silica-H_3PW supported > alumina-H_3PW supported ≅ carbon-H_3PW supported. This acidity order reflects a stronger interaction of H_3PW with alumina and carbon than with silica. FTIR spectrum of H_3PW supported on alumina confirms the interaction of the Keggin anion with the silica and alumina supports. Shifts of the Keggin bands and even loss of the bands in the FTIR spectrum are observed for H_3PW supported on alumina. This explains the decrease in the enthalpy of H_3PW/Al_2O_3 catalyst compared to H_3PW.

APPENDIX

COMPUTER PROGRAM FOR CALCULATION OF CALORIMETRIC DATA IN HOMOGENEOUS SYSTEM

```
C***************************************************************************
C
C                     FORTRAN
C   PROGRAM: CALOR1.FOR
C
C
C   PURPOSE:
C      THIS PROGRAM WILL CALCULATE FROM  CALORIMETRIC  TITRATION DATA
C      THE ENTHALPIES OF DEPROTONATION, THE EQUILIBRIUM CONSTANTS AND
C      THE RESPECTIVE STANDARD  DEVIATIONS  FOR SYSTEMS  OF  ACIDS  WITH
C      ONE, TWO, OR THREE PROTONS IN NON AQUEOUS SOLUTIONS.
C***************************************************************************
C
C   REAL VARIABLES:
C
C   B    (R*4)    = BASE CONCENTRATION
C   BH   (R*4)    = PROTONATED BASE CONCENTRATION
C   DEFIND (R*8,6)  = DEFINED VARIABLES IN THE ORDER K1, K2, K3,
C               WTOT, BTOT, H.
C   RESULT  (R*8,6) = CONCENTRATIONS IN ORDER B,BH,WH3,WH2,WH1,WH0
C
C***************************************************************************
C   AUTHOR: TOM MAIER 02/27/97  INITIAL PROGRAM (Version 1.5)
C***************************************************************************
C   THE VERSION OF THIS PROGRAM FOR IBM/PC WAS ADAPTED BY JOSE A. DIAS
C   ON MARCH  1997 USING A MICROSOFT FORTRAN POWER STATION VERSION 1.0
C   FOR WINDOWS 3.1.
C
C   A FILE WITH INSTRUCTIONS ACCOMPANY THE DOCUMENTATION OF THIS PROGRAM.
C***************************************************************************

     IMPLICIT NONE
     REAL*8  Y(1000), BNON(6), X(1000,6), Z(1000), VAR, YH(1000)
     REAL*8  BASE(1000), D(1000,6), DY(1000), HEATIN(1000), VOL(1000)
     REAL*8  K1, K2, K3, H1, H2, H3, SVART, ACID(1000), SSQE, STD
     REAL*8  DUMMY, K1IN, K2IN, K3IN, H1IN, H2IN, H3IN, STDE(6)
     INTEGER  I, ICON, IN(6), ITMAX, J, NERR, NSIG, ND, NPTOT, NPF, NPV
     INTEGER  NFIRST, NLAST, NPR, IFIX(6), INF(6), CASE
     CHARACTER*5   CHAR*80, VARY1(6), VARY2(6), VARY3(6)
     CHARACTER*80 INFILE, OUTFILE

     DATA IN / 1, 2, 3, 4, 5, 6/
     DATA VARY1 / '  K1 ',' H1 ','    ','    ','    '/
     DATA VARY2 / '  K1 ',' K2 ',' H1 ',' H2 ','    '/
     DATA VARY3 / '  K1 ',' K2 ',' K3 ',' H1 ',' H2 ',' H3 '/

 1   PRINT *,''
     PRINT *,' THERE ARE THREE CASES WHICH THIS PROGRAM WILL HANDLE:'
     PRINT *,''
     PRINT *,'  1  ONE PROTON ON THE ACID'
     PRINT *,'       AH + B = A + BH  '
     PRINT *,''
     PRINT *,'  2  TWO PROTONS ON THE ACID'
     PRINT *,'       AH2 +  B = AH +  BH  '
```

```
      PRINT *,'      AH  +  B = A  +  BH  '
      PRINT *,'      AH2 + 2B = A  + 2BH  (TOTAL REACTION)'
      PRINT *,' '
      PRINT *,' 3  THREE PROTONS ON THE ACID'
      PRINT *,'      AH3 +  B = AH2 +  BH  '
      PRINT *,'      AH2 +  B = AH  +  BH  '
      PRINT *,'      AH  +  B = A   +  BH    '
      PRINT *,'      AH3 + 3B = A   +  3BH  (TOTAL REACTION)'
      PRINT *,' '
      PRINT *,' WHICH CASE DO YOU WANT TO USE?'
      READ(5,*) CASE
      IF (CASE .LT. 1  .OR.  CASE .GT. 3) GO TO 1
      NPR = 0
      PRINT *,' '
C  OPEN THE INPUT FILE.
      NPR = 0
      WRITE (6,3)
 3   FORMAT (5X,'Name of Input File?')
      READ (5,'(A80)') INFILE
      OPEN(UNIT=8,FILE=INFILE,STATUS='OLD')
      READ (8,*) NFIRST, NLAST
      DO I=NFIRST,NLAST
      J=I-NFIRST + 1
      READ (8, *) ACID(J), BASE(J), HEATIN(J), VOL(J)
      END DO
      ND = NLAST - NFIRST + 1
      CLOSE (8)
C THE DATA I AM USING HAS FOUR COLUMNS IN THE ORDER, ACID, BASE,
C HEAT MEASURED, AND TOTAL VOLUME OF THE SOLUTION.
C THE UNITS ARE MOL/L, MOL/L, CALORIES, AND LITERS RESPECTIVELY.
C ONE CAN USE DIFFERENT UNITS IF CORRECTLY DIMMENSIONED.

C  OPEN THE OUTPUT FILE.

      WRITE (6,4)
 4   FORMAT (5X, 'Name of Output File?')
      READ (5,'(A80)') OUTFILE
      OPEN (UNIT=43,FILE=OUTFILE )

C  START THE CALCULATIONS

      GO TO (20, 30, 40) CASE
 20  PRINT *,' '
      PRINT *,' ENTER AN INITIAL EST OF K1'
      READ (5,*) K1
      PRINT *,' '
      PRINT *,' ENTER AN INIT EST OF ENTHALPY, H1'
      PRINT *,' H1 IS FOR THE REACTION AH +  B -> A +  BH'
      PRINT *,' '
      READ (5,*) H1
      PRINT *,' '
      PRINT *,' HERE ARE THE VALUES YOU ENTERED, IN THE ORDER YOU'
      PRINT *,' ENTERED THEM. IF YOU WANT A TERM TO VARY IN THE'
      PRINT *,' REGRESSION, PUT A 1 UNDER THE NUMBER. IF YOU WANT'
      PRINT *,' IT TO STAY THE SAME (NO CHANGE BY THE REGRESSION), '
      PRINT *,' PUT A 0 UNDER THE NUMBER.'
      PRINT *,' '
      WRITE(6,FMT='(2X,6D10.2)') K1, H1
      DO I=3,6
        IFIX(I) = 0
        END DO
      READ (5,*) IFIX(1), IFIX(2)
      GO TO 50
 30   PRINT *,' '
      PRINT *,' ENTER AN INITIAL EST OF K1 AND K2'
      READ (5,*) K1, K2
      PRINT *,' '
      PRINT *,' ENTER AN INIT EST OF EHTHALPIES H1 AND H2'
      PRINT *,'  H1 IS FOR THE REACTION AH2 +  B -> AH  +  BH'
      PRINT *,'  H2 IS FOR THE REACTION AH2 + 2B -> A   + 2BH'
      PRINT *,' '
      READ (5,*)  H1, H2
      PRINT *,' '
      PRINT *,' HERE ARE THE VALUES YOU ENTERED, IN THE ORDER YOU'
      PRINT *,' ENTERED THEM. IF YOU WANT A TERM TO VARY IN THE'
      PRINT *,' REGRESSION, PUT A 1 UNDER THE NUMBER. IF YOU WANT'
      PRINT *,' IT TO STAY THE SAME (NO CHANGE BY THE REGRESSION), '
      PRINT *,' PUT A 0 UNDER THE NUMBER.'
      PRINT *,' '
      WRITE(6,FMT='(2X,6D10.2)') K1, K2, H1, H2
      IFIX(5) = 0
      IFIX(6) = 0
      READ (5,*) IFIX(1), IFIX(2), IFIX(3), IFIX(4)
      GO TO 50
 40   PRINT *,' '
      PRINT *,' ENTER AN INITIAL EST OF K1, K2, K3'
      READ (5,*) K1, K2, K3
      PRINT *,' '
      PRINT *,' ENTER AN INIT EST OF ENTHALPIES H1, H2, H3'
      PRINT *,' H1 IS FOR THE REACTION AH3 +  B -> AH2 +  BH'
      PRINT *,' H2 IS FOR THE REACTION AH3 + 2B -> AH1 + 2BH'
      PRINT *,' H3 IS FOR THE REACTION AH3 + 3B -> A   + 3BH'
      PRINT *,' '
      READ (5,*) H1, H2, H3
      PRINT *,' '
      PRINT *,' HERE ARE THE VALUES YOU ENTERED, IN THE ORDER YOU'
      PRINT *,' ENTERED THEM. IF YOU WANT A TERM TO VARY IN THE'
      PRINT *,' REGRESSION, PUT A 1 UNDER THE NUMBER. IF YOU WANT'
      PRINT *,' IT TO STAY THE SAME (NO CHANGE BY THE REGRESSION), '
      PRINT *,' PUT A 0 UNDER THE NUMBER.'
      PRINT *,' '
      WRITE(6,FMT='(2X,6D10.2)') K1, K2, K3, H1, H2, H3
      READ (5,*) IFIX
 50   K1IN = K1
      K2IN = K2
      K3IN = K3
      H1IN = H1
      H2IN = H2
      H3IN = H3
      NPF = 0
      NPV = 0
      DO I=1,6
      IF (IFIX(I) .EQ. 0) THEN
      NPF = NPF + 1
      INF(NPF) = I
      END IF
      IF (IFIX(I) .NE. 0) THEN
      NPV = NPV + I
      IN(NPV) = I
      END IF
      END DO
      DO I=1,NPF
      IN(NPV+I) = INF(I)
      END DO
 1002 FORMAT(6A5)
      IF (CASE .EQ. 1) THEN
      IF (NPV .GT. 0) THEN
      PRINT *,' '
      PRINT *,' THESE ARE THE TERMS WHICH WILL VARY:'
      PRINT *,' '
      WRITE(6,1002) (VARY1(IN(I)),I=1,NPV)
      END IF
      IF (NPF .GT. 0) THEN
      PRINT *,' '
      PRINT *,' THESE ARE THE TERMS WHICH WILL BE FIXED:'
      PRINT *,' '
      WRITE(6,1002) (VARYI(IN(NPV+I)),I=1,NPF)
      END IF
      END IF
      IF (CASE .EQ. 2) THEN
      IF (NPV .GT. 0) THEN
      PRINT *,' '
      PRINT *,' THESE ARE THE TERMS WHICH WILL VARY:'
      WRITE(6,1002) (VARY2(IN(I)),I=1,NPV)
      PRINT *,' '
      END IF
      IF (NPF .GT. 0) THEN
      PRINT *,' '
      PRINT *,' THESE ARE THE TERMS WHICH WILL BE FIXED:'
      PRINT *,' '
      WRITE(6,1002) (VARY2(IN(NPV+I)),I=1,NPF)
      END IF
      END IF
      IF (CASE .EQ. 3) THEN
      IF (NPV .GT. 0) THEN
      PRINT *,' '
      PRINT *,' THESE ARE THE TERMS WHICH WILL VARY:'
      PRINT *,' '
      WRITE(6,1002) (VARY3(IN(I)),I=I,NPV)
      END IF
      IF (NPF .GT. 0) THEN
      PRINT *,' '
      PRINT *,' THESE ARE THE TERMS WHICH WILL BE FIXED:'
      PRINT *,' '
      WRITE(6,1002) (VARY3(IN(NPV+I)),I=I,NPF)
```

```
END IF
END IF
PRINT *,' '
PRINT *,' HOW MANY ITERATIONS DO YOU WANT THE REGRESSION TO TRY?'
PRINT *,' IF YOU ENTER 0, IT WILL DO NO REGRESSION, BUT IT WILL'
PRINT *,' DO THE CALCULATIONS WITH YOUR INPUT VALUES.'
PRINT *,' IF YOU ENTER A NUMBER GREATER THAN 0, IT WILL DO THAT'
PRINT *,' NUMBER OF ITERATIONS.'
PRINT *,' '
READ (5,*) ITMAX
PRINT *,' '
NPTOT = 6
NSIG = 3
SVART = 1000000.
DO I=1,ND
Y(I) = HEATIN(I)
END DO
BNON(3) = 0.0
BNON(4) = 0.0
BNON(5) = 0.0
BNON(6) = 0.0
IF (CASE .EQ. 1) THEN
BNON(1) = K1
BNON(2) = H1
END IF
IF (CASE .EQ. 2) THEN
BNON(1) = K1
BNON(2) = K2
BNON(3) = H1
BNON(4) = H2
END IF
IF (CASE .EQ. 3) THEN
BNON(1) = K1
BNON(2) = K2
BNON(3) = K3
BNON(4) = H1
BNON(5) = H2
BNON(6) = H3
END IF
PRINT *,' '
NPR = 0
CALL CHEAT(BNON, Z, ND, BASE, ACID, VOL, NPR, CASE)
SSQE=0.0
DO I=1,ND
YH(I)=Z(I)
DUMMY= Y(I)-Z(I)
SSQE=SSQE+DUMMY*DUMMY
END DO
IF (NPV.GT.0 .AND. ITMAX.GT.0)  CALL NLREG(NPTOT,ND,X,Y,D,BNON,
*ICON,Z,YH,DY,NPF,NPV,IN,ITMAX,NSIG,VAR,BASE,ACID,VOL,CASE,
*STDE)

PRINT *,' '
IF (ICON.GT. 0) PRINT *,' NLREG CONVERGED',ICON,' ITERATIONS'
IF (ICON.EQ.-1) PRINT *,' NLREG STOPPED, TOO MANY ITERATIONS'
```

```
   IF (ICON.EQ.-2) PRINT *,' NLREG STOPPED, XPX MATRIX SINGULAR'
   IF (ICON.EQ.-3) PRINT *,' NLREG STOPPED, NO BETTER SOLUTION'

   IF (CASE .EQ. 1) THEN
   K1 = BNON(1)
   H1 = BNON(2)
   END IF
   IF (CASE .EQ. 2) THEN
   K1 = BNON(1)
   K2 = BNON(2)
   H1 = BNON(3)
   H2 = BNON(4)
   END IF
   IF (CASE .EQ. 3) THEN
   K1 = BNON(1)
   K2 = BNON(2)
   K3 = BNON(3)
   H1 = BNON(4)
   H2 = BNON(5)
   H3 = BNON(6)
   END IF
   NPR = 0
   CALL CHEAT(BNON, Z, ND, BASE, ACID, VOL, NPR, CASE)
   SSQE=0.0
   DO I=1,ND
   YH(I)=Z(I)
   DUMMY= Y(I)-Z(I)
   SSQE=SSQE+DUMMY*DUMMY
   END DO
   VAR = SSQE/(ND-6)
   STD = DSQRT(VAR)
   PRINT *,' BEST FIT FOUND:'
   PRINT *,' '
1000 FORMAT(A34, 2D14.4)
1001 FORMAT(34X, A31)
1003 FORMAT(/A34,2D14.4)

   IF (CASE .EQ. 1) THEN
   WRITE(6,1001) '   BEST FIT    INITIAL VALUE'
   WRITE(6,1000) ' AH  +  B -> A   +  BH       K1 =', K1, K1IN
   WRITE(6,1000) ' AH  +  B -> A   +  BH ENTHALPY =', H1, H1IN
   WRITE(6,1003) ' SUM OF SQUARES ERROR          =', SSQE
   WRITE(6,1000) ' VARIANCE                      =', VAR
   WRITE(6,1000) ' STANDARD DEVIATION            =', STD
   WRITE(6,1003) ' STANDARD ERROR OF K1          =', STDE(1)
   WRITE(6,1000) ' STANDARD ERROR OF ENTHALPY    =', STDE(2)

   WRITE(43,1001) '   BEST FIT    INITIAL VALUE'
   WRITE(43,1000) ' AH  +  B -> A   +  BH       K1 =',K1, K1IN
   WRITE(43,1000) ' AH  +  B -> A   +  BH ENTHALPY =',H1, H1IN

   WRITE(43,1003) ' SUM OF SQUARES ERROR          =',SSQE

   WRITE(43,1003) ' STANDARD ERROR OF K1          =', STDE(1)
WRITE(43,1003) ' STANDARD ERROR OF ENTHALPY    =', STDE(2)
END IF

IF (CASE .EQ. 2) THEN
WRITE(6,1001) '   BEST FIT   INITIAL VALUE'
WRITE(6,1000) ' AH2 +  B -> AH1 +  BH      K1 =', K1, K1IN
WRITE(6,1000) ' AH1 +  B -> A   + 2BH      K2 =', K2, K2IN
WRITE(6,1003) ' AH2 +  B -> AH1 +  BH ENTHALPY =', H1, H1IN
WRITE(6,1000) ' AH1 + 2B -> A   + 2BH ENTHALPY =', H2, H2IN
WRITE(6,1003) ' SUM OF SQUARES ERROR         =', SSQE
WRITE(6,1000) ' VARIANCE                     =', VAR
WRITE(6,1000) ' STANDARD DEVIATION           =', STD
WRITE(6,1003) ' STANDARD ERROR OF K1         =', STDE(1)
WRITE(6,1000) ' STANDARD ERROR OF K2         =', STDE(2)
WRITE(6,1003) ' STANDARD ERROR OF ENTHALPY 1  =', STDE(3)
WRITE(6,1000) ' STANDARD ERROR OF ENTHALPY 2  =', STDE(4)

WRITE(43,1001) '   BEST FIT   INITIAL VALUE'
WRITE(43,1000) ' AH2 +  B -> AH1 +  BH      K1 =',K1, K1IN
WRITE(43,1000) ' AH1 +  B -> A   +  BH      K2 =',K2, K2IN

WRITE(43,1003) ' AH2 +  B -> AH1 +  BH ENTHALPY =',H1, H1IN
WRITE(43,1000) ' AH2 + 2B -> A   + 2BH ENTHALPY =',H2, H2IN

WRITE(43,1003) ' SUM OF SQUARES ERROR         =',SSQE

WRITE(43,1003) ' STANDARD ERROR OF K1         =', STDE(1)
WRITE(43,1000) ' STANDARD ERROR OF K2         =', STDE(2)

WRITE(43,1003) ' STANDARD ERROR OF ENTHALPY 1  =', STDE(3)
WRITE(43,1000) ' STANDARD ERROR OF ENTHALPY 2  =', STDE(4)
END IF

IF (CASE .EQ. 3) THEN
WRITE(6,1001) '   BEST FIT   INITIAL VALUE'
WRITE(6,1000) ' AH3 +  B -> AH2 +  BH      K1 =', K1, K1IN
WRITE(6,1000) ' AH2 +  B -> AH1 +  BH      K2 =', K2, K2IN
WRITE(6,1000) ' AH1 +  B -> A   +  BH      K3 =', K3, K3IN
WRITE(6,1003) ' AH3 +  B -> AH2 +  BH ENTHALPY =', H1, H1IN
WRITE(6,1000) ' AH3 + 2B -> AH1 + 2BH ENTHALPY =', H2, H2IN
WRITE(6,1000) ' AH1 + 3B -> A   + 3BH ENTHALPY =', H3, H3IN
WRITE(6,1003) ' SUM OF SQUARES ERROR         =', SSQE
WRITE(6,1000) ' VARIANCE                     =', VAR
WRITE(6,1000) ' STANDARD DEVIATION           =', STD
WRITE(6,1003) ' STANDARD ERROR OF K1         =', STDE(1)
WRITE(6,1000) ' STANDARD ERROR OF K2         =', STDE(2)
WRITE(6,1000) ' STANDARD ERROR OF K3         =', STDE(3)
WRITE(6,1003) ' STANDARD ERROR OF ENTHALPY 1  =', STDE(4)
WRITE(6,1000) ' STANDARD ERROR OF ENTHALPY 2  =', STDE(5)
WRITE(6,1000) ' STANDARD ERROR OF ENTHALPY 3  =', STDE(6)

WRITE(43,1001) '   BEST FIT   INITIAL VALUE'
WRITE(43,1000) ' AH3 +  B -> AH2 +  BH      K1 =',K1, K1IN
WRITE(43,1000) ' AH2 +  B -> AH1 +  BH      K2 =',K2, K2IN
WRITE(43,1000) ' AH1 +  B -> A   +  BH      K3 =',K3, K3IN
```

```
      WRITE(43,1003) ' AH3 +  B -> AH2 +  BH ENTHALPY =',H1, H1IN
      WRITE(43,1000) ' AH3 + 2B -> AH1 + 2BH ENTHALPY =',H2, H2IN
      WRITE(43,1000) ' AH3 + 3B -> A   + 3BH ENTHALPY =',H3, H3IN

      WRITE(43,1003) ' SUM OF SQUARES ERROR         =',SSQE

      WRITE(43,1003) ' STANDARD ERROR OF K1         =', STDE(1)
      WRITE(43,1000) ' STANDARD ERROR OF K2         =', STDE(2)
      WRITE(43,1000) ' STANDARD ERROR OF K3         =', STDE(3)

      WRITE(43,1003) ' STANDARD ERROR OF ENTHALPY 1  =', STDE(4)
      WRITE(43,1000) ' STANDARD ERROR OF ENTHALPY 2  =', STDE(5)
      WRITE(43,1000) ' STANDARD ERROR OF ENTHALPY 3  =', STDE(6)
      END IF
      IF (ITMAX .GT. 0)
     *WRITE(43,1003) ' VARIANCE                  =', VAR
      IF (ITMAX .GT. 0)
     *WRITE(43,1000) ' STANDARD DEVIATION          =', STD
      IF (ITMAX .EQ. 0)
     *WRITE(43,FMT='(A32,D14.4)') ' NO REGRESSION WAS DONE.     '
      WRITE(43,FMT='(//,A32,/)') ' RECONSTRUCTION OF INPUT DATA: '
      WRITE(43,FMT='(A36,A13  )') ' POINT    MEASURED    PREDICTED  '
     * , ' DIFFERENCE '
      DO I=1,ND
      WRITE(43,FMT='(I6,3F14.6)') I, Y(I), Z(I),  (Y(I)- Z(I))
      END DO
      IF (CASE .EQ. 1) THEN
      WRITE(43,FMT='(//,5X,A4,8X,A4,6X,A9,3X,A9,2(6X,A3,3X))')
     *'ACID','BASE','FREE BASE','PROT BASE','AH1','AH0'
      END IF
      IF (CASE .EQ. 2) THEN
      WRITE(43,FMT='(//,4X,A4,6X,A4,3X,A9,2X,A9,3(4X,A3,3X))')
     *'ACID','BASE','FREE BASE','PROT BASE','AH2','AH1','AH0'
      END IF
      IF (CASE .EQ. 3) THEN
      WRITE(43,FMT='(//,4X,A4,5X,A4,4X,A9,2X,A9,4(4X,A3,3X))')
     *'ACID','BASE','FREE BASE','PROT BASE','AH3','AH2','AH1','AH0'
      END IF
      NPR = 1
      CALL CHEAT(BNON, Z, ND, BASE, ACID, VOL, NPR, CASE)
      CLOSE(43)
      STOP
      END

C=================================================================
C SUBROUTINE CHEAT(BNON, Z, ND, BASE, ACID, VOL, NPR, CASE)
C
C PURPOSE
C   THIS SUBROUTINE SETS UP THE CALCULATION FOR EACH TITRATION
C   POINT AND CALCULATES THE HEAT OF REACTION.
C
C VARIABLES
C  BNON   (R*8,6) = KS AND HS, DEPENDING ON CASE.
C  Z     (R*8,1000)= PREDICTED HEATS
```

```
C  ND     (I*4)   = NUMBER OF DATA POINTS
C  ACID   (R*8,1000)= TOTAL ACID CONCENTRATIONS
C  BASE   (R*8,1000)= TOTAL BASE CONCENTRATIONS
C  CASE   (I*4)   = 1=1 PROTON ACID, 2=2 PROTONS, 3=3 PROTONS
C  A      (R*8)   = ACID WITHOUT ANY PROTONS
C  AH     (R*8)   = ACID WITH ONE PROTON
C  AH2    (R*8)   = ACID WITH TWO PROTONS
C  AH3    (R*8)   = ACID WITH THREE PROTONS
C  B      (R*8)   = FREE BASE
C  BH     (R*8)   = PROTONATED BASE
C  DEFIND  (R*8,6) = DEFINED VARIABLES IN THE ORDER K1, K2, K3,
C                   WTOT, BTOT, H.
C  RESULT  (R*8,6) = CONCENTRATIONS IN ORDER B, BH, WH3, WH2, WH1, W
C
C==================================================================

      SUBROUTINE CHEAT(BNON, Z, ND, BASE, ACID, VOL, NPR, CASE)

      IMPLICIT NONE

      REAL*8 DEFIND(6), RESULT(6), WTOT, WH0, WH1, WH2, WH3
      REAL    EXPJ
      REAL*8   ATOT, BTOT, ONE, TWO, THREE, FOUR
      REAL*8   BNON(6), Z(1000), BASE(1000), ACID(1000), VOL(1000)
      REAL*8   K1, K2, K3, A, AH, AH2, AH3, B, BH, C, D, E
      REAL*8   DEL1, DEL2, BETA, BESAVE(2), PLOST, PONB
      INTEGER  CASE, I, J, ND, NPR
      DATA ONE   / 1.0D00/
      DATA TWO   / 2.0D00/
      DATA THREE / 3.0D00/
      DATA FOUR  / 4.0D00/
      IF (CASE .EQ. 1) THEN
      K1 = BNON(1)
      DO  I=1,ND
      BTOT = BASE(I)
      ATOT = ACID(I)

C  THE CASE OF ONE PROTON CAN BE SOLVED BY A QUADRATIC EQUATION,
C    E*A**2 + D*A + C = 0
C    A = (-D +- SQRT(D*D - 4*E*C)) / (2*E)

        E = ONE - K1
        D = (ATOT + BTOT) * K1
        C = -K1 * ATOT * BTOT
        C = DSQRT(D*D - FOUR * E * C)
        A = (-D + C) / (TWO * E)
     IF (A.LT.0.0 .OR. A.GT.ATOT .OR. A.GT.BTOT)
     *        A = (-D - C) / (TWO * E)
     IF (A.LT.0.0 .OR. A.GT.ATOT .OR. A.GT.BTOT)
     *PRINT *,' ERROR IN CALCULATING CONCENTRATIONS ON POINT ',
     *         I
        BH = A
        AH = ATOT - A
        B = BTOT - BH
        Z(I) = VOL(I) * A * BNON(2)
     IF (NPR .EQ. 1) WRITE(43,FMT='(6D12.3)') ACID(I), BASE(I),
    *     B, BH, AH, A
     END DO
     RETURN
     END IF

C  IN CASE 2, THERE ARE FIVE EQUATIONS FOR FIVE UNKNOWNS, AH2, AH, A,
C   B, AND BH (ASSUMING K1 AND K2 ARE KNOWN). I REDUCED THE FIVE
C   EQUATIONS IN FIVE UNKNOWNS TO TWO EQUATIONS IN TWO UNKNOWNS.
C   HERE IS AN ATTEMPT TO SOLVE FOR THOSE TWO UNKNOWNS. THE KEY IS
C   TO ASSUME BETA (= BH/B, WHICH ALLOWS THE CALCULATION OF B AND BH)
C   CALCULATE AH, AND FROM AH CALCULATE AH2 AND A. THEN CHECK
C   WHETHER THE ASSUMED BETA IS CORRECT BY DOING A MASS BALANCE ON
C   THE PROTONS (THE PROTONS ON BH MUST HAVE BEEN THE ONES LOST FROM
C   AH AND AH2). WHEN THE PROTONS BALANCE, THE EQUATIONS HAVE BEEN
C   SOLVED.

     IF (CASE .EQ. 2) THEN
       K1 = BNON(1)
       K2 = BNON(2)
       DO  I=1,ND
         BTOT = BASE(I)
         ATOT = ACID(I)
         BESAVE(1) = 0.0
         BESAVE(2) = 0.0
         DEL2 = 0.000001D00 * ATOT
         DO J=1,50
          IF (J .LT. 3) THEN
            EXPJ = 20.
            IF (J .EQ. 2) EXPJ = -20.
            EXPJ = 10.0**EXPJ
            BETA = EXPJ
            END IF
          IF (J .GT. 2)  BETA = DSQRT(BESAVE(1) * BESAVE(2))
          BH = BTOT / (ONE + ONE/BETA)
          B = BH / BETA
          AH = ATOT / (ONE + BETA/K1 + K2/BETA)
          A = K2*AH/BETA
          AH2 = AH*BETA/K1
          PLOST = TWO*A + AH
          PONB = BH
          DEL1 = DABS(PLOST - PONB)
          IF (PLOST .GT. PONB) BESAVE(1) = BETA
          IF (PLOST .LT. PONB) BESAVE(2) = BETA
          IF (DEL1 .LT. DEL2) GO TO 10
          END DO

     PRINT *,' WARNING, POINT', I, ' DID NOT CONVERGE.'

 10       Z(I) = VOL(I) * (AH * BNON(3) + A * BNON(4))
        IF (NPR .EQ. 1) WRITE(43,FMT='(7D10.3)') ACID(I), BASE(I),
    *     B, BH, AH2, AH, A
     END DO
     RETURN
     END IF
```

```
C  IN CASE 3 THIS PROGRAM WILL USE A PREVIOUS SOBROUTINE WHERE THE SPECIES
C  CONCENTRATIONS ARE CALCULATED SEPARETEDLY BY OTHER SUBROUTINE
"CONCEN"

      IF (CASE .EQ. 3) THEN
       K1 = BNON(1)
       K2 = BNON(2)
       K3 = BNON(3)
       DO  I=1,ND

     BTOT = BASE(I)
     WTOT = ACID(I)
     IF (ABS(BTOT-3.0*WTOT) .LT. 0.01*WTOT)    GO TO 100
     DEFIND(1) = BNON(1)
     DEFIND(2) = BNON(2)
     DEFIND(3) = BNON(3)
     DEFIND(4) = WTOT
     DEFIND(5) = BTOT
     DEFIND(6) = 3.0D00*WTOT
     IF (I .EQ. 1) THEN
     RESULT(1) = 0.0000000001
     RESULT(2) = BTOT
     RESULT(3) = 0.00000000001
     RESULT(4) = 0.00000000001
     RESULT(5) = 0.000000001
     RESULT(6) = WTOT
     END IF
     IF (I .GT. 1)  RESULT(2) = BTOT
     IF (BTOT-3.0D0*WTOT .GT. 0.0) RESULT(2) = 3.0D0*WTOT

     CALL CONCEN (RESULT, DEFIND, I)

     B   = RESULT(1)
     BH  = RESULT(2)
     WH0 = RESULT(3)
     WH1 = RESULT(4)
     WH2 = RESULT(5)
     WH3 = RESULT(6)
     Z(I) = VOL(I) * (WH2*BNON(4) + WH1*BNON(5) + WH0*BNON(6))
     IF (NPR .EQ. 1)
    * WRITE(43,FMT='(8D10.3)') ACID(I), BASE(I), B, BH, WH3, WH2,
    *     WH1, WH0


  100 CONTINUE
     END DO
     RETURN
     END IF

     END
C==============================================================
C  SUBROUTINE CONCEN(RESULT, DEFIND, NP)
C
C  PURPOSE
```

```
C   GIVEN ALL THE DEFINED VARIABLES, THIS ROUTINE CALCULATES THE
C   CONCENTRATIONS OF B, BH, WH3, WH2, WH1, WH0. THIS IS AN
C   ITERATIVE SEARCH ROUTINE.
C
C  VARIABLES
C   DEFIND (R*8,6) =  DEFINED VARIABLES IN THE ORDER K1, K2, K3,
C                     WTOT, BTOT, H.
C   RESULT (R*8,6) =  CONCENTRATIONS IN ORDER B, BH, WH3, WH2, WH1, WH0
C   DEFI   (R*4,4) =  INPUT VARIABLES K1/K2, WTOT, H/ K2/K3
C   DEFE   (R*4,4) =  ESTIMATES OF THE VARIABLES IN DEFI
C
C  TOM MAIER  2/96
C=====================================================================
      SUBROUTINE CONCEN(RESULT, DEFIND, NP)

      IMPLICIT NONE

      REAL*8 DEFIND(6), RESULT(6), DELTA(4), WF, WFF
      REAL*8 B, BH, WH3, WH2, WH1, WH0, K1, K2, K3, K12, K23
      REAL*8 DEFI(4), DEFE(4)
      REAL*8 WTOT, BTOT, HTOT, ERRAIM(4), DELW
      REAL*8 WH0N, WH1N, WH2N, WH3N, F012, F123, BHB, DENOM
      INTEGER I, J, KOUNT, NL012, NL123, NP
      INTEGER NF012(1155), NF123(1155)

      KOUNT = 0
      F012 = 1.0D00
      F123 = 1.0D00
      B   = RESULT(1)
      BH  = RESULT(2)
      WH0 = RESULT(3)
      WH1 = RESULT(4)
      WH2 = RESULT(5)
      WH3 = RESULT(6)
      K1  = DEFIND(1)
      K2  = DEFIND(2)
      K3  = DEFIND(3)
      K12 = K1/K2
      K23 = K2/K3
      WTOT = DEFIND(4)
      BTOT = DEFIND(5)
      HTOT = DEFIND(6)
      DEFI(1) = K12
      DEFI(2) = WTOT
      DEFI(3) = HTOT - BTOT
      DEFI(4) = K23
      IF (DEFI(3) .LT. 0.0) THEN
      DEFI(3) = HTOT
      BH = 3.0*WTOT
      B = BTOT - BH
      BHB = BH/B
      DENOM = 1.0D00 + BHB/K3 + BHB*BHB/(K3*K2) +
     *        BHB*BHB*BHB/(K3*K2*K1)
      WH0 = WTOT/DENOM
      WH1 = WH0*BHB/K3
      WH2 = WH1*BHB/K2
      WH3 = WH2*BHB/K1
      RESULT(1) = B
      RESULT(2) = BH
      RESULT(3) = WH0
      RESULT(4) = WH1
      RESULT(5) = WH2
      RESULT(6) = WH3
      RETURN
      END IF
      ERRAIM(1) = 1.0D-05*DEFI(1)
      ERRAIM(2) = 1.0D-04*DEFI(2)
      ERRAIM(3) = 1.0D-04*DEFI(3)
      ERRAIM(4) = 1.0D-05*DEFI(4)
      IF (ERRAIM(3) .LT. 1.0D-08) ERRAIM(3) = 1.0D-08


C ESTIMATE THE KNOWN VALUES, DEFI  ARE INPUT, DEFE  ARE ESTIMATES.
C DEFI(1) = K1/K2, DEFI(2) = WTOT, DEFI(3) = H-BH, DEFI(4) = K2/K3

   10 KOUNT = KOUNT + 1
      WF = WH3 + WH2 + WH1 + WH0
      DEFE(1) = WH2*WH2/(WH1*WH3)
      DEFE(2) = WH3 + WH2 + WH1 + WH0
      DEFE(3) = 3.0D00*WH3 + 2.0D00*WH2 + WH1
      DEFE(4) = WH1*WH1/(WH2*WH0)

C ADJUST TOTAL W BY MULTIPLYING CALCULATED CONCENTRATIONS BY WF.

      WF = DEFI(2) / DEFE(2)
      WH3 = WF * WH3
      WH2 = WF * WH2
      WH1 = WF * WH1
      WH0 = WF * WH0

C ADJUST BASE CONCENTRATIONS BY MULTIPLYING BY WF.

      IF (KOUNT .GT. 2) THEN
      WF = BTOT / (B + BH)
      B = WF * B
      BH = WF * BH
      DEFI(3) = HTOT - BH
      END IF

C ADJUST TOTAL H CONCENTRATION BY ADJUSTING WHi CONCENTRATIONS.

      DEFE(3) = 3.0D00*WH3 + 2.0D00*WH2 + WH1
      WF = DEFI(3)  - DEFE(3)
   15 I = 0
      IF (DABS(WF) .LT. 1.0D-10) I = 1
      IF (WF .GT. 0.0) THEN
      IF (WF .LT. WH0) THEN
      I = 1
      WH0 = WH0 - WF
      WH1 = WH1 + WF
      GO TO 20
      END IF
      IF (WF .LT. WH1) THEN
      I = 1
      WH1 = WH1 - WF
      WH2 = WH2 + WF
      GO TO 20
      END IF
      IF (WF .LT. WH2) THEN
      I = 1
      WH2 = WH2 - WF
      WH3 = WH3 + WF
      GO TO 20
      END IF
      END IF
      IF (WF .LT. 0.0) THEN
      WFF = - WF
      IF (WFF.LT. WH3) THEN
      I = 1
      WH3 = WH3 - WFF
      WH2 = WH2 + WFF
      GO TO 20
      END IF
      IF (WFF.LT. WH2) THEN
      I = 1
      WH2 = WH2 - WFF
      WH1 = WH1 + WFF
      GO TO 20
      END IF
      IF (WFF.LT. WH1) THEN
      I = 1
      WH1 = WH1 - WFF
      WH0 = WH0 + WFF
      GO TO 20
      END IF
      END IF
  20  IF (I .EQ. 0) THEN
      WF = 0.8D0*WF
      GO TO 15
      END IF

C CHECK TO SEE HOW WELL WE HAVE DONE.

      IF (WH3 .LE. 0.0) WH3 = 1.0D-10
      IF (WH2 .LE. 0.0) WH2 = 1.0D-10
      IF (WH1 .LE. 0.0) WH1 = 1.0D-10
      IF (WH0 .LE. 0.0) WH0 = 1.0D-10
      DEFE(1) = WH2*WH2/(WH1*WH3)
      DEFE(2) = WH3 + WH2 + WH1 + WH0
      DEFE(3) = 3.0D00*WH3 + 2.0D00*WH2 + WH1
      DEFE(4) = WH1*WH1/(WH2*WH0)
      DO I=1,4
      DELTA(I) = DEFI(I)  - DEFE(I)
      END DO
      IF (DABS(DELTA(I)) .LT. ERRAIM(I) .AND.
     *   DABS(DELTA(2)) .LT. ERRAIM(2) .AND.
     *   DABS(DELTA(3)) .LT. ERRAIM(3) .AND.
     *   DABS(DELTA(4)) .LT. ERRAIM(4)) THEN
      RESULT(1) = B
      RESULT(2) = BH
      RESULT(3) = WH0
      RESULT(4) = WH1
      RESULT(5) = WH2
      RESULT(6) = WH3
      RETURN
      END IF
C THE ABOVE CALCULATIONS LINEARLY BALANCED CONCENTRATIONS. NOW
C MAKE ADJUSTMENTS BASED ON THE EQUILIBRIUM CONSTANTS, ACTUALLY THE
C THE RATIOS OF THE Ks: K1/K2 and K2/K3 (THESE RATIOS ELIMINATE B/BH)

      NL012 = 0
      IF (WH2 .LT. WH0) NL012 = 2
      NL123 = 1
      IF (WH3 .LT. WH1) NL123 = 3
      IF (NL123 .EQ. 1) THEN
      WH1N = WH2*WH2/(WH3*K12)
      DELW = F123 * (WH1 - WH1N)
      IF (DELW .GT. 0.6D0*WH1) DELW = 0.6D0*WH1
      IF (DELW .GT. 0.6D0*WH3) DELW = 0.6D0*WH3
      IF (-2.0D0*DELW .GT. 0.6D0*WH2) DELW = -0.3D0*WH2
      WH1 = WH1 - DELW
      WH2 = WH2 + DELW + DELW
      WH3 = WH3 - DELW
      END IF
      IF (NL123 .EQ. 3) THEN
      WH3N = WH2*WH2/(WH1*K12)
      DELW = F123 * (WH3 - WH3N)
      IF (DELW .GT. 0.6D0*WH1) DELW = 0.6D0*WH1
      IF (DELW .GT. 0.6D0*WH3) DELW = 0.6D0*WH3
      IF (-2.0D0*DELW .GT. 0.6D0*WH2) DELW = -0.3D0*WH2
      WH1 = WH1 - DELW
      WH2 = WH2 + DELW + DELW
      WH3 = WH3 - DELW
      END IF
      IF (NL012 .EQ. 0) THEN
      WH0N = WH1*WH1/(WH2*K23)
      DELW = F012 * (WH0 - WH0N)
      IF (DELW .GT. 0.6D0*WH0) DELW = 0.6D0*WH0
      IF (DELW .GT. 0.6D0*WH2) DELW = 0.6D0*WH2
      IF (-2.0D0*DELW .GT. 0.6D0*WH1) DELW = -0.3D0*WH1
      WH0 = WH0 - DELW
      WH1 = WH1 + DELW + DELW
      WH2 = WH2 - DELW
      END IF
      IF (NL012 .EQ. 2) THEN
      WH2N = WH1*WH1/(WH0*K23)
      DELW = F012 * (WH2 - WH2N)
      IF (DELW .GT. 0.6D0*WH0) DELW = 0.6D0*WH0
      IF (DELW .GT. 0.6D0*WH2) DELW = 0.6D0*WH2
      IF (-2.0D0*DELW .GT. 0.6D0*WH1) DELW = -0.3D0*WH1
      WH0 = WH0 - DELW
      WH1 = WH1 + DELW + DELW
      WH2 = WH2 - DELW
      END IF
      IF (WH3.GT.WH2) B = WH2*BH/(WH3*K1)
      IF (WH2.GT.WH3) B = WH1*BH/(WH2*K2)
      IF (WH0.GT.WH1) B = WH0*BH/(WH1*K3)

      DEFE(1) = WH2*WH2/(WH1*WH3)
      DEFE(2) = WH3 + WH2 + WH1 + WH0
      DEFE(3) = 3.0D00*WH3 + 2.0D00*WH2 + WH1
      DEFE(4) = WH1*WH1/(WH0*WH2)
      DO I=1,4
      DELTA(I) = DEFI(I)  - DEFE(I)
      END DO

      NF012(KOUNT) = 1
      IF (DELTA(4) .LT. 0.0) NF012(KOUNT) = -1
      NF123(KOUNT) = 1
      IF (DELTA(1) .LT. 0.0) NF123(KOUNT) = -1
      IF (KOUNT .GT. 2) THEN
        J = NF012(KOUNT-1)*NF012(KOUNT)
        IF (J.LT.0 .AND. F012.GT.0.001) F012 = 0.8D00*F012
        J = NF123(KOUNT-1)*NF123(KOUNT)
        IF (J.LT.0 .AND. F123.GT.0.001) F123 = 0.8D00*F123
        END IF

C CHECK TO SEE HOW WELL WE HAVE DONE.

      IF (DABS(DELTA(1)) .LT. ERRAIM(1) .AND.
     *   DABS(DELTA(2)) .LT. ERRAIM(2) .AND.
     *   DABS(DELTA(3)) .LT. ERRAIM(3) .AND.
     *   DABS(DELTA(4)) .LT. ERRAIM(4)) THEN
          RESULT(1) = B
          RESULT(2) = BH
          RESULT(3) = WH0
          RESULT(4) = WH1
          RESULT(5) = WH2
          RESULT(6) = WH3
          RETURN
          END IF
      DO I=1,4
      DELTA(I) = DELTA(I) / ERRAIM(I)
      END DO

      IF (KOUNT.LT.1150) GO TO 10

   55 PRINT *,'WARNING, SLOW CONVERGENCE ON POINT', NP
      RESULT(1) = B
      RESULT(2) = BH
      RESULT(3) = WH0
      RESULT(4) = WH1
      RESULT(5) = WH2
      RESULT(6) = WH3
      RETURN
      END

C=====================================================================
C SUBROUTINE NLREG (NPTOT, ND, X, Y, D, BNON, ICON, Z, YH, DY, NPF, NPV,
C         IN, ITMAX, NSIG, VAR, BASE, ACID, VOL, CASE, STDE)
C
C *** NON-LINEAR REGRESSION SUBROUTINE ***
C=====================================================================

      SUBROUTINE NLREG (NPTOT, ND, X, Y, D, BNON, ICON, Z, YH, DY, NPF,
     *       NPV, IN, ITMAX, NSIG, VAR, BASE, ACID, VOL, CASE, STDE)

C     IMPLICIT NONE
      REAL*8  X(ND,NPTOT), Y(ND), BNON(1), D(ND,NPTOT), Z(ND), YH(ND)
      REAL*8  BASE(ND), DY(ND), ACID(ND), VOL(ND), STDE(6)
      REAL*8  XPX(6,6), XPY(6), COREC(6), COR(12), C(6)
      REAL*8  DD, DEL, G, GF, GG, QBEST, QNEW, QOLD, SIG, SUM, TP, VAR
      INTEGER CASE, I, ICON, ITER, J, NCOR, ND, NPF, NPR, NPV, NSIG
      INTEGER ICOR, IN(NPTOT), ITMAX, K, KI, KJ, NBEST, NPTOT

      DATA COR/1.0D0,0.5D0,0.2D0,0.4D0,0.6D0,0.8D0,
     * 0.02D0,0.04D0,0.06D0,0.1D0,-0.1D0,-0.5D0/,NCOR/12/
C ********************************************************************
C
C ***          INPUT ARGUMENTS              ***
C
C NPTOT      TOTAL NUMBER OF NON-LINEAR PARAMETERS.
C ND         TOTAL NUMBER OF OBSERVED DATA POINTS.
C X          ND X NPTOT MATRIX.
C Y          ND VECTOR OF RESPONSES.
C D          MATRIX OF SIZE AT LEAST ND X NPTOT.
C BNON       VECTOR OF LENGTH NPTOT
C            ON INPUT, CONTAINS INITIAL VALUES FOR NON-LINEAR
C            PARAMETERS.  ON OUTPUT, CONTAINS ESTIMATES OF
C            PARAMETERS.
C ICON       CONVERGENCE INDICATOR RETURNED FROM NLREG:
C            ICON=NO. OF ITERATION ( CONVERGENCE ATTAINED)
C               =-1  TOO MANY ITERATIONS ( HAS NOT CONVERGED)
C               =-2  XPX MATRIX SINGULAR
C               =-3  NO IMPROVEMENT.
C Z          WORK VECTOR OF SIZE AT LEAST ND.
C YH         PREDICTED VALUES RETURNED FROM NLREG.
C NPF        NUMBER OF NON-LINEAR PARAMETERS FIXED (NOT VARYING).
C NPV        NUMBER OF NON-LINEAR PARAMETERS VARYING.
C IN         NPTOT VECTOR INDICATING INDICES OF NON-LINEAR PARAMETERS
C            VARYING.
C ITMAX      MAXIMUM NUMBER OF ITERATIONS ALLOWED. ON OUTPUT, ITMAX
C          CONTAINS THE ACTUAL NUMBER OF ITERATIONS.
C NSIG       NUMBER OF SIGNIFICANT DIGITS DESIRED IN PARAMETER
C            ESTIMATES.
C VAR        ESTIMATED VARIANCE OF OBSERVATIONS RETURNED FROM NLREG
C
C STDE       STANDARD DEVIATION FOR EACH CALCULATED PARAMETER
C
C    *****           NOTE:              *****
```

```
C    *****    THIS SUBROUTINE IS CURRECTLY SET UP FOR A MAXIMUM OF
C    *****    6 PARAMETERS.
C ***********************************************************************

      SIG=NSIG
      TP=10.0**(-SIG)
      ICON=0
      ITER=0
      DO  I=1,6
      COREC(I)=0.0D0
      END DO
  100 NPR = 0
      CALL CHEAT(BNON, Z, ND, BASE, ACID, VOL, NPR, CASE)
      QOLD=0.0
      DO  I=1,ND
      YH(I) = Z(I)
      DEL = Y(I) - YH(I)
      QOLD = QOLD + DEL*DEL
      END DO

      IF (MOD(ITER,4) .EQ. 1) THEN
      PRINT *,' '
      PRINT *,' *****************************************************'
      WRITE(6,FMT='(3X,A21,I4,3X,A23,D12.5)') 'AT END OF ITERATION ',
     * ITER, ' SUM OF SQUARES ERROR =', QOLD
      IF (CASE .EQ. 1) PRINT *,' K1 AND H1 ARE:'
      IF (CASE .EQ. 2) PRINT *,' K1, K2, H1, AND H2 ARE:'
      IF (CASE .EQ. 3) PRINT *,' K1, K2, K3, H1, H2, AND H3 ARE:'
      WRITE(6,FMT='(2X,6D11.3)') (BNON(I),I=1,2*CASE)
      PRINT *,' *****************************************************'
      PRINT *,' '
      END IF

      CALL DERV (X,Y,BNON,D,Z,YH,NPF,NPV,IN,NPTOT,ND,BASE,ACID,
     * VOL, CASE)
      CALL XPRMX (D,ND,ND,NPV,XPX)
      DO  J=1,ND
      DY(J) = Y(J) - YH(J)
      END DO
      CALL XPRMY (D,DY,ND,NPV,XPY)
      CALL INVERT (XPX,NPV,DD)
      IF (DD.NE.0.0D0) GO TO 120
C ***********************************************************************
C *** XPX MATRIX IS SINGULAR - ICON=-2 - ZERO OUT MATRICES AND RETURN *
C ***********************************************************************
      DO 110 I=1,NPTOT
      DO 110 J=1,NPTOT
  110 D(J,I)=0.D0
      VAR=0.0
      DO  I=1,ND
      VAR=VAR+(Y(I)-YH(I))*(Y(I)-YH(I))
      END DO
      VAR=VAR/(ND-NPV)
      ICON=-2
      RETURN
```

```
C ************************************************************************
C *** END XPX MATRIX SINGULAR SECTION                    *****
C ************************************************************************
C  ***  FINISH IF ICON IS NOT EQUAL TO ZERO OR ITMAX IS ZERO
C ************************************************************************
 120 IF (ICON .NE. 0) GO TO 200
    IF (ITMAX .EQ. 0) GO TO 200
C *** COREC IS THE AMOUNT BY WHICH TO ADJUST EACH BNON ELEMENT.
     DO I=1,NPV
     KJ=IN(I)
     SUM=0.0D0
     DO J=1,NPV
     SUM=SUM + XPX(I,J)*XPY(J)
     END DO
     COREC(KJ)=SUM
     END DO
     ITER=ITER+1
     GF = 1.8D0
     DO I=1,NPV
     IF (COREC(I) .NE. 0.0) THEN
     GG = DABS(BNON(I)/COREC(I))
     IF (GG .LT. GF) GF = GG
     END IF
     END DO
     GF = 0.5D0*GF

C *** PARTIAL CORRECTION ROUTINE FOR PARAMETERS
C *** TRY THE FRACTIONAL CORRECTIONS CONTAINED IN THE VECTOR COR.

     NBEST = 0
     QBEST = QOLD
     DO  ICOR=1,NCOR
     G = GF*COR(ICOR)
     DO  K=1,NPTOT
     C(K)=BNON(K)+G*COREC(K)
     END DO
     NPR = 0
     CALL CHEAT(C, Z, ND, BASE, ACID, VOL, NPR, CASE)
     QNEW=0.0
     DO  I=1,ND
     YH(I)=Z(I)
     QNEW=QNEW+(Y(I)-YH(I))*(Y(I)-YH(I))
     END DO
     IF (QNEW .LT. QBEST) THEN
     NBEST = ICOR
     QBEST = QNEW
     END IF
     END DO
     IF (NBEST .GT. 0) THEN
     G = GF*COR(NBEST)
     DO  K=1,NPTOT
     C(K)=BNON(K)+G*COREC(K)
     END DO
     GO TO 130
     END IF
```

```
C ***********************************************************************
C ***  ALL CORRECTIONS TRIED; NO IMPROVEMENT
C ***  DEFINE ICON=-3
C ***********************************************************************
     ICON = -3
     GO TO 200
C ***  CHECK PARAMETERS FOR CONVERGENCE ***
  130 DO  J=1,NPTOT
     IF (BNON(J).EQ.0.0D0) GO TO 140
     IF (DABS((C(J)-BNON(J))/C(J)).GT.TP) GO TO 150
     END DO
C ***********************************************************************
C CONVERGED, DEFINE ICON = NUMBER OF ITERATIONS USED
C ***********************************************************************
  140 ICON = ITER
  150 DO  J=1,NPTOT
     BNON(J) = C(J)
     END DO
     IF (ICON.GT.0) GO TO 200
     IF (ITER .LT. ITMAX) GO TO 100
C ***********************************************************************
C *** TOO MANY ITERATIONS - SET ICON = -1
C ***********************************************************************
     ICON = -1

C CALCULATE STD ERRORS FOR ALL PARAMETERS

  200 NPR = 0
     CALL CHEAT(C, Z, ND, BASE, ACID, VOL, NPR, CASE)
     VAR = 0.0
     DO  I=1,ND
     YH(I)=Z(I)
     VAR=VAR+(Y(I)-YH(I))*(Y(I)-YH(I))
     END DO
     VAR = VAR / (ND-NPV)
     DO 210 I=1,ND
     DO 210 J=1,NPTOT
  210 D(I,J) = 0.0
     DO 215 I=1,6
     DO 215 J=1,6
  215 XPX(I,J) = 0.0

C  CALCULATE XPX MATRIX

     CALL DERV(X,Y,BNON,D,Z,YH,NPF,NPV,IN,NPTOT,ND,BASE,ACID,VOL,CASE)
     CALL XPRMX (D,ND,ND,NPV,XPX)
     DO 220 I=1,NPTOT
     DO 220 J=1,I
  220 D(J,I) = 0.0D0
     CALL INVERT (XPX,NPV,DD)
     IF (DD .EQ. 0.0D0) THEN
     WRITE (6,FMT='(/,A40,/)')
    *' XPX MATRIX SINGULAR ON FINAL ITERATION'
     RETURN
     END IF
```

```
      DO 230 I=1,NPV
      KI = IN(I)
      DO 230 J=1,I
      KJ = IN(J)
      D(KJ,KI) =  XPX(I,J)*VAR
      IF (KI .EQ. KJ) THEN
      STDE(KI) = DSQRT(D(KJ,KI))
      PRINT *,' KI, BNON, STDE =', KI, BNON(KI), STDE(KI)
      END IF
  230 CONTINUE

      RETURN
      END
C============================================================
      SUBROUTINE INVERT (XPX,NROW,DD)
      IMPLICIT NONE
      REAL*8  XPX(6,6), AI(36), DD
      INTEGER I, J, K, L(6), M(6), NROW

C SUBROUTINE TO INVERT A MATRIX

      K = 0
      DO 100 I=1,NROW
      DO 100 J=1,NROW
      K = K + 1
  100 AI(K) = XPX(I,J)
      CALL DMINV (AI,NROW,DD,L,M)
      K = 0
      DO 200 I=1,NROW
      DO 200 J=1,NROW
      K = K + 1
  200 XPX(I,J) = AI(K)
      RETURN
      END
C============================================================
      SUBROUTINE XPRMY (X,Y,NR,NCOL,XPY)
C     IMPLICIT NONE
      REAL*8  X(NR,NCOL), Y(NR), XPY(NCOL)
      INTEGER NCOL, NR, I, J

C SUBROUTINE TO CALCULATE XPY MATRIX

      DO  I=1,NCOL
      XPY(I) = 0.0D0
      DO  J=1,NR
      XPY(I) = XPY(I) + Y(J)*X(J,I)
      END DO
      END DO
      RETURN
      END
C============================================================
      SUBROUTINE XPRMX (X,ND,NR,NCOL,XPX)
C     IMPLICIT NONE
      REAL*8  X(ND,NCOL), XPX(6,6), SUM
      INTEGER I, J, K, NCOL, ND, NR

C CALCULATE XPX MATRIX

      DO 10 I=1,NCOL
      DO 10 J=1,I
      SUM = 0.0D0
      DO  K=1,NR
      SUM = SUM + X(K,I)*X(K,J)
      END DO
      XPX(I,J) = SUM
   10 XPX(J,I) = SUM
      RETURN
      END
C==============================================================
      SUBROUTINE DERV (X,Y,BNON,D,Z,YH,NPF,NPV,IN,NPTOT,ND,BASE,
     *ACID,VOL,CASE)

C  THIS SUBROUTINE CALCULATES DERIVATIVES AS DELTA YH/DELTA BNON
C  FOR EACH DATA POINT (YH) AND EACH BNON VARIABLE.

C     IMPLICIT NONE
      REAL*8  X(ND,NPTOT), Y(1), BNON(1), D(ND,NPTOT), YH(ND)
      REAL*8  Z(ND), BASE(ND), ACID(ND), VOL(ND), YHSAVE(1000)
      REAL*8  BHOLD, DEL, DELTA, VAR
      INTEGER CASE, I, IN(1), J, KI, ND, NPF, NPR, NPTOT, NPV

      DEL=0.1D-3
      DO  J=1,ND
      YHSAVE(J) = YH(J)
      END DO
      DO 100 I=1,NPV
      KI = IN(I)
      BHOLD = BNON(KI)
      DELTA = DEL * BNON(KI)
      IF (ABS(DELTA) .LT. 0.000001) DELTA=0.000001
      BNON(KI) = BNON(KI) + DELTA
      NPR = 0
      CALL CHEAT(BNON, Z, ND, BASE, ACID, VOL, NPR, CASE)
      VAR = 0.0
      DO  J=1,ND
      YH(J) = Z(J)
      DEL = Y(J) - YH(J)
      VAR = VAR + DEL*DEL
      END DO
      DO  J=1,ND
      D(J,I) = (YH(J) - YHSAVE(J)) / DELTA
      END DO
      BNON(KI) = BHOLD
  100 CONTINUE

      DO I=1,ND
      YH(I) = YHSAVE(I)
      END DO
      RETURN
      END
C ***********************************************************************
      SUBROUTINE DMINV(A,N,D,L,M)
C ***********************************************************************
      IMPLICIT NONE
      REAL*8  DABS, A(1), D, BIGA, HOLD
      INTEGER I, IJ, IZ, J, JI, JP, K, KI, KK, L(1), M(1), N, NK
      INTEGER IK, JK, JQ, JR, KJ

C     SEARCH FOR LARGEST ELEMENT

      D=1.0
      NK=-N
      DO 80 K=1,N
      NK=NK+N
      L(K)=K
      M(K)=K
      KK=NK+K
      BIGA=A(KK)
      DO 20 J=K,N
      IZ=N*(J-1)
      DO 20 I=K,N
      IJ=IZ+I
      IF(DABS(BIGA)-DABS(A(IJ))) 15,20,20
   15 BIGA=A(IJ)
      L(K)=I
      M(K)=J
   20 CONTINUE

C     INTERCHANGE ROWS

      J=L(K)
      IF(J-K) 35,35,25
   25 KI=K-N
      DO 30 I=1,N
      KI=KI+N
      HOLD=-A(KI)
      JI=KI-K+J
      A(KI)=A(JI)
   30 A(JI) =HOLD

C     INTERCHANGE COLUMNS

   35 I=M(K)
      IF(I-K) 45,45,38
   38 JP=N*(I-1)
      DO 40 J=1,N
      JK=NK+J
      JI=JP+J
      HOLD=-A(JK)
      A(JK)=A(JI)
   40 A(JI) =HOLD

C     DIVIDE COLUMN BY MINUS PIVOT (VALUE OF PIVOT ELEMENT IS
C     CONTAINED IN BIGA)
```

```
 45 IF(BIGA) 48,46,48
 46 D=0.0
    RETURN
 48 DO 55 I=1,N
    IF(I-K) 50,55,50
 50 IK=NK+I
    A(IK)=A(IK)/(-BIGA)
 55 CONTINUE

C      REDUCE MATRIX

    DO 65 I=1,N
    IK=NK+I
    HOLD=A(IK)
    IJ=I-N
    DO 65 J=1,N
    IJ=IJ+N
    IF(I-K) 60,65,60
 60 IF(J-K) 62,65,62
 62 KJ=IJ-I+K
    A(IJ)=HOLD*A(KJ)+A(IJ)
 65 CONTINUE

C      DIVIDE ROW BY PIVOT

    KJ=K-N
    DO 75 J=1,N
    KJ=KJ+N
    IF(J-K) 70,75,70
 70 A(KJ)=A(KJ)/BIGA
 75 CONTINUE

C      REPLACE PIVOT BY RECIPROCAL

    A(KK)=1.0/BIGA
 80 CONTINUE

C      FINAL ROW AND COLUMN INTERCHANGE

    K=N
100 K=(K-1)
    IF(K) 150,150,105
105 I=L(K)
    IF(I-K) 120,120,108
108 JQ=N*(K-1)
    JR=N*(I-1)
    DO 110 J=1,N
    JK=JQ+J
    HOLD=A(JK)
    JI=JR+J
    A(JK)=-A(JI)
110 A(JI) =HOLD
120 J=M(K)
    IF(J-K) 100,100,125
```

```
125 KI=K-N
   DO 130 I=1,N
   KI=KI+N
   HOLD=A(KI)
   JI=KI-K+J
   A(KI)=-A(JI)
130 A(JI) =HOLD
   GO TO 100
150 RETURN
   END
```

LIST OF REFERENCES

1. Greenwood, N. N.; Earnshaw, A. *Chemistry of the Elements*, Pergmon Press, Oxford, reprinted 1994.

2. Pope, M. T. *Heteropoly and Isopoly Oxometalates*, Springer-Verlag, Berlin, 1983.

3. Pauling, L. C. *J. Am. Chem. Soc.* **1929**, 51, 2868.

4. (a) Keggin, J. F. *Nature* **1933**, 131, 908.
   (b) Keggin, J. F. *Proc. Roy. Soc. A* **1934**, 144, 75.

5. Evans, H. T. Jr. *J. Am. Chem. Soc.* **1948**, 70, 1291.

6. (a) Lindqvist, I. *Arkiv Kemi* **1950**, 2, 325.
   (b) Evans, H. T. Jr. *J. Am. Chem. Soc.***1968**, 90, 3275.

7. Kepert, D. L. Prog. *Inorg. Chem.* **1962**, 4, 199.

8. Kepert, D. L. *Comprehensive Inorganic Chemistry*, Bailar, J. C., Jr.; Emeléus, H. J.; Nyholm, R.; Trotman-Dickenson, A. F. Eds., Pergmon Press, Oxford, vol. 4, 1973.

9. Tsigdinos, G. A. *Top. Curr. Chem.* **1978**, 76, 1.

10. Cotton, F. A.; Wilkinson G. *Advanced Inorganic Chemistry*, Fifth Edition, John Wiley & Sons, New York, 1988

11. Misono, M. *Catal. Rev.- Sci. Eng.* **1987**, *29*, 269.

12. Baker, L. C. W.; Figgs, J. S. *J. Am. Chem. Soc.* **1970**, 92, 3794.

13. Evans, H. T. Jr. *Acta Cryst.* **1974**, B30, 2095.

14. Waugh, J. C. T.; Schoemaker, D. P.; Pauling, L. *Acta Cryst.* **1954**, 7, 438.

15. Pope, M. T.; Müller, A. *Angew. Chem. Int. Ed. Engl.* **1991**, 30, 34.

16. Shannon, R. D.; Prewitt, C. T. *Acta Cryst.* **1969**, B25, 925.

17. Ma, L.; Liu, S.; Zubieta, J. *Inorg. Chem.* **1989**, 28, 175.

18. Müller, A.; Krickemeyer, M.; Penk, M.; Wittneben, V.; Döring, J. *Angew. Chem. Int. Ed. Engl.* **1990**, 29, 88.

19. Porai-Koshits, M. A.;Atovmyan, L. O. *Russ. J. Inorg. Chem.* **1981**, 26, 1697.

20. (a) Kuikova, O. M.; Maksimovskaya, R. I.; Kulikov, S. M.; Kozhevnikov, I. V. *Russ. Chem. Bull.* **1992**, 496.
(b) Maksimov, G. M.; Maksimovskaya, R. I.; Kozhevnikov, I. V. *Russ. J. Inorg. Chem.* **1992**, 496.

21. Simon, S. J.; Boltz, D. F. *Anal. Chem.* **1975**, 47, 1758.

22. Gullstrom, D.; Mellon, M. G. *Anal. Chem.* **1953**, 25, 1809.

23. Fogg, A. G.; Bsebsu, N. K.; Birch, B. J.*Talanta* **1981**, 28, 473.

24. Pope, M. T.; Müller, A. *Polyoxometalates: from Platonic solids to anti-retrovirial activity*, M. T. Pope and A. Müller Eds., Klumer, Dordrech, 1994.

25. (a) Hardwick, A.; Dickens, P. G.; Slade, R. T. C. *Solid State Ionics* **1984**, 13, 345.
(b) Nakamura, O.; Kodama, T.; Ogino, I.; Miyake, Y. *Chem. Lett.* **1979**, 17.
(c) Tatsumisago, M.; Minomi, T. *J. Am. Ceram. Soc.* **1989**, 72, 484.

26. (a) Shimidzu, T.; Ohtani, A.; Aiba, M.; Honda, K. *J. Chem. Soc. Faraday Trans.* **1988**, 1 84, 3941.
(b) Sheen, S.-R.;Shih, J.-S. *Analyst* **1992**, 117, 1691.

27. Okuhara, T.; Mizuno, N.; Misono, M. *Adv. Catal.* **1996**, *41*, 113.

28. Hill, C. L.; Prosser-McCartha, C. M. *Coord. Chem. Rev.* **1995**, *143*, 407.

29. (a) Kozhevnikov, I. V. *Catal. Rev.-Sci. Eng.* **1995**, *37*, 311.
(b) Kozhevnikov, I. V *Russ. Chem. Rev.* **1993**, 62, 473.

30. Corma, A. *Chem. Rev.* **1995**, *95*, 559.

31. Izumi,Y.; Urabe, K.; Onaka, M. *Zeolite, Clay, and Heteropoly Acid in Organic Reactions*; VCH: Tokyo, 1992.

32. (a) Vide references 2, 9, 11, 15, and 27-31.
(b) Mateev, K. I.; Kozhevnikov, I. V. *Russ. Chem. Rev.* **1982**, *51*, 1075.
(c) Tanabe, K.; Misono, M.; Ono, Y.; Hattoni, H. *New Solid Acids and Bases - their Catalytic Properties*; Elsevier: Tokyo, 1989.

33. (a) Johansson, G.; Pettersson, L.; Ingri, N. *Acta. Chem. Scand.* **1974**, A28, 1119.
(b) Johansson, G.; Pettersson, L.; Ingri, N. *Acta. Chem. Scand.* **1978**, A32, 407.
(c) Johansson, G.; Pettersson, L.; Ingri, N. *Acta. Chem. Scand.* **1978**, A32, 681.
(d) Levy, H. A.; Agron, P. A.; Danford, M. D. *J. Chem. Phys.* **1959**, 30, 1486.

34. Barkza, L.; Pope, M. T. *J. Phys. Chem.* **1975**, 79, 92.

35. Kozhevnikov, I. V. *Russ. Chem. Bull.* **1980**, 2213.

36. Kulikov, S. M.; Kozhevnikov, I. V. *Russ. Chem. Bull.* **1981**, 348.

37. Ghosh, A. K.; Moffat, J. B. *J. Catal.* **1986**, *101*, 238.

38. Farcasiu, D.; Li, J. Q. *J. Catal.* **1995**, *152*, 198.

39. (a) Misono, M.; Okuhara, T. *CHEMTECH* **1993**, 23, 23.
(b) Gillespie, R. J. *Acc. Chem. Res.* **1968**, 1, 202.
(c) Olah, G. A.; Prakash, G. K.; Sommer, J. *Superacids*; Wiley: New York, 1985.

40. Jozefowicz, L. C.; Karge, H. G.; Vasilyeva, E.; Moffat, J. B. *Micropor. Mater.* **1993**, *1*, 313.

41. Kapustin, G. I.; Brueva, T. R.; Klyachko, A. L.; Timofeeva, M. N.; Kulikov, S. M.; Kozhevnikov, I. V. *Kinet. and Catal.* **1990**, *31*, 896.

42. Lefebvre, F.; Liu-Cai, F. X.; Auroux, A. *J. Mater. Chem.* **1994**, *4*, 125.

43. This difference is significant in light of our previous claim that gas-solid calorimetry fails to differentiate sites of different strength in HZSM-5 because the equilibrium constants are comparable at elevated temperatures. Drago, R. S.; Dias, S. C.; Torrealba, M; de Lima, L. *J. Am. Chem. Soc.* **1997**,119, 4444.

44. West, F. S.; Audrieth, L. F. *J. Phys. Chem.* **1955**, *59*, 1069.

45. Hodnett, B. K.; Moffat, J. B. *J. Catal.* **1984**, *88*, 253.

46. Hayashi, H.; Moffat, J. B. *J. Catal.* **1982**, *77*, 473.

47. Hodnett, B. K.; Moffat, J. B. *J. Catal.* **1985**, 91, 93.

48. Rocchiccioli-Deltcheff, C.; Thouvenot, R.; Franck, R. *Spectrochim. Acta.* **1976,** 32A, 587.

49. Rocchiccioli-Deltcheff, C.; Fournier M.; Franck, R.; Thouvenot, R. *Inorg. Chem.* **1983**, *27*, 207.

50. Highfield, J. G.; Moffat, J. B. *J. Catal.* **1984,** *88*, 177.

51. Southward, B. W. L.; Vaughan, J. S.; O'Conor, C. T. *J. Catal.* **1995,** *153*, 293.

52. Kanda, Y.; Lee, K. Y.; Nakata, S.; Asaoka, S.; Misono, M. *Chem. Lett.* **1988,** 139.

53. Kozhevnikov, I. V. *J. Mol. Catal.* **1990,** 60, 65.

54. Drago, R. S. *Struct. and Bonding* **1973,** *15*, 73.

55. Drago, R. S. *Coord. Chem. Rev.* **1980,** *33*, 251.

56. Drago, R. S. *Applications of Electrostatic-Covalent Models in Chemistry*, Surfiside Scientific Publishers, Gainesville, 1994.

57. Reichardt, C. *Solvents and Solvent Effects in Organic Chemistry*, 2nd ed.; VCH: Weinheim, 1988.

58. Meek, D. W.; Drago, R. S. *J. Am. Chem. Soc.* **1961,** *83*, 4322.

59. Drago, R. S.; Chronister, C. W. *J. Am. Chem. Soc.* **1993,** *115*, 793.

60. Connors, K. A. *Binding Constants - The Measurement of Molecular Complex Stability*, John Wiley & Sons: New York, 1987.

61. For a general comparison, see references 40-42, 44-46, 62 and 63.

62. Rocchiccioli-Deltcheff, C.; Aouissi, A.; Bettahar, M. M.; Launay, S.; Fournier, M. *J. Catal.* **1996,** *164*, 16.

63. Payen, E.; Kasztelan, S.; Moffat, J. B. *J. Chem. Soc. Faraday Trans.* **1992,** *88*, 2263.

64. Varga, G. M. Jr.; Papaconstantinou, E.; Pope, M. T. *Inorg. Chem.* **1970,** *9*, 662.

65. Hill, C. L.; Bouchard, D. A. *J. Am. Chem. Soc.* **1985,** *107*, 5148.

66. Prosser-McCartha, C. M.; Kadkhodayan, M.; Williamson, M. M.; Bouchard, D. A.; Hill, C. L. *J. Chem. Soc., Chem. Commun.* **1986,** 1747.

67. Hill, C. L.; Bouchard, D. A.; Kadkhodayan, M.; Williamson, M. M.; Schmidt, J. A.; Hilinski, E. F. *J. Am. Chem. Soc.* **1988**, *110*, 5471.

68. Williamson, M. M.; Bouchard, D. A.; Hill, C. L. *Inorg. Chem.* **1987**, *26*, 1436.

69. Izutsu, K. *Acid-Base Dissociation Constants in Dipolar Aprotic Solvents, Chemical Data Series No. 35*, Blackwell Scientific Publications, Oxford, 1990.

70. Angelici, R. *J. Acc. Chem. Res.* **1995**, *28*, 51.

71. Drago, R. S.; Joerg, S. *J. Am. Chem. Soc.* **1996**, *118*, 2654.

72. Izutsu, K. *Acid-Base Dissociation Constants in Dipolar Aprotic Solvents, Chemical Data Series No. 35*, Blackwell Scientific Publications, Oxford, 1990.

73. Drago, R. S. *Inorg. Chem.* **1990**, *29*, 1379.

74. Drago, R. S.; Dias J. A.; Maier, T. O. *J. Am. Chem. Soc.* **1997**, 119, 7702.

75. Brown, G. M.; Noe-Spirlet, M. R.; Busing, W. R.; Levy, H. A. *Acta. Cryst.* **1977**, B33, 1038.

76. Nishimura, T.; Okuhara, T.; Misono, M. *Appl. Catal*. **1991**, 73, L7.

77. Okuhara, T.; Nishimura, T.; Misono, M. *Chem. Lett.* **1995**, 155.

78. Corma, A.; Martínez, A.; Martínez, C. *J. Catal.* **1996**, 164, 422.

79. Tatematsu, S.; Hibi, T.; Okuhara, T.; Misono, M. *Chem. Lett.* **1984**, 865.

80. Mizuno, N.; Misono, M. *Chem. Lett.* **1987**, 967.

81. Okuhara, T.; Nishimura, T.; Watanabe, H.; Misono, M. *J. Mol. Catal.* **1992**, 74, 247.

82. Bonardet, J. L.; Fraissard, J.; McGarvey, G. B.; Moffat, J. B. *J. Catal.* **1995**, 151, 147.

83. Moffat, J. B. *J. Mol. Catal.* **1989**, 51, 169.

84. McGarvey, G. B.; Moffat, J. B. *J. Colloid Interface Sci.* **1988**, 125, 51.

85. Taylor, D. B.; McMonagle, J. B.; Moffat, J. B. *J. Colloid Interface Sci.* **1985**, 108, 278.

86. Lapham, D.; Moffat, J. B. *Langmuir* **1991**, 7, 2273.

87. Lim, Y. Y.; Drago, R. S.; Babich, M. W.; Wong, N.; Doan, P. E. *J. Am. Chem. Soc.* **1987**, 109,169.

88. Drago, R. S.; Kob, N. *J. Phys. Chem. B* **1997**, 101, 3360.

89. Okuhara, T.; Nishimura, T.; Ohashi, K.; Misono, M. *Chem. Lett.* **1990**, 1201.

90. Lee, K. Y.; Arai, T.; Nakata, S.; Asaoka, S.; Okuhara, T.; Misono, M. *J. Am. Chem. Soc.* **1992**, 114, 2836.

91. Parry, E. P. *J. Catal.* **1963**, 2, 371.

92. Mastikhin, V. M.; Kulikov, S. M.; Nosov, A. V.; Kozhevnikov, I. V.; Mudrakovsky, I. L.; Timofeeva, M. N. *J. Mol. Catal.* **1990**, 60, 65.

93. Hayashi, H.; Moffat, J. B. *J. Catal.* **1983**, 83, 192.

94. Izumi, Y.; Hasebe, R.; Urabe, K. *J. Catal.* **1983**, 84, 402.

95. Shikata, S.; Nakata, S.; Okuhara, T.; Misono, M. *J. Catal.* **1997**, 166, 263.

96. Lefebvre, F. *J. Chem. Soc. Chem. Commun.* **1992**, 756.

97. Kulikov, S. M.; Timofeeva, M. N.; Kozhevnikov, I. V.; Zaikovskii, V. I.; Plyasova, L. M.; Ovsyannikova, L. A. *Russ. Chem. Bull.* **1989**, 763.

98. Rao, K. M.; Gobetto, R.; Iannibello, A.; Zecchina, A. *J. Catal.* **1989**, 119, 512.

99. Cheng, W.; Luthra, N. P. *J. Catal.* **1988**, 109, 163.

100. Nowinska, K.; Fiedorow, R. Adamiec, J. *J. Chem. Soc. Faraday Trans.* **1991**, 87, 749.

101. Izumi, Y.; Urabe, K. *Chem. Lett.* **1981**, 663.

102. Lefebvre, F.; Dupont, P.; Auroux, A. *React. Kinet. Catal. Lett.* **1995**, 55, 3.

103. Lefebvre, F.; Jouguet, B.; Auroux, A. *React. Kinet. Catal. Lett.* **1994**, 53, 297.

104. Schwegler, M. A.; van Bekkum, H.; de Munck, N. A. *Appl. Catal.* **1991**, 74, 191.

105. Drago, R. S.; Joerg, S. manuscript in preparation.

106. Drago, R. S.; Burns, D. S.; Lafrenz, T. J. *J. Phys. Chem.* **1996**, 100, 1718.

BIOGRAPHICAL SKETCH

José A. Dias was born September 18, 1962, in Jataí, a city located in the state of Goiás, central-west of Brazil, to parents Sebastião Dias and Luzia A. Dias. He attended Colégio da CASEB Elementary School and Objetivo High School in Brasília, Distrito Federal, where he graduated in December 1980. He entered the Universidade de Brasília, Brazil as a chemistry major in March of 1981. He graduated in December of 1985 with B.S. degree.

He started graduate school at the Department of Chemistry in the Universidade de Brasília, Brazil in March of 1986. He married Sílvia C. Loureiro on February 27th, 1987. In March of 1987 he was hired as Auxiliary Professor at the Universidade de Brasília. He graduated with a M. S. in Chemistry, in the area of Inorganic Chemistry, under the guidance of Dr. David P. Geeverghese in March of 1989. His thesis title was "Complexes of Iron (III) with DL(±) Malic Acid in Aqueous Solution." In October of 1990, he was approved, based on a written and a public oral qualify exam, to work as a full Professor in the Department of Chemistry at the Universidade de Brasilia. In March of 1991, he became Assistant Professor of that university.

He was admitted to graduate school at the University of Florida in January 1994 to pursue his doctorate in chemistry under guidance of Dr. Russell S. Drago. His research has focused on the acidity characterization of heteropoly acids and its salts.

The author has published a paper and is currently working on two others. Upon receiving the degree of Doctor of Philosophy, he will return to the Universidade de Brasília as Associate Professor, where he intends to continue his academic career teaching and developing research.

I certify that I have read this study and that in my opinion it conforms to acceptable standards of scholarly presentation and is fully adequate, in scope and quality, as a dissertation for the degree of Doctor of Philosophy.

Russell S Drago

Dr. Russell S. Drago, Chair
Graduate Research Professor of Chemistry

I certify that I have read this study and that in my opinion it conforms to acceptable standards of scholarly presentation and is fully adequate, in scope and quality, as a dissertation for the degree of Doctor of Philosophy.

Dr. Daniel R. Talham
Associate Professor of Chemistry

I certify that I have read this study and that in my opinion it conforms to acceptable standards of scholarly presentation and is fully adequate, in scope and quality, as a dissertation for the degree of Doctor of Philosophy.

Dr. David E. Richardson
Professor of Chemistry

I certify that I have read this study and that in my opinion it conforms to acceptable standards of scholarly presentation and is fully adequate, in scope and quality, as a dissertation for the degree of Doctor of Philosophy.

Samuel O. Colgate

Dr. Samuel O. Colgate
Professor of Chemistry

I certify that I have read this study and that in my opinion it conforms to acceptable standards of scholarly presentation and is fully adequate, in scope and quality, as a dissertation for the degree of Doctor of Philosophy.

Joseph H. Simm

Dr. Joseph H. Simmons
Professor of Materials Science Engineering

This dissertation was submitted to the Graduate Faculty of the Department of Chemistry in the College of Liberal Arts and Sciences and to the Graduate School and was accepted as partial fulfillment of the requirements for the degree of Doctor of Philosophy.

December, 1997

____

Dean, Graduate School